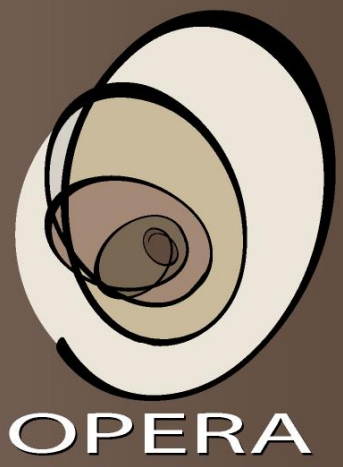

Corrosion behaviour of spent research reactor fuel under OPERA repository conditions

OPERA-PU-IBR511B

Radioactive substances and ionising radiation are used in medicine, industry, agriculture, research, education and electricity production. This generates radioactive waste. In the Netherlands, this waste is collected, treated and stored by COVRA (Centrale Organisatie Voor Radioactief Afval). After interim storage for a period of at least 100 years radioactive waste is intended for disposal. There is a world-wide scientific and technical consensus that geological disposal represents the safest long-term option for radioactive waste.
Geological disposal is emplacement of radioactive waste in deep underground formations. The goal of geological disposal is long-term isolation of radioactive waste from our living environment in order to avoid exposure of future generations to ionising radiation from the waste. OPERA (OnderzoeksProgramma Eindberging Radioactief Afval) is the Dutch research programme on geological disposal of radioactive waste.
Within OPERA, researchers of different organisations in different areas of expertise will cooperate on the initial, conditional Safety Cases for the host rocks Boom Clay and Zechstein rock salt. As the radioactive waste disposal process in the Netherlands is at an early, conceptual phase and the previous research programme has ended more than a decade ago, in OPERA a first preliminary or initial safety case will be developed to structure the research necessary for the eventual development of a repository in the Netherlands. The safety case is conditional since only the long-term safety of a generic repository will be assessed. OPERA is financed by the Dutch Ministry of Economic Affairs, Agriculture and Innovation and the public limited liability company Electriciteits-Produktiemaatschappij Zuid-Nederland (EPZ) and coordinated by COVRA. Further details on OPERA and its outcomes can be accessed at www.covra.nl.

OPERA-PU-IBR511B
Title: Corrosion of spent research reactor fuels
Authors: Guido Deissmann (BS), Kirsten Haneke (BS), André Filby (BS), Rob Wiegers (IBR)
Date of publication: 2016
Keywords: spent research reactor fuels, UAl_x-Al, U_3Si_2-Al, corrosion rates, source term

Summary

The present report summarises the results of the evaluation of the corrosion behaviour of and the radionuclide release from research reactor spent fuels (RRSF) under disposal conditions expected in a geological repository in Boom Clay in the Netherlands. The results address directly the safety function "delay and attenuation of releases" relevant after the failure of the waste canisters, when the waste forms come into contact with the near field water. Due to the temporal evolution of the cementitious near field in the repository and the uncertainty regarding the lifetime of the waste canister, different scenarios regarding the composition of the near field water are discussed. Research reactor fuels relevant within OPERA are plate-shaped dispersion type fuels consisting of uranium aluminide (UAl_x) or uranium silicide (U_3Si_2) fuel particles dispersed in an aluminium matrix with an aluminium cladding, containing high enriched uranium (up to 93 wt.% ^{235}U) or low-enriched uranium (up to 20 wt.% ^{235}U), respectively.

Experimental investigations on the corrosion behaviour of RRSF in the repository environment are rather limited, and studies under cementitious near field conditions are lacking to date. Corrosion data obtained for RRSF in salt brines, granite waters, or clay waters indicate a – with respect to the time scales relevant for geological disposal – practically instantaneous corrosion after failure of the waste canisters. A similar behaviour is expected here for disposal in a cementitious repository in Boom Clay, taking into account the high aluminium corrosion rates under anoxic and alkaline conditions. Thus with respect to the OPERA safety case it is suggested here that it is sensible to assume an instantaneous corrosion of and radionuclide release from RRSF after failure of the waste canisters.

Samenvatting

In dit rapport wordt de evaluatie van zowel de corrosie als het vrijkomen van radionucliden uit afgewerkte splijtstoffen (RRSF) onder ondergrondse eindberging condities behandeld. De resultaten hebben betrekking op het veiligheidsaspect "delay and attenuation releases" die de situatie beschrijft na aantasting van de opslagvaten (cannisters), waardoor het afval direct in contact komt met het water uit de directe omgeving van de ondergrondse eindberging. Gezien de in de tijd veranderende omstandigheden in de near field omstandigheden en de onzekerheden in de levensduur van de cannisters, zijn er verschillende scenario’s aangaande de samenstelling van het near field water beschouwd. Voor OPERA is het z.g. plate shapes dispersion type brandstof van belang, waarbij er sprake is van hetzij hoog verrijkt (tot 93 gew-%) dan wel laag verrijkt (tot 20 gew-%) uranium.

Er is slechts een beperkt aantal experimenten uitgevoerd ten aanzien van het optreden van corrosie van RRSF onder eindberging condities en helemaal geen ten aanzien van de condities in een cementgebonden eindberging omgeving. Gegevens betreffende corrosie in een zoute, graniet- of kleiwater omgeving indiceren een bijna instantaan (in relatie tot de relevante tijdschaal) optreden van corrosie na het bezwijken van de cannisters. Overeenkomstig gedrag wordt verwacht in een cementgebonden eindberging in Boomse klei, waarbij rekening wordt gehouden met de hoge corrosiesnelheid van aluminium onder anoxidische en alkalische condities. Derhalve wordt voorgesteld om het instantaan optreden van corrosie, alsmede het vrijkomen van radionucliden van de RRSF zorgvuldig te beschouwen.

1. Introduction

1.1. Background

The five-year research programme for the geological disposal of radioactive waste − OPERA − started on 7 July 2011 with an open invitation for research proposals. In these proposals, research was proposed for the tasks described in the OPERA Research Plan.

The required long-term isolation of radioactive wastes from the biosphere can be achieved by a multiple barrier system, consisting of a combination of a man-made engineered barrier system (EBS) with a suitable geological barrier, the repository host rock. Within a multibarrier concept for the disposal of high-level radioactive waste (HLW), the waste form acts as the first barrier against the release of radionuclides from the waste into the repository near-field. In as such, the performance of the waste form under repository conditions plays an important role with respect to the isolation of the radioactive waste and the radionuclides contained therein from the biosphere. The understanding of the corrosion behaviour of and the consequent radionuclide release from the disposed HLW forms thus an integral part of a safety assessment for a geological repository. HLW intended for future geological disposal in the Netherlands comprises vitrified wastes (glass) from the reprocessing of light water reactor (LWR) fuels from commercial nuclear reactors, research reactor spent fuels (RRSF), spent uranium targets from molybdenum production as well as non-heat generating wastes such as compacted hulls and ends from fuel assemblies packaged in CSD-C containers and legacy wastes.

Compared to UO_2-based fuels for LWR for nuclear power generation, nuclear fuel types employed in research and prototype reactors are generally very different in design (e.g. regarding fuel composition, enrichment, cladding materials) and irradiation history (i.e. irradiation temperatures, burn-up) resulting in distinct differences regarding (i) the microstructure development and (ii) concentration, distribution and speciation of fission/activation products after irradiation. These structural and compositional differences lead also to significant differences in their long-term behaviour in the repository environment.

1.2. Objectives

In this report, the execution and results of the research proposed for task *5.1.1* with the following title in the Research Plan: *HLW waste matrix corrosion processes* is described. This report refers to the work performed with respect to spent fuel from research reactors.

The aim of this report is to provide information on the corrosion behaviour of and the radionuclide release from spent fuel from research reactors in a generic repository in Boom Clay in the Netherlands to assess and quantify the safety function ‘delay and attenuation of releases’ in the context of the envisaged safety case. Based on existing data and information obtained from the literature, relevant corrosion processes under the expected conditions in the repository are investigated and discussed to increase the understanding of waste form evolution (i.e. leaching and dissolution behaviour) with time. The results of these investigations comprise data and ranges for corrosion rates of spent research reactor fuels under repository conditions and the associated release rates of safety relevant radionuclides that can be used in performance assessments for a geological repository in the Netherlands. In addition to the waste form corrosion rates, processes that may retain the leached radionuclides in the immediate near field by interaction with degradation products from the engineered barrier system (i.e. metal corrosion products, and concrete degradation products) will be addressed to derive radionuclide source terms.

1.3. Realisation

The literature study presented in this report was performed by a consortium formed by IBR Consult BV (IBR, Haelen, The Netherlands) and Brenk Systemplanung GmbH (BS, Aachen, Germany). The work reported here was carried out in the period January 2013 to March 2016 and the report is based upon, and solely refers to, information available at that time. Thus, for example, where the report refers to 'current knowledge' this should be read to mean 'knowledge existing at the time the work was carried out'.

1.4. Explanation contents

Chapter 2 provides an overview on the general characteristics of research reactor fuels and the research reactors operated in the Netherlands. Issues concerning the inventory of research reactor spent fuels within OPERA are addressed in chapter 3. Chapter 4 discusses bounding conditions for the HLW disposal in the Netherlands with respect to the disposal concept and the environmental conditions to be expected in the repository near field and its evolution. Chapter 5 details the results of the review of literature data and other available information on the corrosion behaviour of research reactor spent fuels. Based on the results of this review, in chapter 6 the available information is evaluated with respect to the derivation of corrosion rates and radionuclide release rates under repository conditions relevant to OPERA. Conclusions and recommendations resulting from the work performed in the frame of this project are given in chapter 7. References cited throughout this report are compiled in chapter 8.

2. Research reactor fuels

2.1. Dispersion type intermetallic fuels

Nuclear fuels employed in research reactors are generally very different in design (e.g. regarding fuel composition, enrichment, cladding materials) from the Zircaloy-clad ceramic UO_2 fuels used in power reactors. Furthermore, irradiation temperatures and burn-ups are rather different in research reactors compared to power reactors used for electricity generation, resulting in distinct differences regarding (i) the microstructure development and (ii) concentration, distribution and speciation of fission/activation products in the fuels after irradiation. These structural and compositional differences of the spent fuels lead also to significant differences in their long-term behaviour in the repository environment.

The purpose of research and test reactors is to produce neutrons used for research, production of radioisotopes for medicine and industry and other purposes, rather than power. Thus research reactors require fuels that can operate at high-power density and exhibit low neutron absorption capacity. Current research reactor fuels are predominantly thin plate-shaped dispersion type fuels composed of fuel particles dispersed in an inert matrix and sandwiched between metal cladding [Kim 2012]. The fuelled zone in a dispersion fuel plate (cf. Figure 2.1) – sometimes called the 'fuel meat' or 'fuel core' – frequently consists of uranium-aluminide (UAl_x) or uranium-silicide (e.g. U_3Si, U_3Si_2, or USi) fuel particles (size mainly between 40 and 150 µm) dispersed in an aluminium matrix that is metallurgicaly bonded to aluminium cladding ([Kim 2012], [Hofman 2015]). Aluminium is chosen for the matrix due to its low neutron absorption cross section, low costs, and good fabricability. Various aluminium alloys (e.g. 1100Al, 5052Al, 6061Al [Sindelar 1996], AlMg2 [Curtius 2006], or AlFeNi [Wintergerst 2009]) are used as cladding materials due to their high thermal conductivities and, again, the low neutron absorption cross-sections. Unlike moderately enriched commercial fuels for light-water reactors (LWR) (4 to 5 wt.% ^{235}U), research reactor fuels are more highly enriched (typically about 20 wt.% ^{235}U or higher). Since highly-enriched uranium (HEU, i.e. >20 wt.% ^{235}U) allowed for higher neutron fluxes and more compact reactor cores, many reactors up to the 1980s used HEU-cores with 93 wt.% enriched fuel.

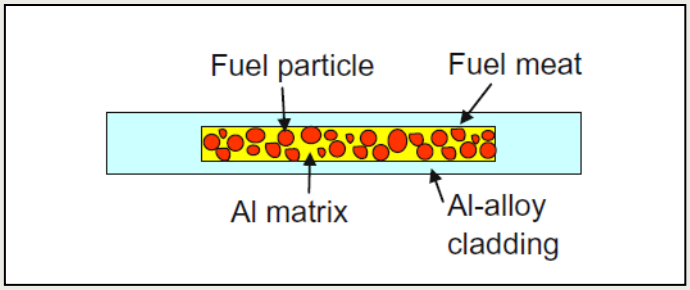

Figure 2-1 **Schematic cross section of a dispersion type fuel plate used in research and test reactors**

A broad variety of designs for research reactor fuels has been developed throughout the last decades depending on the type and purpose of the reactor. Most research reactors in Europe employ plate-type fuels with assemblies of thin flat or curved plates arranged in various types of fuel assemblies (e.g. box- or tube-shaped, cf. Figure 2.2) [Van den Berghe 2010]. Comprehensive reviews of the composition and fabrication of dispersion type intermetallic fuels and their chemical, mechanical, and thermophysical properties and their irradiation behaviour are provided for example by [Kim 2012] and [Hofman 2015].

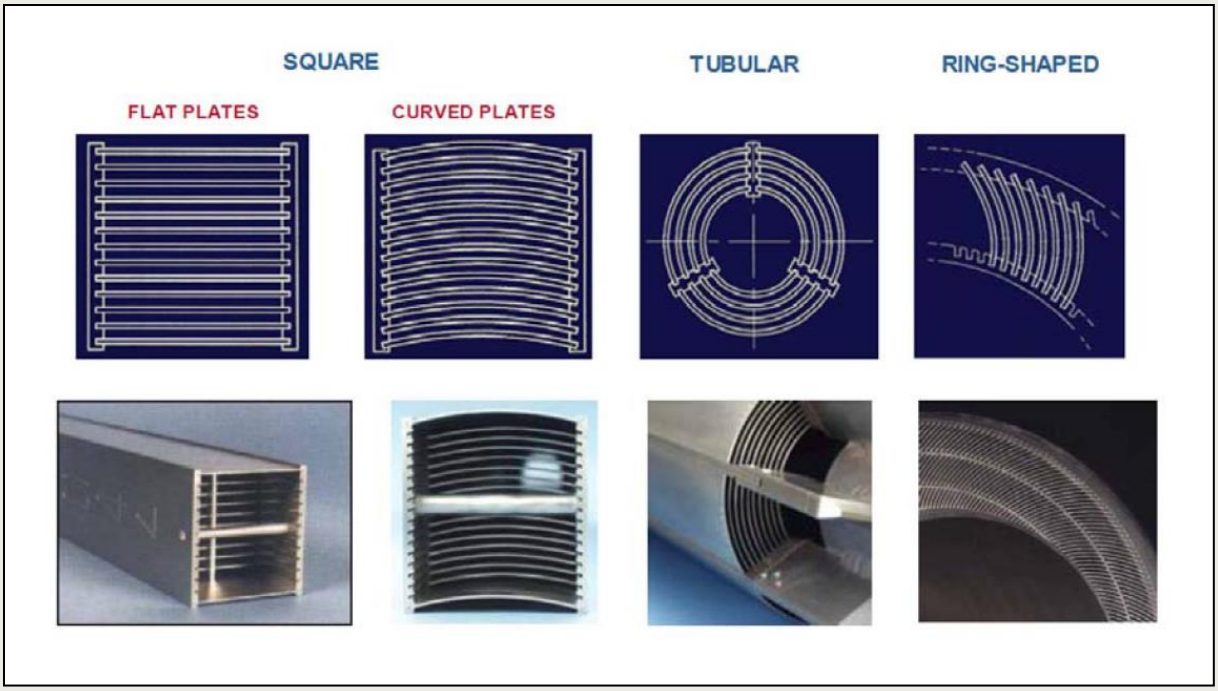

Figure 2-2 Examples for different designs of research reactor fuels [Van den Berghe 2010]

The first uranium intermetallic fuels chosen for research and test reactor purposes were U-Al alloys consisting of mixtures of UAl_2, UAl_3, and/or UAl_4, thus known as UAl_x, dispersed in aluminium employing HEU [Kim 2012]. In 1978, the U.S. Department of Energy (US DOE) initiated the Reduced Enrichment for Research and Test Reactors (RERTR) Program to develop technical means to convert research reactors and isotope production processes using HEU to low enriched uranium (LEU) to reduce risks associated with proliferation. The threshold between HEU and LEU was set to 20 wt.% ^{235}U. The use of LEU-fuels in research reactors required the development of new fuels with higher uranium densities to compensate for the reduced fraction of fissile materials in the fuel elements. This requirement lead to the development of LEU fuels using uranium silicides (e.g. U_3Si_2, U_3Si, or USi) dispersed in aluminium, due to the significantly higher achievable uranium density in the fuels. At present, U_3Si_2 is considered as the best qualified fuel for research and test reactors with respect to uranium loading and performance. Due to its swelling behaviour, U_3Si is unsuitable for usage in plate-type fuels but can be used in fuel rods [Kim 2012].

Compared to power reactors, research reactors typically operate at lower temperatures (e.g. coolant temperature below 100 °C) but at higher power densities and achieve higher fuel burn-up, so the fuel must withstand structural damage from fission and accommodate high quantities of fission products. However, due to the lower proportion of ^{238}U even in LEU fuels, spent research reactor fuels contain less actinides and produce less heat from radioactive decay than spent LWR fuels. Depending on operating temperature and fission rate during reactor operation of UAl_x-Al-fuels, the three uranium aluminide compounds undergo amorphisation, with higher amorphisation rates at lower irradiation temperatures and higher fission rates. The amorphisation resistance decreases in the order UAl_2 > UAl_3 > UAl_4 [Kim 2012]. Uranium silicides such as U_3Si and U_3Si_2 are also amorphised under irradiation due to damage induced by fission. Moreover, during reactor operation the dispersed uranium silicides react with the aluminium in the fuel meat to form reaction rims (interaction layers, IL) consisting of (nonstoichiometric) intermetallic U-Al-Si compounds, which become amorphous during irradiation. The growth of the IL can be expressed as function of fission rate, temperature, and irradiation time [Kim 2012].

2.2. Research reactors in the Netherlands and their fuels

Within the nuclear programme of the Netherlands, there are currently two research reactors in operation: the High Flux Reactor (HFR) of the EU Joint Research Centre (JRC) in Petten, operated by NRG, and the Hoger Onderwijs Reactor (HOR) at the Reactor Institute Delft on the premises of the Delft University of Technology [MEAAI 2014]. The Low Flux Reactor (LFR) located in Petten was taken out of operation in 2010. NRG has plans for the construction of a replacement for the ageing HFR in Petten known as PALLAS. In January 2012, the Dutch government gave its approval for the construction of the new reactor, which is not likely to be operational until around 2024 [WNN 2013a]. At present, spent fuel from three Dutch research reactors is stored at COVRA, namely from LFR, HFR and HOR [MEAAI 2014], that has to be considered for geological disposal within OPERA. The basic characteristics of these research reactors are summarised in Table 2-1. Spent fuels from test and research reactors in the Netherlands that were shut down in the 1970s such as the Biologische Agrarische Reactor Nederland (BARN), the Atoomkernreactor Technische Hogeschool Eindhoven NEderland (ATHENE) and the KEMA Suspensie Test Reactor (KSTR) were sent back to the USA within the frame of the US non-proliferation policy (cf. [Dodd 2000], [MEAAI 2014], [Verhoef 2016]).

Table 2-3 Test and research reactors in the Netherlands ([Dodd 2000], [Hart 2014])

Reactor	Location	Owner	Criticality	Status	Type	Design power	Maximum power
LFR	Petten	ECN/NRG	28/09/1960	shut down	Argonaut	10 kW	30 kW
HFR	Petten	JRC	09/11/1961	operating	Tank	20 MW	45 MW
HOR	Delft	TU Delft	25/04/1963	operating	Pool	200 kW	3 MW

The following sections provide a brief overview of each of these reactors and a description of the fuel elements.

2.2.1. Low Flux Reactor (LFR)

The Lage Flux Reactor or Low Flux Reactor (LFR) was a small research reactor used for the production of neutrons for biological and physical research, as well as for general training purposes. The LFR, located in Petten and owned by ECN/NRG, was not operated on a regular basis and was permanently taken out of operation in 2010 [MEAAI 2014]. At present, its decommissioning is being prepared. The LFR was a light water moderated research reactor of the type 'Argonaut' with a ring-shaped core box and internal and external graphite reflectors ([Braak 1987], [Stecher-Rasmussen 1996]). The LFR started its operation in 1960 with an initial maximum reactor power of 10 kW, which was increased in 1983 to 30 kW. The fuel elements used in the LFR had a horizontal cross section of 75 mm x 75 mm and a length of 840 mm, containing 9 fuel plates or trim plates. The LFR employed aluminium-clad UAl_x-Al dispersion type fuels containing HEU (enrichment approximately 90 wt.% ^{235}U). The number of fuel plates (21.3 g ^{235}U) and 'trim' plates (10 g ^{235}U) per fuel element could be varied to vary the amount of fissile material in the reactor core [Dodd 2000]. The consumption of fuel in the LFR was very low and the original fuel elements were still in use at the time of the shut-down of the reactor in 2010 [MEAAI 2014]. The spent HEU fuel was removed from the reactor in 2013 and transferred to COVRA in December 2013 ([WNN 2013b], [MEAAI 2014]).

2.2.2. High Flux Reactor (HFR)

The Hoge Flux Reactor or High Flux Reactor (HFR), also located at Petten, is a multi-purpose research reactor used for materials testing, radioisotope production and general research purposes. Over the operating period beginning in 1960, its use has been shifted

from testing of nuclear materials to fundamental research and the production of medical radioisotopes. The reactor is operated by ECN/NRG on behalf of the European Union's Joint Research Centre (JRC) and has supplied a large share of the world's supply of radioisotopes for medical purposes. The HFR is a 'tank-in-pool' type of reactor using light water as coolant and moderator and employs beryllium reflectors. The initial design power output of the HFR was 20 MW. The power was increased in 1966 to 30 MW, and to the present 45 MW in 1970. The reactor core consists of a 9 x 9 lattice, containing 33 fuel elements, 6 control assemblies, 25 beryllium reflector elements, and 17 experimental positions [Thijssen 2006].

The HFR fuel assemblies (height 924 mm, horizontal cross section 81 x 77 mm) contain 23 vertically arranged parallel, curved, fuel plates with a height of 625 mm. Initially, the HFR employed aluminium-clad UAl_x-Al HEU dispersion fuels with an enrichment of 93 wt.% ^{235}U. The conversion of the HFR core from HEU to LEU using U_3Si_2-Al dispersion fuels with approximately 20 wt.% ^{235}U started in 2005 and was completed in 2006 [Thijssen 2006]. This step was in line with the worldwide move to abandon the use of HEU due to non-proliferation reasons [MEAAI 2014]. The larger thickness of fuel plates for LEU has resulted in less fuel plates per fuel assembly. Thus LEU fuel assemblies contain 20 instead of 23 fuel plates [Thijssen 2006]. Prior to being transferred to COVRA for long-term storage, the spent fuel from HFR is stored in the spent fuel pools [MEAAI 2014]. Usually a cooling period of five years is applied. The last HEU fuel elements from the HFR were transported to COVRA in March 2011 [MEAAI 2014]. Table 2-2 summarises some of the main characteristics of HEU and LEU fuels used in the HFR.

Table 2-2 Main characteristics of HFR fuels [Thijssen 2006]

Characteristic	HEU-fuel	LEU-fuel
fuel type	UAl_x-Al	U_3Si_2-Al
U-density	1 g cm^{-3}	4.8 g cm^{-3}
enrichment [%]	93 %	19.75 %
No. of plates in fuel / control element	23 / 19	20 / 17
^{235}U mass in fuel / control element	450 g /310 g	550 g / 440 g
burnable poison	1000 mg ^{10}B	40 ^{113}Cd wires (diameter 0.5 mm)

2.2.3. Hoger Onderwijs Reactor (HOR)

The Hoger Onderwijs Reactor (HOR) located at Delft University is a multi-purpose research reactor used for basic and applied research as well as for educational purposes, mainly in the fields of neutron and positron beam physics research, radiochemistry and neutron activation analysis, as well as reactor physics. It is owned by the Delft University of Technology and operated by the Interfaculty Reactor Institute. The HOR is a 'swimming pool' type of reactor using light water as coolant and moderator and utilises beryllium as reflector material. The initial maximum operating power of 200 kW was increased to 500 kW in the beginning of 1967. After extensive modifications, the operating power of the HOR was increased to 2 MW later in 1967 and to the currently licensed maximum power of 3 MW in 1969. The core lattice of the HOR is a 7 x 6 array.

The fuel and control elements used in the HOR contain 19 and 10 fuel plates, respectively. The HOR was originally designed for and operated with HEU fuels (UAl_x-Al) with an enrichment of approximately 93 wt.% ^{235}U. The HEU standard core of the HOR consisted of 28 HEU fuel assemblies and 4 HEU control assemblies with the 10 remaining lattice

positions part of the water reflector [Dodd 2000]. The HEU to LEU conversion at HOR Delft started in March 1998 with the first full LEU core in January 2005 [De Vries 2006]. The LEU fuels employed at the HOR are U_3Si_2-Al dispersion fuels with an enrichment of 19.75 wt.% ^{235}U. The LEU compact core of the HOR consists of 16 LEU fuel assemblies, 4 LEU control assemblies and 21 beryllium reflector elements with the last position meant as Central Irradiation Facility. After interim storage in the spent fuel pool facility at Delft, spent fuels from the HOR are transferred to COVRA. The last HEU fuel elements from the HOR were shipped to COVRA in May 2011 [MEAAI 2014]. Table 2-3 summarises important properties of HEU and LEU fuels employed in the HOR.

Table 2-3 Main characteristics of HOR fuels [De Vries 1997, 2006]

Characteristic	HEU-fuel	LEU-fuel
fuel type	UAl_x-Al	U_3Si_2-Al
U-density	0.58 g cm^{-3}	4.3 g cm^{-3}
enrichment [%]	93 %	19.75 %
No. of plates in fuel / control element	19 / 10	19 / 10
^{235}U mass in fuel / control element	190 g /100 g	300 g / 158 g
burnable poison	B	B

3. Research reactor spent fuel in OPERA

The release rates of radionuclides from wastes disposed in a geological repository depend, inter alia, on the processes controlling waste form corrosion and the mechanisms leading to a release of radionuclides from the waste matrices. The release of radionuclides from the waste into the repository near-field strongly depends on the distribution and speciation of the radionuclide in the waste form. The matrix compositions and the radiological inventories of the various waste categories included in the OPERA disposal concept [Verhoef 2014a] are addressed in [Meeusen 2014] and [Hart 2014], respectively. In order to determine reliable radionuclide source terms for the safety assessments within OPERA, waste families were defined as groups of radioactive wastes from the same origin, with similar nature, and identical or rather close conditioning characteristics, while belonging to the same category of the current waste classification used in the Netherlands [Verhoef 2016]. For each of these waste families, standardised compositions were derived to be used in the further analysis and assessments of waste form corrosion and radionuclide release mechanisms within OPERA. These standardised compositions include inventories of radionuclides per waste container, the expected distribution of the radionuclides in the respective waste matrices and the chemical composition of the wastes as well as the dimensions/properties of the waste containers and − if relevant − the expected heat output in 2130. The information and the level of detail match the requirements of the various tasks within OPERA and reflect the available information [Verhoef 2016]. The following sections summarise the information on the standardised composition and the waste inventories with respect to the waste family research reactor spent fuel (RRSF).

3.1. Characteristics of spent research reactor fuels within OPERA

RRSF to be considered within OPERA comprises the spent fuels from the three research reactors from which spent fuel is stored at COVRA, namely the Low Flux Reactor (LFR), the High Flux Reactor (HFR), and the Hoger Onderwijs Reactor (HOR) (cf. section 2.2). The characteristics of RRSF in OPERA derived in [Verhoef 2016] are based mainly on the information available on fuels used in the HFR (e.g. [Ahlf 1993], [Dodd 2000], [Thijssen 2006], [NRG 2012]) The characteristics of the spent fuels from the two other research reactors LFR and HOR are similar to those of the HFR [Verhoef 2016] with differences for example regarding the ^{235}U mass per fuel element/control element and the number of plates per fuel assembly. According to [Verhoef 2016], these differences are assumed to be not relevant in the preliminary phase of research into geological disposal of radioactive waste in the Netherlands within OPERA. Thus, for the following consideration it is assumed that all RRSF has the same characteristics as the fuel used in the HFR. Both, spent HEU and LEU fuels are considered within OPERA. Table 3-1 summarises the main characteristics of RRSF according to [Verhoef 2016].

3.2. Waste canisters for RRSF and packaging

The spent fuel elements of the research reactors are delivered to COVRA in a cask containing a stainless steel (type 32) basket with circa 33 elements ([MEAAI 2014], [Meeussen 2014]). Inside COVRA the basket with fuel elements is removed from the cask and placed in a steel canister (ECN canister), which is welded tight and filled with an inert gas (helium). The ECN canister (Figure 3-1) has an internal diameter of 740 mm and is made of stainless steel Type 304 [Verhoef 2014a]. If filled with 33 fuel elements, each ECN-canister contains 16 kg HEU fuel or 97 kg LEU fuel, respectively [Verhoef 2016].

Table 3-1 Characteristics of research reactor spent fuel (RRSF) used within OPERA [Verhoef 2016]

Characteristic	unit	HEU-fuel	LEU-fuel
fuel type	[-]	UAl_x	U_3Si_2
U-density	[g cm^{-3}]	1	4.8
fuel meat thickness	[mm]	0.51	0.76
fuel meat length	[mm]	600	600
enrichment	[%]	93	19.75
^{235}U mass in fuel / control element (BOI)	[g]	450 / 310	550 / 440
^{235}U mass in fuel / control element (EOI)	[g]	177 / 119	200 / 225
maximum burn-up	[%]	55	70 / 60
No. of plates in fuel/control element	[-]	23 / 19	20 / 17
cladding/framing material	[-]	Al	AG3NE or equivalent
matrix	[-]	Al	Al
thickness of cladding on both sides inner /outer fuel plate	[mm]	0.38 / 0.57	0.38 / 0.57
burnable poison	[-]	1000 mg ^{10}B (in Al side plates)	40 Cd wires (diameter 0.5 mm)

BOI : Begin Of Irradiation, EOI: End of Irradiation

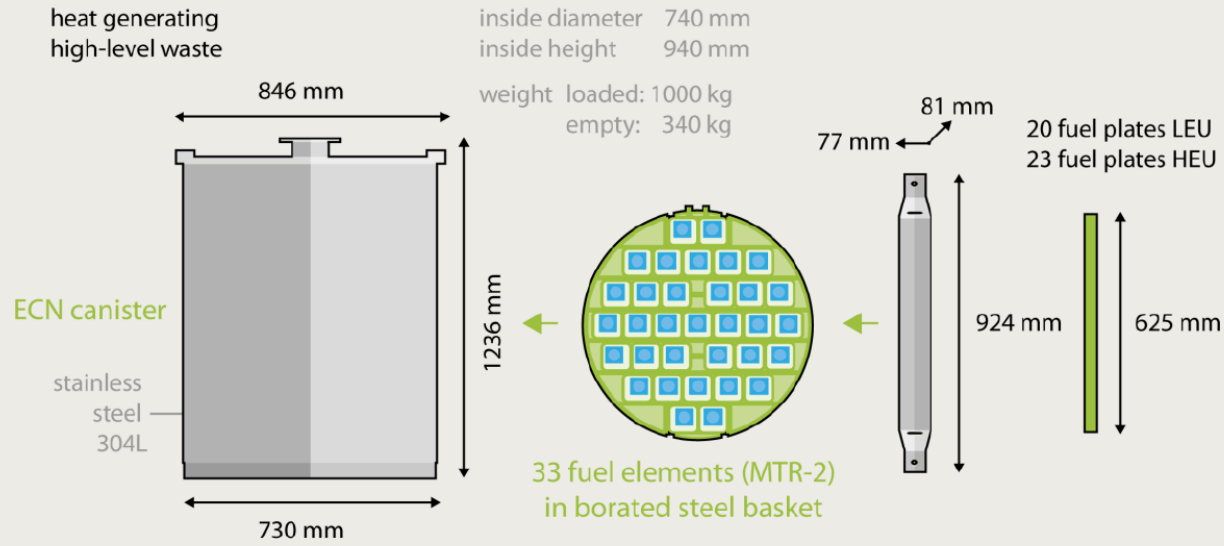

Figure 3-2 Schematics of ECN-container used for storage and disposal of RRSF, dimensions in mm [Verhoef 2016]

According to the waste inventory provided in the disposal concept [Verhoef 2014a], 150 ECN waste canisters containing RRSF are intended for final disposal [Verhoef 2016]. It is assumed that 30 waste canisters contain spent HEU fuel and 120 waste canisters contain spent LEU fuel [Verhoef 2016]. The maximum heat production of each waste canister at disposal time (i.e. after a storage period of at least 100 years) can be assumed to be 33 W [Verhoef 2016]. Within the OPERA disposal concept in clay, it is assumed that two ECN-canisters are placed into one supercontainer (cf. chapter 4.1) for final disposal [Verhoef 2014a].

3.3. Radionuclide inventory

A reference radionuclide inventory for ECN-canister containing spent HEU and LEU fuels at disposal time was derived in [Verhoef 2016], based in particular on information on the radionuclide inventory of RRSF in [Dodd 2000], and assuming that each ECN canister holds 33 fuel elements to simplify the input for the research tasks in OPERA. The activity of radionuclides per ECN canister containing RRSF at disposal time is summarised in Table A-1 in Appendix 1. At disposal time, the activity inventory of a waste canister containing 33 LEU fuel elements is about a factor of two larger than for a canister with 33 HEU elements, due to the higher initial $^{238/235}$U content of the LEU fuel elements that results in (i) significantly higher amounts of transuranium elements and (ii) higher amounts of fission products per fuel element after irradiation. The uranium content of the control elements is smaller than in the respective HEU/LEU fuel elements leading to lower actinide and fission product contents per element at the time of fuel unloading from the reactor. Thus the assumption of disposing ECN-canisters containing only 33 fuel elements each is conservative with respect to the radionuclide inventory of the waste canisters at disposal time. According to [Verhoef 2016], an ECN canister loaded with 33 spent fuel elements contains 16 kg of fissile material in the case of HEU fuel, or 97 kg in the case of LEU fuel, which is above the reported critical masses of 14.4 kg for HEU and 43 kg for LEU (cf. [Dodd 2000]). The baskets holding the spent fuel elements in the ECN canister are fabricated from borated steel to ensure that criticality cannot occur [Verhoef 2016]. Nevertheless, it is deemed worthwhile to investigate the disposal of a single ECN canister with in a supercontainer [Verhoef 2016].

Within the RRSF the radionuclides are not expected to be homogeneously distributed as, for example, in vitrified waste from the reprocessing of LWR-fuels. Regarding RRSF, the radionuclides can assumed to be contained mainly in the fuel meat of the fuel plate in the fuel assembly [Verhoef 2016].

The total radionuclide inventory of the wastes to be considered for final disposal within OPERA was estimated in [Hart 2014]. [Hart 2014] derived the radionuclide inventories in the various waste categories included in the OPERA disposal concept [Verhoef 2014a] such as low and intermediate level waste (LILW), non-heat generating HLW, RRSF or vitrified HLW in the year 2130. Only radionuclides with half-lives greater than 10 years were taken into account as relevant for the long-term safety of the repository [Hart 2014]. The inventories of radionuclides relevant for the long-term safety in RRSF in the year 2130 are provided in Appendix 1 (Table A-2), including inventories originating from spent uranium filters from ^{99}Mo production at the HFR in Petten [Hart 2014]. A potential uncertainty of the radionuclide inventory in the spent fuel section of the repository is related to the anticipated replacement of the HFR considered in the extrapolation of the inventories [Hart 2014]. In case that a replacement reactor for the HFR (PALLAS) will not be built, the inventory of the spent fuel section of the repository will be significantly lower [Hart 2014].

4. Conditions in the near field

The evaluation of the long-term behaviour of nuclear wastes in a deep geological disposal facility requires an understanding of the environmental conditions to which the material will be exposed. The durability of the waste forms and the long-term radionuclide release are affected by intrinsic properties of the waste forms as well as by the interaction with the disposal environment, i.e. the engineered barriers system and the geological environment, and the near-field conditions that may evolve over time. Thus with respect to the disposability of the waste forms and the safety case for a repository, assessments and predictions of the long-term durability of the waste forms in the repository environment, and radionuclide release rates under realistic repository conditions are essential.

Near field characteristics that affect waste form performance and radionuclide source terms include hydrogeological (e.g. groundwater flow regimes and flow rates) as well as geochemical conditions (e.g. pH, redox potential, temperature, ionic strength, and groundwater composition), which both depend on the repository design and the geological environment. The deep geological disposal of LILW and HLW addressed within OPERA is at present at a site-generic stage, i.e. no potential repository site has been selected. However, the preselection of a potential geological formation (Boom Clay) for the repository and the development of a disposal concept [Verhoef 2014a] for the OPERA safety case allow constraining the near field conditions in the repository to some degree. The following section 4.1 provides an overview on the disposal concept pursued within OPERA. Aspects regarding the expected evolution of the repository near field are discussed in section 4.2.

4.1. OPERA disposal concept

The disposal concept pursued within OPERA considers the installation of a multi-barrier repository system within the poorly indurated Boom Clay formation in the Netherlands. A multi-barrier system intended for the long-term isolation of radioactive wastes from the biosphere typically comprises a combination of a man-made engineered barrier system (EBS) with a suitable geological barrier, the repository host rock. An outline of the disposal system in clay has been provided by [Verhoef 2010] and [Verhoef 2014a]. The generic disposal concept for HLW pursued within this context is based on the Belgian ONDRAF/NIRAS supercontainer concept (cf. [ONDRAF 2004], [Bel 2006], [ONDRAF 2013]).

The OPERA disposal facility consists of both surface and underground facilities, connected by two vertical shafts and (optionally) an inclined ramp [Verhoef 2014a]. The surface facilities comprise the waste conditioning facilities required for receiving, inspecting, and conditioning of the different waste types and the construction and supply facilities, i.e. the support infrastructure for construction, operation, and closure of the underground disposal facilities.

The underground disposal facilities contain separate disposal sections for different types of wastes, a pilot facility and a workshop for maintenance work, all connected by the main gallery, which is an orbicular structure. The disposal drifts are horizontal boreholes supported by wedge-shaped concrete blocks. The disposal drifts used for vitrified HLW and RRSF have a length of 45 m and are directly connected to the main gallery. The dimensions of the disposal tunnels in the different sections of the OPERA disposal facility are provided in Table 4-1.

Table 4-1 Dimensions of the disposal drifts in different sections of the OPERA disposal facility [Verhoef 2014a]

Waste section	Number of drifts [-]	Length [m]	Diameter (outer/inner) [m]	Concrete support thickness [m]	Spacing [m]
heat-generating HLW	47	45	3.2/2.2	0.50	50
RRSF	6	45	3.2/2.2	0.50	50
non-heat-generating HLW	36	200	3.2/2.2	0.50	50
LILW and DU	65	200	4.8/3.7	0.55	50

The functions and compositions of various cementitious materials utilised within the OPERA disposal concept in clay (e.g. for mechanical support, waste conditioning, backfilling) are discussed in [Verhoef 2014b].-The mechanical support during the constructional and operational phase of the geological disposal facility is provided by the gallery lining. In [Verhoef 2014b] concrete segments made with Portland fly ash cement (CEM II) are proposed for this purpose. The suggested composition of the concrete used for the gallery lining and the mechanical support of the disposal tunnels is provided in Table 4-2.

Table 4-2 Suggested composition of concrete used for the mechanical support of the disposal tunnels [Verhoef 2014b]

Component/Parameter	Type	
cement	CEM II/A to B-(V)	386 kg m^{-3}
water		125 kg m^{-3}
plasticiser	Woermann BV 514	1.33 kg m^{-3}
superplasticiser	Woermann FM 30	3.65 kg m^{-3}
fine aggregate	quartz sand: 0-2 mm	615 kg m^{-3}
coarse aggregate	quartz gravel: 2-8 mm	612 kg m^{-3}
coarse aggregate	quartz gravel: 8-16 mm	700 kg m^{-3}
w/c-ratio		0.39

Prior to disposal, the ECN-canisters containing RRSF (as well as canisters with vitrified HLW and non-heat generating HLW) will be overpacked in supercontainers [Verhoef 2014a]. In the supercontainer concept, the waste canister, overpack and buffer are transported and disposed of as one entity. The OPERA supercontainer, adopted from the Belgian supercontainer concept (cf. [Bel 2006]), consists of a carbon steel overpack (30 mm), a concrete buffer (600 to 700 mm) and a stainless steel envelope (4 mm) [Verhoef 2016]. Supercontainers with a length of 2.5 m will contain one CSD-V canister with vitrified HLW or one CSD-C canister with compacted reprocessing wastes, respectively, whereas supercontainers with a length of 3.0 m will contain two ECN canisters with either RRSF or other non-heat generating HLW [Verhoef 2014a]. Taking into account the length of a single disposal drift in the HLW section of the OPERA disposal facility, each disposal drift can hold 15 supercontainers with a length of 2.5 m containing vitrified HLW (CSD-V) and/or compacted wastes (CSD-C). For the supercontainers with a length of 3 m used for RRSF and other (non-heat generating) HLW packaged in ECN-canisters, the emplacement of 12 supercontainers in each disposal drift are considered in [Verhoef 2014a]. The provisional properties of the OPERA supercontainer for RRSF are shown in Table 4-3.

Table 4-3 Provisional properties of the OPERA supercontainer for RRSF [Verhoef 2014a]

Property	
outer container diameter	1.9 m
outer container length	3.0 m
waste container(s)	2 ECN canisters
steel overpack thickness	3 cm
concrete buffer thickness	0.6-0.7 m
steel envelope thickness	0.4 cm
weight	approx. 20,000 to 24,000 kg
maximum dose rate at container surface	≤10 mSv/h

Potential compositions of the concrete to be used in the OPERA supercontainer are discussed in [Verhoef 2014b], based on compositions studied by the Belgian waste management organisation ONDRAF/NIRAS. In [Verhoef 2014b] concrete made with sulphate-resistant Portland cement (CEM I) and limestone aggregates is proposed for the OPERA supercontainer (cf. Table 4-4). As an alternative, self-compacting concrete investigated by ONDRAF/NIRAS (cf. [van Humbeeck 2007]) was suggested in [Verhoef 2014b].

Table 4-4 Suggested composition of concrete used for the OPERA supercontainer [Verhoef 2014b]

Component/Parameter	Type	
cement	CEM I/42.5 N HS LA (LH)	350 kg m^{-3}
water		175 kg m^{-3}
filler	Calcitec 2001 ME	50 kg m^{-3}
plasticiser	Glenium 27/20	4.41 kg m^{-3}
fine aggregate	limestone: 0-4 mm	708 kg m^{-3}
coarse aggregate	limestone: 2-6 mm	414 kg m^{-3}
coarse aggregate	limestone: 6-14 mm	191 kg m^{-3}
coarse aggregate	limestone: 6-20 mm	465 kg m^{-3}
w/c-ratio		0.50

N usual initial strength, HS High Sulphate resistance, LA Low Alkali content, (LH Low Hydration heat)

After the emplacement of the waste packages in the disposal drifts, the tunnels are backfilled with grout to fill the voids between the gallery lining and emplaced waste packages and hydraulically sealed off using a plug [Verhoef 2014a]. For simplicity it is presumed in OPERA that the type of backfill is independent of the type of emplaced waste, i.e. the same mortar is used as backfill in all waste sections of the disposal facility. Foam concrete made either with Portland cement (CEM I) or blast furnace slag cement (CEM III) and fine aggregates is proposed and investigated within OPERA for the backfill providing the enclosure of the emplaced waste packages (cf. [Verhoef 2014a, b]). The composition of the foam concrete for the backfill suggested in OPERA is given in Table 4-5 for two different densities [Verhoef 2014b].

Table 4-5 Suggested composition of the foam concrete used for the backfill in OPERA [Verhoef 2014b]

Component/Parameter	Type	Density 1200	Density 1600
cement	CEM I	360 kg m^{-3}	400 kg m^{-3}
water		140 kg m^{-3}	160 kg m^{-3}
foaming agent	TM 80/23 (synthetic)	1 kg m^{-3}	1 kg m^{-3}
water		21.3 kg m^{-3}	13.6 kg m^{-3}
fine aggregate	quartz sand: 0-4 mm	750 kg m^{-3}	1100 kg m^{-3}
w/c-ratio		0.45	0.43

4.2. Near field evolution

The long-term performance of a waste form in a deep geological repository cannot be assessed without an understanding of the conditions to which the material will be exposed. Besides intrinsic properties of the waste matrix (e.g. material composition, chemical and mechanical properties), the interaction with the disposal environment, i.e. the engineered barriers system and the geological environment, and the conditions prevailing in the near field affect the waste form durability and the radionuclide release. Near field factors substantially affecting the radionuclide source term for a waste form comprise hydrogeological (e.g. groundwater flow/exchange rates) and geochemical conditions (notably pH, redox potential, temperature, gas partial pressures, groundwater salinity/composition, microbial activity), which essentially depend on the repository design and the geological environment. In general after closure of the repository, the near-field will be influenced by a number of complex, inter-related processes such as (i) heat generation from the emplaced high-level wastes, (ii) resaturation of the repository, (iii) consumption of oxygen, (iv) gas generation due to corrosion, microbial degradation, and radiolysis of water and organic materials, (v) corrosion of waste containers, and (vi) the evolution/degradation of engineered barriers by interaction with the local groundwater (e.g. [Beattie 2012]). The extent and chronology of these processes will vary between different repository concepts [Beattie 2012].

The hydraulic conductivity of the host rock is important with respect to a variety of aspects related to the performance of the repository, e.g. the time required for the resaturation of the repository after closure, the mass transport to and from the disposal tunnels and waste containers (including the transport/flow of potentially deleterious groundwater constituents into the near field, and the transport of radionuclides released from the wastes into the far field), or the time frame for the leaching of cementitious backfill or buffer materials. Furthermore, the porosity and permeability affect the gas flow out of the near field (e.g. mode and rate of transport of H_2 generated by metal corrosion) and the potential for the formation of a separate gas phase in the repository. The composition of the groundwater in the surrounding host rock formation can affect the chemical conditions within the repository near-field as well as the degradation rates of cementitious barriers and the corrosion of metallic waste containers, due to the presence of potentially deleterious components (e.g. sulphate and magnesium with respect to cement degradation; sulphides and chloride with respect to metal corrosion, etc.) in elevated concentrations.

Although the properties of the Boom Clay and the groundwater composition at a potential repository site in Boom Clay in the Netherlands cannot be defined in detail at this time due to the inherent variability of the Boom Clay formation throughout the Netherlands (i.e. no

"reference" conditions are available), the general evolution of the repository near-field and the expected overall conditions relevant to the performance of the disposed high level wastes can be constrained to a certain degree. Section 4.2.1 discusses the probable evolution of pH and pore water composition in the near-field of the HLW-section of the OPERA disposal facility resulting from the interaction between the cementitious barriers and the Boom Clay groundwater. The expected evolution of the redox conditions in the repository near-field is addressed in section 4.2.2. Section 4.2.3 summarises the main conclusions regarding the near-field evolution relevant to the long-term behaviour of high-level radioactive wastes to be disposed in the Netherlands.

4.2.1. Evolution of pH and pore water composition in the HLW section

Within the OPERA disposal concept, cementitious materials are the main constituents of the near-field in the planned repository, e.g. in the supercontainer buffer, the backfill and the gallery linings (cf. section 4.1). The chemical and physical conditions in the repository near-field will thus been determined by the large amounts of hydrated cements for long periods of time (e.g. [Berner 1992], [Atkins 1992], [Glasser 2011], [Drace 2013]). The degradation of the engineered barriers and the evolution of the geochemical conditions will occur due to the disequilibrium between the chemical conditions in the cementitious materials and the groundwater infiltrating into the near-field (cf. [Wieland 2001]), and the cementitious materials will be leached in order to adjust the geochemical conditions in the near field to the groundwater conditions in the long-term.

The cementitious materials in the EBS will contain a number of hydrated cement phases, with the exact mineral assemblage depending on the cement formulation, curing time and temperature. The evolution of the cementitious materials, pore water pH and chemistry in the repository near field under leaching conditions in the post-closure phase is commonly described by various stages, defined by different pH ranges in the pore water and associated buffering phases (cf. [Atkins 1992], [Glasser 2011], [Drace 2013]). In addition to the changes in the chemical conditions and the pH buffering capacity due to the sacrificial dissolution of the hydrated cement phases, also the physical/hydraulic properties (porosity, permeability, and tortuosity) of the cementitious barrier materials are affected (cf. [Drace 2013]).

Initially, the main components of the cementitous materials are expected to be calcium-silica-hydrate (CSH) gels, portlandite ($Ca(OH)_2$), hydrated calcium aluminates, and alkali (i.e. Na, K) hydroxides/sulphates (e.g. [Glasser 2011], [Hoch 2012]). In stage I, the initial cement pore water composition is dominated by the dissolution of the alkali hydroxides (NaOH and KOH) that will condition the pore water to a high pH (i.e. pH >13) (cf. [Wieland 2002], [Glasser 2011]). As groundwater gradually replaces the initial pore water, in stage II the chemistry will be dominated by the dissolution of portlandite, which will maintain a pH of about 12.5 in the pore water. After portlandite depletion, in stage III the pH will be buffered in the range between 10 and 12 by the incongruent dissolution of CSH-phases (i.e. preferential release of calcium), lowering the Ca/Si-ratio over time and reducing the pH value at which the pore water is buffered (e.g. [Berner 1988], [Harris 2002], [Glasser 2011]). The formation of secondary minerals (e.g. calcite, brucite, hydrogarnet, ettringite, and/or hydrotalcite) may occur due to reactions between groundwater constituents and cement phases [Hoch 2012]. After complete depletion of the CSH, the pore water composition and pH can be controlled by secondary phases such as calcite (e.g. [Wang 2013a]) and the pH can continue to decrease to a value buffered by the groundwater in the host rock formation (e.g. [Krupka 1998], [Glasser 2011], [Drace 2013]).

The duration of the different stages and the timescales of pore-water evolution depend on various factors, including the pore volume of the cementitious materials and the connectivity of pore spaces, the hydraulic conductivity of the host rock and the hydraulic

potentials, and the groundwater composition and the concentration of potentially deleterious components (e.g. magnesium and sulphate). Generally it is expected to take thousands to tens of thousands of years until the pH of the cement pore water decreases to values below pH 10 and approaches the pH of the contacting groundwater. In general, a diffusion controlled system, such as in a clay host rock, is expected to maximise the duration of the high pH period [NAGRA 2002]. Simulations performed for the Belgian supercontainer concept indicate that highly alkaline conditions with a pH above 12.5 remain for at least 80,000 years (cf. [Wickham 2008], [Wang 2009a]). [Diomidis 2014] expected highly alkaline conditions to prevail for a considerably longer period of time in the near field of a Swiss L/ILW repository due to larger amounts of cementitious materials in the caverns and thus higher availability of alkalis and portlandite. According to [Wersin 2003], stage II (portlandite stage, pH 12.5) will persist over very long time periods (many hundred thousand to millions of years) in a cementitious repository in Opalinus Clay, due to the very low water exchange rate. Calculations made for the geological disposal programme in the UK indicated a pH above 12.5 for over 100,000 years and a pH above 10.5 for over a million years in a cementitious repository [Kursten 2004].

Based on scoping calculations of the near field evolution in concrete in contact with Boom Clay ground water for a repository according to the supercontainer concept in Boom Clay in Mol, Belgium [Wang 2009a], [Lemmens 2012] described the evolution of the concrete pore water with a decrease from pH 13.5 (young cement water) to 12.5 (evolved cement water) and further to about pH 12 (old cement water). [Lemmens 2012] expected the first two stages (pH 13.5 to 12.5) to last up to several 10^5 years, due to the expected slow transport by diffusion. Figure 4-1 depicts the expected evolution of the pH at the interface between cement and Boom Clay. The simulated cement pore water compositions are provided in Table 4-6 ([Wang 2009a], [Ferrand 2013]). For comparison, the expected cement pore water compositions resulting from the interaction between Opalinus Clay pore water and cementitious materials in a proposed LILW repository in Switzerland are provided in Appendix 2.

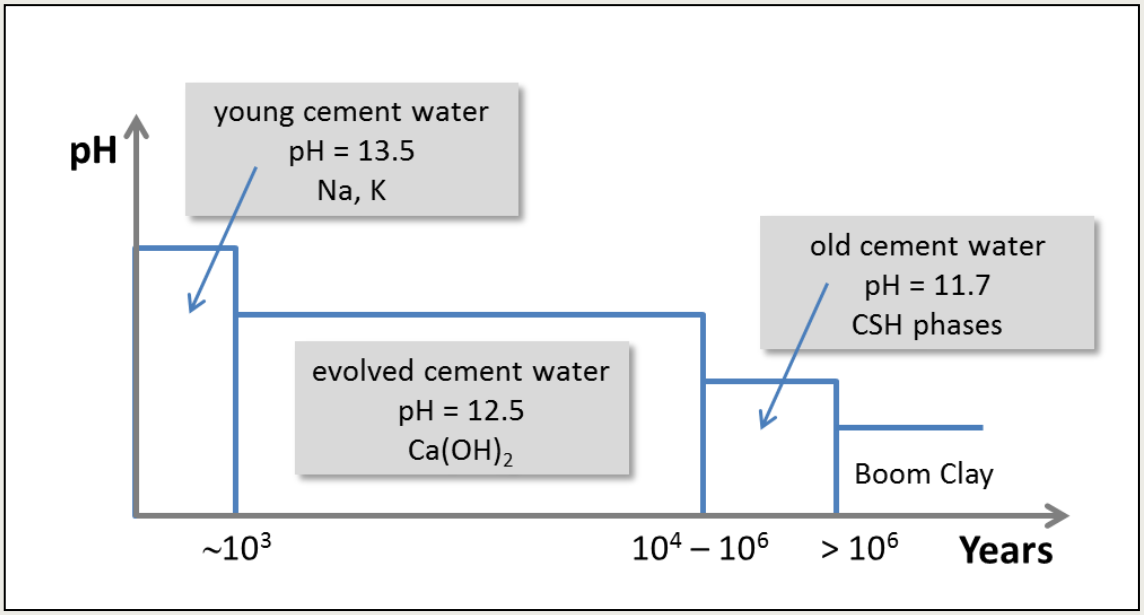

Figure 4-1 **Evolution of the pH in the pore water at the interface between cement and Boom Clay (modified after [Ferrand 2013])**

Table 4-6 Simulated pore water composition in the near-field concrete of a cementitious repository in Boom Clay in Mol (adapted from [Wang 2009a], [Ferrand 2013] and [Cachoir 2015]; Boom Clay pore water from [De Craen 2004]) – concentrations in mmol L^{-1})

	Young cement water	Evolved cement water	Old cement water	Boom Clay pore water
pH	13.5	12.5	11.7	8.5
Eh	~-800 mV	~-800 mV	~-800 mV	-274 mV
Na	141	15.1	15.1	15.6
K	367	0.2	0.2	0.2
Ca	0.7	15.3	0.8	0.05
Mg	$\sim 10^{-7}$	$\sim 10^{-7}$	$\sim 4 \cdot 10^{-6}$	0.06
Si	$3 \cdot 10^{-4}$	$3 \cdot 10^{-6}$	$8 \cdot 10^{-4}$	0.1
Al	0.06	0.005	9.4	$2.4 \cdot 10^{-5}$
CO_3^{-2}	0.3	0.008	0.02	14.4
Cl^-	0.2 … 12	0.2	0.2	0.7
SO_4^{2-}	2	0.007	0.05	0.02

Within OPERA, the evolution of the near-field conditions (e.g. regarding water saturation of the repository components, temperature evolution, and pH conditions) in the HLW/SF-section of the OPERA disposal facility have been addressed by [Kursten 2015] and [Seetharam 2015]. The timescale of resaturation of the repository is mainly dependent on the unsaturated hydraulic properties of the EBS materials and the Boom Clay, the porosity/permeability of the cementitious materials, the hydraulic conductivity of the Boom Clay and the hydraulic gradient (cf. [Wickham 2008]). The calculations of [Kursten 2015] indicate that the concrete buffer of the supercontainer becomes fully water saturated soon after the disposal tunnels are backfilled (i.e. in less than 10 years). However, these calculations were performed without the presence of a stainless steel envelope. One of the main reasons being that it is very difficult to simulate water transport through a single hole, since the envelope will be fabricated from stainless steel, which, under repository conditions, will mainly be susceptible to localized corrosion (e.g. high chloride concentrations could lead to pitting corrosion) [Kursten 2016]. Thus the time frame of resaturation of the supercontainer concrete and thus the arrival of deleterious species at the carbon steel overpack will depend on the lifetime and failure mechanisms of the steel envelope.

Simulations of the temperature evolution in the OPERA disposal facility for the disposal of vitrified HLW show that the surface temperature of the respective supercontainers will not exceed 40 °C, due to the 100 years cooling time of the HLW prior to disposal [Kursten 2015]. The temperature at the surface of the overpack in the simulations reached a peak temperature of 50 °C after about 10 years that decreased to below 30 °C after 100 years [Kursten 2015].

Scoping calculations of the pH evolution in the cementitious pore water of the concrete buffer at the interface to the carbon steel overpack indicate a decrease of the initial pH (13.5, controlled by the dissolved alkalis) to a minimum value of 12.14 after 9 years when temperature reaches its peak value of 50 °C. It is expected that high pH conditions (i.e. pH 13.5) will be resumed in the concrete after the short thermal phase [Kursten 2015]. The further long-term evolution of the pH under isothermal conditions at ambient temperature is shown in Figure 4-2. Conditions with pH ~13.5 will prevail up to about 1,000 years until the concrete buffer gets depleted in Na- and K-hydroxides [Kursten 2015]. Afterwards, the

pH will be determined by portlandite dissolution at about 12.5; this pH is predicted to persist for at least 80,000 years after which it will drop to a value of about 11.3 [Kursten 2015]. The predicted pH evolution is very conservative due to the neglect of (i) pore clogging in the cementitious materials due to calcite precipitation, and (ii) transport limitations in the Boom Clay. Thus it is expected that a pH of 12.5 could be maintained in the concrete buffer for much longer time spans than 80,000 years [Kursten 2015].

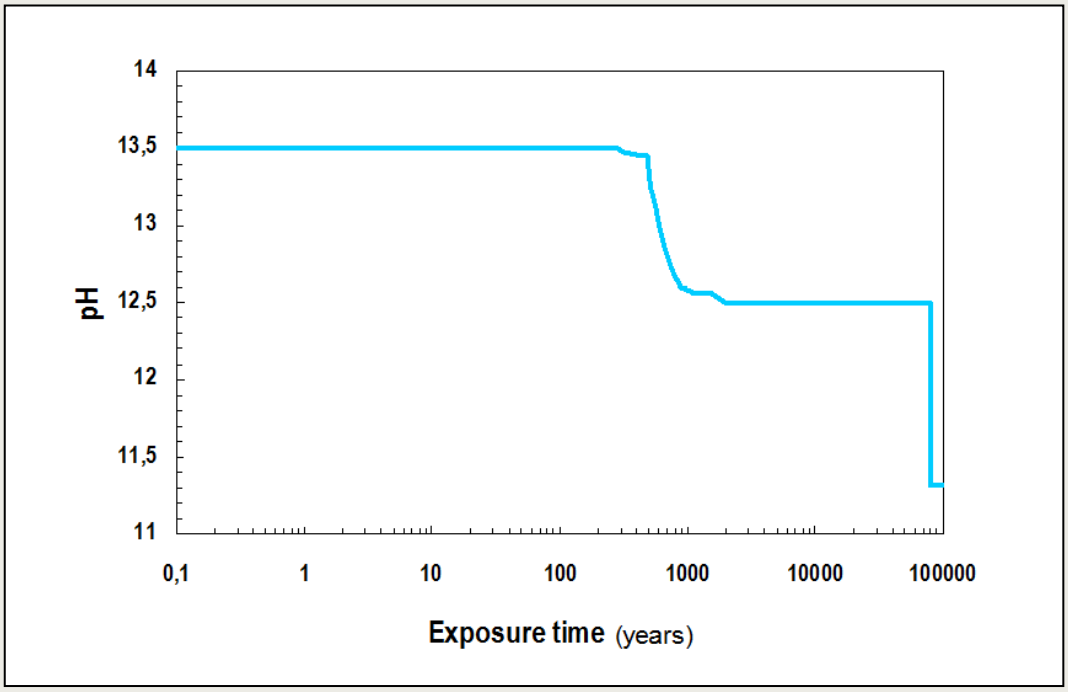

Figure 4-2 **Long-term evolution of the pH in the pore water at the cement/overpack interface of the supercontainer as function of time after repository closure [Kursten 2015]**

4.2.2. Evolution of redox conditions

The presence of oxygen plays a paramount role with respect to the evolution of the redox conditions in the repository in the post-closure phase. Initially after operation and closure of the disposal facility, some oxygen will be trapped in voids in the excavation-disturbed zone and in pores in the buffer/backfill materials, leading to aerobic conditions during resaturation. However, the oxygen remaining after closure will be consumed comparatively fast by a number of processes, such as corrosion of metallic canister materials, oxidation of ferrous iron bearing minerals and sulphides present in the host rocks, reaction with organic matter, and aerobic microbial respiration or other mechanisms (e.g. [Diomidis 2014]). Thus after an initial aerobic phase, anoxic conditions will prevail in the repository near field that are expected to persist indefinitely (cf. [Diomidis 2014], [Kursten 2015]). The duration of the aerobic phase depends on the amount of oxygen present and the rates of the oxygen consuming reactions [Neall 1994]. In general, the rates of oxygen consumption and metal corrosion are strongly dependent on the water saturation which itself depends on the temperature and the hydraulic properties of the host rock formation and the cementitious materials (cf. [Wersin 2003]). The generation of H_2 due to anoxic corrosion of container materials or other metals present can further enhance the reducing conditions in the repository, depending on the nature of the metals and their anoxic corrosion rates.

According to [Diomidis 2014], during the initial oxic phase in which oxygen is still available, a redox potential in the range of 200 mV can be expected. Once oxygen is consumed the only available oxidant is water, and thus a redox potential as low as -750 mV vs. SHE is expected in highly alkaline environments (cf. [Smart 2004], [Diomidis 2014]). The redox conditions will be influenced by various reactions occurring between dissolved and solid redox-active species under cementitious conditions (e.g. [Wersin 2003]). Due to the amounts of iron/steel in the repository environment and the ease of electron transfer between Fe(II) and Fe(III) compared to other redox couples, it is mainly assumed that iron phases control redox conditions in the repository near-field (cf. [Wersin 2003] and references therein, e.g. [Jobe 1997], [King 2000]).

[Berner 2003] estimated the redox conditions in the reference pore water of a cementitious LILW repository in the Opalinus Clay in Switzerland. A possible range of redox conditions was estimated for different combinations of iron bearing solids (including sulphides), assuming that the redox conditions are generally defined by the Fe^{2+}/Fe^{3+}-couple and magnetite is the major corrosion product in equilibrium with the cementitious pore fluid. The calculations based on these assumptions resulted in redox potentials ranging from -750 to -230°mV at a pH of 12.55. For an initial stage pore water at pH ~13.4, a redox potential of -430 mV was calculated [Berner 2003].

More recently, [Berner 2014] derived a pore solution composition for radionuclide solubility calculations in the repository environment based on the equilibration of a cement/ concrete system with Opalinus Clay water for 10,000 years due to diffusion processes. The redox potential of the system of about -500 mV was calculated from the thermodynamic equilibrium with Fe-monocarbonate ($Ca_4Fe^{III}_2(CO_3)(OH)_{12}(H_2O)_5$), Fe-ettringite ($Ca_6Fe^{III}_2(SO_4)_3(OH)_{12}(H_2O)_{26}$), Fe-hydrotalcite ($(MgO)_4Fe^{III}_2O_3(H_2O)_{10}$) and hydrous magnetite ($Fe_3O_4x2H_2O$) [Berner 2014].

[Wang 2009a] performed scoping calculations of the geochemical evolution in the cementitious repository near-field relevant for the Belgian supercontainer concept, taking into account the reference pore water composition in the Boom Clay at Mol, Belgium. Depending on the dominant corrosion products of the metallic barriers under anaerobic conditions, i.e. either magnetite or $Fe(OH)_2$, redox potentials were estimated at the surface of the metallic barriers (cf. Table 4-7). The redox potentials are assumed to be around or below -800 mV as long as some uncorroded iron/steel remains [Wang 2009a]. [Wang 2009a] expected this phase to be followed by the establishment of redox conditions controlled by the E_H of the in-diffusing Boom Clay pore water at about -300 mV.

Table 4-7 Estimated redox conditions in the cementitious near-field of a HLW-repository in Boom Clay in Mol as function of dominant metal corrosion products and pH in the presence of uncorroded metals (after [Wang 2009a])

Corrosion product	pH	Redox potential
Magnetite (Fe_3O_4)	13.5	-884 mV
	12.5	-825 mV
$Fe(OH)_2$	13.5	-850 mV
	12.5	-800 mV

More recently within the context of radionuclide solubilities in the pore water of the supercontainer buffer concrete, [Wang 2013a] discussed again the redox conditions in the different stages of cement degradation in a deep geological repository for HLW in Boom Clay in Belgium. Based on the approach of [Wersin 2003], three different mechanisms were proposed that could control the redox conditions in the cementious system:

(1) the dissolved iron concentration is controlled by iron-cement interactions resulting in a total dissolved iron concentration of 10^{-7} mol kg^{-1} in equilibrium with magnetite as corrosion product;
(2) the dissolved iron concentration is controlled by the solubility of iron oxihydroxides ($Fe(OH)_3$) and magnetite is one of the corrosion products;
(3) the dissolved iron concentration is controlled by the solubility of goethite (FeOOH) and magnetite is one of the corrosion products.
The redox potentials calculated using the NAGRA/PSI 01/01 thermodynamic database [Hummel 2002] ranged between -90 to -800 mV in stage I (pH 13.5) and between -30 and -741 mV in stage II (pH 12.5) [Wang 2013a], depending on the mechanism controlling the total dissolved iron concentration in the cementitious pore water. Moreover it was noted by [Wang 2013a] that distinctively different redox potentials were calculated when using the ANDRA Thermochimie v7b database [Giffaut 2014] instead of the NAGRA/PSI database. [Wang 2013a] concluded that an accurate estimation of the redox potential in the engineered barrier system is difficult due to the uncertainties regarding the mechanisms controlling the redox conditions and the thermodynamic data, but in general the redox potential in the near field of the supercontainer is expected to be reducing.

4.2.3. Résumé

Although representative ("reference") conditions regarding the hydraulic properties and the pore water composition of the Boom Clay for the generic OPERA disposal facility are not available yet (cf. [Seetharam 2015]), the overall evolutionary pathway for the near-field conditions can be described, in which conditions gradually evolve from unsaturated to water saturated and from aerobic to anaerobic/reducing. After a fast resaturation of the system within a few years after closure and a brief thermal phase with peak temperatures not exceeding 50 °C at the cement/overpack interface of the supercontainer, the repository near-field will further evolve under ambient conditions [Kursten 2015]. The chemical evolution of the repository system will be characterised − on the timescale of thousands to hundred thousands of years − by the continuous interaction of the cementitious near-field materials with the Boom Clay pore water and the accompanying mineralogical changes that will buffer the pH to values >12 under anoxic/reducing conditions. The time frame for saturation of the supercontainer concrete will depend on the lifetime and failure mode of the stainless steel envelope, but starting with the failure of the envelope, a similar chemical evolution in the concrete in the supercontainer buffer as in the other cementitious materials (i.e. long-lasting anoxic/reducing conditions at high pH) can be expected.

5. Corrosion of RRSF in the repository environment

The corrosion of plate type RRSF in the repository environment after failure of the waste container when coming in contact with the near-field water can be divided into two steps:

(i) corrosion of the aluminium cladding, followed by

(ii) corrosion of the fuel meat, which contains the vast majority of the radionuclide inventory, after cladding failure.

In the following sections corrosion mechanisms and corrosion rate data relevant to the behaviour of RRSF under conditions relevant to geological disposal are discussed, focusing on corrosion under (highly) alkaline conditions (cf. section 4.2). Section 5.1 addresses the corrosion of aluminium in general, whereas available information and data on the corrosion of RRSF are discussed in Section 5.2.

5.1. Corrosion of aluminium under alkaline conditions

Aluminium is a reactive metal since it is not thermodynamically stable in water, but is nominally passive in the pH range of ~4 to 9 due to the presence of protective oxide and hydroxide films that develop on its surface (cf. [Pourbaix 1974], [Sukiman 2013]). Under conditions deviating from the near neutral range, the continuity of this film can be disrupted due to the higher solubility of aluminium oxides/hydroxides under acidic and alkaline conditions, facilitating the dissolution of aluminium and its alloys. The overall corrosion behaviour of aluminium based on thermodynamic principles can be summarised by Pourbaix diagrams showing the stability of aluminium as a function of pH and potential, and indicating the regions of corrosion, immunity and passivation (cf. Figure 5-1).

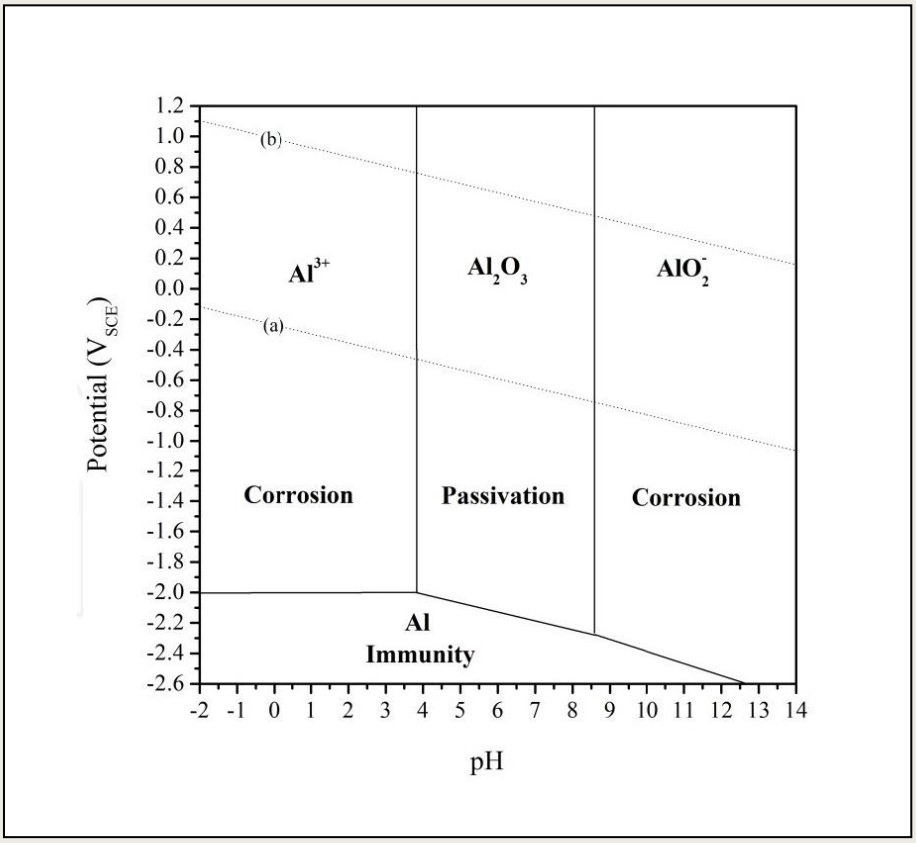

Figure 5-1 **E-pH diagram for pure aluminium at 25 °C in aqueous solution (adapted from [Pourbaix 1974] and [Sukiman 2013]); lines (a) and (b) denote the lower and upper stability of water**

Factors not considered in this approach are (i) presence of alloying elements, (ii) solution composition, for example the presence of chloride ions, (iii) temperature, (iv) the mode of corrosion, and (v) reaction kinetics [Sukiman 2013]. An extended potential vs. pH diagram provided by [Gimenez 1981] (cf. Figure 5-2), indicates that localised corrosion is also possible in the supposedly passive region, and that uniform corrosion (general corrosion) is generally the preferential corrosion mode under more alkaline conditions (cf. [Sukiman 2013]). In general, possible types of aluminium corrosion comprise uniform corrosion, galvanic corrosion, crevice corrosions, pitting corrosion, and stress corrosion cracking, although only the first two types are deemed relevant with respect to the behaviour of aluminium under cementitious repository conditions [Carlsson 2014].

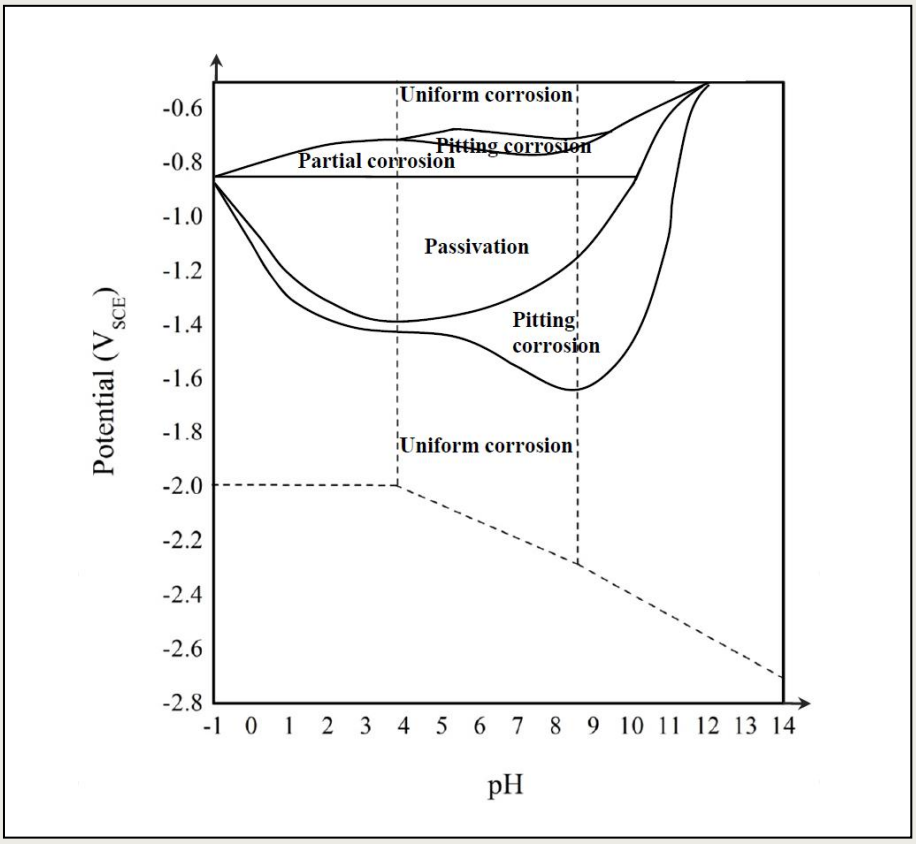

Figure 5-2 **Modes of aluminium corrosion based on experimental data for AA5086 in aqueous solutions containing 0.5 M NaCl at 20 °C (adapted from [Gimenez 1981] and [Sukiman 2013])**

The solubility and corrosion of aluminium in an aqueous environment are closely connected to the pH of the water phase. The anodic dissolution reaction of aluminium in water can be described as:

$$Al_{(s)} \rightarrow Al^{3+} + 3e^-$$

Under alkaline conditions, the cathodic reaction to balance the anodic aluminium dissolution is predominately the reduction of water associated with the production of hydrogen gas:

$$3H_2O + 3e^- \rightarrow 3OH^- + 3/2\ H_2$$

although the corrosion reaction of aluminium can also simultaneously be balanced by reduction of oxygen [Hoch 2010]:

$$O_2 + 2H_2O + 4e^- \rightarrow 4OH^-$$

In alkaline conditions, the dissolved Al^{3+} ion will react with the hydroxyl ions to form dissolved $Al(OH)_4^-$ leading to the overall corrosion reaction (cf. [Höglund 1991], [Armstrong 1996], [Zhang 2009]):

$$Al_{(s)} + OH^- + 3H_2O \rightarrow Al(OH)_4^- + 3/2\ H_2$$

The reaction is highly exothermic (i.e. heat producing) with ΔH°_r = -413.3 kJ mol^{-1} of aluminium).

The corrosion rates of aluminium have been addressed by various experimental approaches such as measurements of weight loss, H_2-gas evolution, and/or oxide layer formation or electrochemical techniques. An extensive review of available corrosion rate data for aluminium in alkaline solutions and under cementitious conditions is provided by [Hoch 2010]. Table A-5 in Appendix 3 summarises corrosion rate data obtained in alkaline and cementitious environments by various methods. In general in the alkaline region, the corrosion rates of aluminium increase at increased pH due to the increased solubility of its oxides and hydroxides (e.g. [Zhang 2009], [Diomidis 2014]).

5.1.1. Corrosion rates in alkaline solutions

The pore water in a cementitious near-field is dominated by KOH, NaOH and $Ca(OH)_2$, depending on the age of the system and the extent of interaction with groundwaters and their composition and properties (cf. chapter 4.2). The corrosion rate of aluminium is at a minimum at around pH 6, corresponding to a minimum in the solubility of the protecting aluminium (hydro)oxide layers (e.g. [Pourbaix 1974], [Vujičic 1985]). In sodium and potassium hydroxide solutions, corrosion rates increase with increasing pH as expected and, at a given pH, increase with temperature (e.g. [Vujičic 1985], [Tabarize 1991]). According to [Straumanis 1949a,b] corrosion rates are higher in NaOH than in KOH. The presence of chloride ions does not affect the general corrosion rate of aluminium in sodium, potassium, or calcium hydroxide solutions significantly, although it does increase the risk of pitting corrosion (e.g. [Takatani 1982], [Hoch 2010]). In alkaline sodium (or potassium) hydroxide solutions, the initial high corrosion rates only slightly decrease with time due to the solubility of the corrosion products [Hoch 2010]. [Tabrizi 1991] found a decrease in corrosion rates in sodium hydroxide solutions at pH 11 and 30 °C from 110 µm a^{-1} at 20 days, via 100 µm a^{-1} at 40 days to about 33 µm a^{-1} after 80 days exposure time. At pH 12 and 30 °C, the corrosion rate was about 530 µm a^{-1} after 20 days exposure. According to [Hoch 2010] the corrosion product in alkali metal hydroxide solutions below pH 12 initially consists of an aluminium hydroxide gel that ages to form boehmite (γ-AlO(OH)), pseudo-boehmite ($Al_2O_3 \cdot xH_2O$ (1<x<2)), bayerite (α-$Al(OH)_3$) and/or hydrargillite/gibbsite (γ-$Al(OH)_3$). The nature and composition of the corrosion products depend on solution composition, pH, temperature and exposure time. At pHs above 12, the corrosion product is too soluble to form a stable film [Hoch 2010], thus rather high corrosion rates sustain in the longer term at these pH-levels.

The corrosion of aluminium in calcium hydroxide solutions has been studied e.g. by [Takatani 1982, 1983] for a variety of aluminium alloys. Generally in calcium hydroxide solutions the corrosion rate decreases with time due to the formation of a (protective) layer of corrosion products, composed predominantly of aluminium hydroxides and calcium aluminates (c.f. [Straumanis 1949b], [Takatani 1982], [Takatani 1983], [Hoch 2010]). The corrosion rate of aluminium alloys decreases in the order Al-Mg-Si >> Al-Zn > Al-Mg ~ Al > Al-Mn > Al-Cu. (e.g. [Takatani 1982], [Takatani 1983]). Experimental data on aluminium corrosion rates in pore fluids extracted from various cementitious grouts, simulated OPC pore water and saturated $Ca(OH)_2$ solutions reviewed by [Hoch 2010] showed the expected

increase in the corrosion rate in alkaline conditions with increasing pH, leading to higher corrosion rates in OPC pore waters than in PFA/OPC and BFS/OPC pore solutions or saturated $Ca(OH)_2$ solutions. Corrosion products formed on aluminium in the presence of $Ca(OH)_2$ or cement comprise aluminium hydroxides (e.g. gibbsite or bayerite [Fujisawa 1997], [Setiadi 2006]), and various calcium aluminates such as $3CaO{\cdot}Al_2O_3{\cdot}xH_2O$ ($8<x<12$) and $6CaO{\cdot}Al_2O_3{\cdot}3SO_3{\cdot}32H_2O$ [Hoch 2010]. In addition, the formation of strätlingite ($2CaO{\cdot}Al_2O_3{\cdot}SiO_2{\cdot}8H_2O$) was observed on aluminium encapsulated in blast furnace slag (BFS) composite cements ([Setiadi 2006] [Kinoshita 2013]). [Fujisawa 1997] demonstrated the importance of the corrosion product layer with respect to the decrease in corrosion rates with time in cementitious conditions. In an experimental setup where the corrosion products could not adhere to the aluminium surface, only slightly decreasing corrosion rates of 10,200 µm a^{-1} (day 1), 7,400 µm a^{-1} (day 4) and 6,700 µm a^{-1} (day 40) with time were derived in mortar equilibrated water (pH ~12) at 15 °C.

5.1.2. Corrosion rates in cementitious media

A number of studies have been performed within the nuclear industry with respect to the effect of aluminium corrosion on waste encapsulation grouts and on the integrity of waste forms. [Hoch 2010] reviewed various not publicly available studies on the encapsulation of aluminium in grouts performed in the UK, including, inter alia, OPC, 9:1 BFS/OPC, 3:1 BFS/OPC, and PFA/OPC grouts. Most of these studies, using mainly hydrogen evolution measurements and electrochemical techniques for the determination of aluminium corrosion rates, were relatively short-term experiments performed for periods of less than 150 days. In general, a strong decrease of the very high initial corrosion rates (1,000 to 22,000 µm a^{-1} in the first day) to rates of the order of some 10 µm a^{-1} or below after about 1,000 to 2,000 hours was observed in most systems. The highest longer-term corrosion rates were generally observed in OPC-based systems. In a longer-term study on aluminium corrosion in 3:1 BFS/OPC, 9:1 BFS/OPC and 3:1 PFA/OPC grouts lasting for 667 days, the high initial corrosion rates (1,000 to 13,000 µm a^{-1} in the first 30 hours) decreased with time to ~100 µm a^{-1} after 400 hours, ~10 µm a^{-1} after 900 to 1800 hours, 1–2 µm a^{-1} after 4000 to 5000 hours, and 0.1-0.5 µm a^{-1} after 16000 hours (667 days) [Hoch 2010]. Moreover, [Hoch 2010] concluded with respect to the corrosion of aluminium in grouts that (i) corrosion rates increase with the proportion of OPC in the grouts and are determined by water availability and the permeability of the grout, (ii) corrosion rates in simulated pore waters are higher than in grouts, possibly due to the limited supply of water in the grouts, and (iii) different aluminium alloys produce gas at different rates.

Similar results regarding the corrosion behaviour of aluminium in cementitious grouts were derived in experiments performed by [Fujisawa 1997] under anoxic conditions. Commercial pure aluminium (JIS A 1070) was placed in mortar equilibrated water (pH 12.6) in contact to pulverised mortar grains made from an OPC/sand mixture at 15 °C, to simulate disposal conditions in which aluminium is solidified with mortar. The corrosion rate was determined by the amount of evolved H_2. In the initial immersion period, aluminium corroded rapidly with a corrosion rate of 10 to 20 °mm a^{-1}, but the corrosion rate decreased with time to reach a constant level of 1 to 10 µm a^{-1} after 1000 hours [Fujisawa 1997]. Similar longer-term rates (i.e. at times > 1000 hours) were obtained in experiments using aluminium specimens solidified in mortar [Fujisawa 1997], although the initial corrosion rates were about an order of magnitude lower than in the experiments with the aluminium specimens in pulverised mortar. [Fujisawa 1997] attributed the reduction in the corrosion rates to the accumulation of corrosion products on the surface of the aluminium plates, namely in form of gibbsite. The same trends in the corrosion rates were observed by [Kinoshita 2013] who investigated the corrosion reactions of aluminium encapsulated in OPC, OPC/BFS and calcium aluminate cement (CAC) based systems. For aluminium embedded in a 3:1 BFS/OPC grout, the measured hydrogen evolution indicated a decrease in the aluminium corrosion rate from 2,250 µm a^{-1} (0 to 7 days) to 22 µm a^{-1} (7 to 28 days) [Kinoshita 2013].

5.1.3. Corrosion rates used in safety assessments

The corrosion rates of aluminium in cementitious environments and the associated generation of H_2-gas have been addressed and evaluated repeatedly within the context of safety assessments for geological repositories for radioactive wastes (cf. Table 5-1). [Prítrský 2006] expected a rapid corrosion of aluminium alloys in alkaline and anoxic repository environments with corrosion rates in the range of 1 to 10 mm a^{-1}. [Skagius 1999] evaluated the amounts of gas that can be generated in the waste packages and in the vaults in the planned SFL 3-5 repository for the disposal of long-lived low- and intermediate-level waste in Sweden. Regarding the H_2-generation from the corrosion of aluminium under alkaline conditions, a corrosion rate of 1 mm a^{-1} was adopted in this study, corresponding to typical rates quoted elsewhere (cf. [Savage 2002]). The amount of gas generated by corrosion of metals, microbial degradation and radiolytic decomposition of the wastes disposed in the SFR repository for low-level operational wastes from NPP in Sweden was estimated by [Moreno 2001]. The assumed aluminium corrosion rate of 1 mm a^{-1} for anoxic high pH conditions corresponded to corrosion of all aluminium in the waste material within a few years. Similar corrosion rates were derived in a status report from the European Commission on gas migration and two-phase flow in deep geological repositories [Rodwell 1999].

Table 5-1 Corrosion rates of aluminium under alkaline conditions adopted in the context of safety assessments for nuclear waste disposal

Repository	Country	Corrosion rate	Source
RU RAO Mochovce	Slovakia	1 … 10 mm a^{-1}	[Prítrský 2006]
SFL 3-5	Sweden	1 mm a^{-1}	[Skagius 1999]
SFR	Sweden	1 mm a^{-1}	[Moreno 2001]
SMA	Switzerland	1 mm a^{-1}	[Grogan 1992]
ILW	Switzerland	1 mm a^{-1}	[NAGRA 2004]
L/ILW	Switzerland	0.1 mm a^{-1}	[NAGRA 2008]
L/ILW	Switzerland	0.01 mm a^{-1}	[Diomidis 2014]
L/ILW	UK	15.3 mm a^{-1} *) 0.0245 mm a^{-1} **)	[Hoch 2010]

*) initial acute rate; **) chronic rate

Gas generation processes in a deep geological repository for radioactive wastes within the context of short-lived low and intermediate level waste (LILW) disposal in Switzerland according to the NAGRA SMA repository programme were examined by [Grogan 1992]. Based on earlier evaluations by [Wiborgh 1986], a corrosion rate of 1 mm a^{-1} was assumed for aluminium under cementitious conditions. The issue of how gas generation in and transport from waste repositories may influence the disposal system performance was further discussed in [NAGRA 2004] for a repository for spent fuel, vitrified high-level waste and long-lived intermediate-level waste sited in the Opalinus Clay in Switzerland. It was argued that the adopted aluminium corrosion rate of 1 mm a^{-1} under cementitious conditions might be an overestimate considering the data reported by [Fujisawa 1997]. However, since these results were dependent on preserving the (unstable) corrosion layer on the surface, and galvanic coupling with steel might occur in the waste containers, the corrosion rate of 1 mm a^{-1} was retained in [NAGRA 2004]. Moreover, effects of post-disposal gas generation in a repository for L/ILW in the Opalinus Clay of Northern Switzerland were assessed in [NAGRA 2008]. It was concluded that it is prudent to adopt a corrosion rate for aluminium of 0.1 mm a^{-1} as a rather pessimistic reference case rate that is about 3 to 10 times higher than experimentally measured steady-state values from [Fujisawa 1997] and [Smart 1998]. More recently, [Diomidis 2014] suggested a reference corrosion rate of

10 µm a^{-1} for aluminium under alkaline and anoxic conditions, based on expert judgment and the experimental data from [Fujisawa 1997] and [Smart 1998].

[Hoch 2010] compiled and reviewed data for corrosion rates of reactive metals present in the UK National Inventory of intermediate-level and certain low-level radioactive wastes to be used in gas generation modelling. The corrosion rate for aluminium in the modelling tool SMOGG (Simplified Model of Gas Generation) used in packaging proposal and safety assessment studies is specified as [Hoch 2010]:

$$\frac{ds}{dt} = -k_a e^{-\frac{t}{t_a}} f_a(T) - k_c e^{-\frac{t}{t_c}} f_c(T)$$

where s is the position of the surface of the aluminium [m], t the time of corrosion [a], k_a the initial acute corrosion rate (at a reference temperature T_{ref}, for which $f_a = 1$) [m a^{-1}], t_a a characteristic time for the acute corrosion [a], f_a a factor that specifies the dependence of the acute corrosion rate on temperature [-], T the temperature [K], k_c the initial chronic corrosion rate (defined at a reference temperature T_{ref}, for which $f_c = 1$) [m a^{-1}], t_c a characteristic time for the chronic corrosion [a], and f_c a factor that specifies the dependence of the chronic corrosion rate on temperature [-]. Based on a fit to experimental data, the following recommended parameters were derived for aluminium corrosion in an alkaline cementitious environment for use in SMOGG [Hoch 2010]:

- an initial acute corrosion rate of 15.3 mm a^{-1} independent of temperature,
- a characteristic time for the acute corrosion of 0.001 a (i.e. the initial acute corrosion rate drops to the chronic rate within about 3 days), and
- a (constant) chronic corrosion rate of 24.5 µm a^{-1} that is independent of temperature, oxygen and chloride concentrations [Hoch 2010].

5.2. Corrosion of RRSF under alkaline conditions

The corrosion of RRSF in aqueous environments under conditions relevant to geological disposal has not yet received widespread attention. Thus in contrast to LWR oxide fuels, information on the behaviour of spent dispersion type fuels from research reactors under repository conditions is rather sparse. Many uranium alloys, for example with niobium, molybdenum, silicon or zirconium, can trace their history back to work performed during the 1940s and 1950s, within the development of corrosion resistant metallic fuels for nuclear (power) reactors (cf. [Lillard 2005]). Moreover, pure metallic uranium has also been used in reactors by roll cladding with aluminium (e.g. [Howe 1956]). Therefore also the corrosion resistance of uranium-aluminium alloys was studied to some degree in the 1950s, often by boiling water corrosion tests or with superheated steam (e.g. [Waber 1952], [Whirtler 1952]). Based mainly on tests in distilled water and at elevated temperatures it was concluded at that time that the general corrosion of high-aluminium uranium alloys is similar to that of pure aluminium, and that uranium alloys containing silicon were somewhat more corrosion resistant than pure metallic uranium, especially alloys containing more than 16 at.% of silicon.

With respect to the corrosion of uranium aluminide fuels, [Kaminski 2002] proposed the following mechanism in dry air (cf. also [Openshaw 1964]):

$$UAl_x + O_2 \rightarrow UO_2 + xAl$$

and a reaction mechanism similar to the corrosion of metallic aluminium and uranium in the presence of water:

$$UAl_x + (1.5x + 2 + n)\ H_2O \rightarrow UO_2 + (1.5x + 2)\ H_2 + (0.5x\ Al_2O_3)\ n\ H_2O.$$

Under oxidising conditions a rapid oxidation of UO_2 to (dissolved) uranyl species was expected by [Kaminski 2002], based also on the lack of UO_2 surface layers observed inter alia by [Openshaw 1964]. Based on the results of corrosion experiments under anoxic conditions, the formation of amorphous $U(OH)_4$ as solubility controlling uranium phase was proposed (cf. [Curtius 2011], [Curtius 2015]). Thus for alkaline and anoxic conditions, where the solubility of aluminium hydroxides is high (cf. section 5.1), the corrosion reaction can be described as:

$$UAl_x + (3x + 4)\ H_2O + xOH^- \rightarrow U(OH)_4 + (1.5x + 2)\ H_2 + xAl(OH)_4^-$$

where $U(OH)_4$ refers to the dissolved U^{IV} species as well as to an amorphous solid phase. An analogous reaction is proposed here for the corrosion of intermetallic uranium silicide fuels (e.g. U_3Si_2):

$$U_3Si_2 + 2OH^- + 18H_2O \rightarrow 3U(OH)_4 + 10H_2 + 2SiO(OH)_3^-$$

or alternatively, if an amorphous hydrous silica gel is formed:

$$U_3Si_2 + (16 + n)\ H_2O \rightarrow 3U(OH)_4 + 10H_2 + 2SiO_2\ n\ H_2O$$

The corrosion behaviour of metallic uranium fuels and various intermetallic fuels has been investigated and discussed in the United States throughout the last decades with respect to disposal conditions in the proposed national repository in Yucca Mountain, Nevada (e.g. [Wiersma 1998], [Gray 1998], [Lam 2000], [Kaminski 2001], [Kaminski 2002]). Investigations into the behaviour of aluminium-clad intermetallic research reactor fuels (UAl_x-Al and U_3Si_2-Al) under conditions relevant to deep geological disposal have been performed in Germany since the 1990s in particular at Research Centre Jülich (e.g. [Brodda 1995], [Fachinger 2000], [Mazeina 2003], [Brücher 2007], [Klinkenberg 2010], [Curtius 2011], [Curtius 2015]). The following sections summarise the main findings regarding the corrosion rates of uranium aluminide fuels (section 5.2.1) and uranium silicide fuels (section 5.2.2) as well as the observations on secondary phase formed during the corrosion process (section 5.2.3) relevant to the OPERA safety case. However, at present to our best knowledge, no information and data on the corrosion behaviour of RRSF under anoxic conditions representative for the highly alkaline, cementitious near-field to be expected in the OPERA disposal concept are available. Moreover, the findings on corrosion behaviour and reported corrosion rates are not always directly comparable and sometimes seemingly contradictory, due to the use of different sample materials and sample pre-treatment, and the broad range of rather different, often non-standardised experimental set-ups (e.g. static batch tests, single pass flow through tests, unsaturated drip tests, etc.) employed. In addition the available experimental data were obtained under highly variable conditions, for example with respect to temperature (ambient to several hundred °C), redox conditions (oxic vs. anoxic) and solution compositions (e.g. distilled water, different natural groundwaters and brines).

5.2.1. Aqueous corrosion of uranium aluminide fuels

The corrosion behaviour and long-term performance of Department of Energy (DOE) spent nuclear fuels (DSNF), including intermetallic aluminium-clad uranium aluminide fuels, has been addressed in several studies with respect to interim storage and conditions expected in a mined geologic disposal system.

Within the development of acceptance criteria for interim dry storage, [Sindelar 1996] evaluated the corrosion behaviour of dispersion fuels consisting of a mixture of 10 to 50 vol.% UAl_x particles (x = 3 or 4) within a matrix of commercial 1100 aluminium. The

reported corrosion rates in water at 290 °C (test duration 60 days) ranged from 0.53 to 0.94 g m^{-2} d^{-1} depending on the uranium content, and were about a factor 2 higher than those of an 8001 aluminium alloy at the same temperature. In contrast, the corrosion rates of 8001 aluminium and an aluminium-10 % uranium alloy at room temperature were found to be approximately similar (about 0.03 g m^{-2} d^{-1}). A similar conclusion was drawn in the parameter selection for the Yucca Mountain viability assessment by [Fillmore 1998], who assumed that the aluminium matrix and the enclosed uranium aluminide particles dissolve at about the same rate, which would be about one tenth of the rate for uranium metal.

Taking into account that U-Al-alloys are thermodynamically unstable in the presence of water and atmospheric oxygen to approximately the same degree as aluminium metal, [CRWMS M&O 1998a] assumed that the uranium aluminide fuel matrix would corrode at a rate resembling that for aluminium metal, leading in consequence to a rather rapid corrosion. With the assumed corrosion rate of 0.225 g m^{-2} d^{-1} [CRWMS M&O 1998b] for a water chemistry derived from the J-13 well water at Yucca Mountain reacting with degrading waste forms (pH 9 to 10, oxidising conditions), the aluminium fuel matrix would completely corrode within 10 years [CRWMS M&O 1998a].

[Lam 2000] tested the corrosion of aluminium-uranium alloys (10 and 18 wt.% uranium) due to exposure to saturated water vapour at 200 °C for up to about 12 weeks. The test data indicated that the corrosion rates of the aluminium-uranium materials at 100 % relative humidity were initially up to four times higher than those for commercial 1100 aluminium, but approached similar rates to 1100 aluminium at the end of the tests, presumably due to the formation of a passivating oxide layer. [Hilton 2000] critically evaluated the reaction kinetics of metallic uranium, various uranium alloys, and aluminium-based dispersion fuels with oxygen, water vapour, and water, based on a review of available literature data. The aspect of water-corrosion was limited to pure water, due to a lack of data on corrosion in (ground)waters relevant to the repository environment. Thus the processes and kinetics discussed were not directly applicable to corrosion rates of spent nuclear fuels under disposal conditions. According to [Hilton 2000], the reaction rate of UAl_x-Al with water is governed by the corrosion behaviour of the aluminium matrix, with the reaction rates of UAl_x-Al essentially the same as for aluminium alloys with water, which are much smaller than the reaction rates of metallic uranium with water. The reaction rates of UAl_x-Al alloys in saturated water vapour at 200 °C (0.05 to 0.19 g m^{-2} d^{-1}) were essentially the same as the reaction rates in pure water at similar temperatures (0.18 g m^{-2} d^{-1}), indicating that the oxidation rates of UAl_x-Al are equivalent for water and water vapour, just as the oxidation rates of metallic uranium [Hilton 2000]. The reaction rates of UAl_x-Al and aluminium alloys with water were found to depend moderately on temperature, increasing by a factor of ten between 200 and 350 °C [Hilton 2000].

Moreover, within the U.S. National Spent Nuclear Fuel Program, the behaviour of uranium aluminide fuels was investigated experimentally under conditions that might exist in the proposed repository at Yucca Mountain, Nevada. The various tests performed with unirradiated and irradiated fuels included static batch tests [Wiersma 1998], single pass flow through tests ([Wiersma 1998], [Gray 1998]) or unsaturated drip tests ([Kaminski 2001], [Kaminski 2002]) and employed mainly J-13 well water, a lowly mineralised (I = 0.003 mol L^{-1}), slightly alkaline (pH 8.5) Na-HCO_3-type water (cf. [Wiersma 1998]), or variants thereof. [Wiersma 1998] performed static batch tests with uranium-aluminium alloy samples (i.e. surrogates) submerged in variants of J-13 water at 25°C and 90 °C for up to one month. The dissolution of uranium at 90 °C was most severe in J-13 water adjusted to pH 11, followed by J-13 water adjusted to pH 3, followed by nominal J-13 water (relative dissolution rate ratio 5:2:1). Galvanic coupling with stainless steel produced the same trend but with higher corrosion rates ([Wiersma 1998], [Kaminski 2003]).

Dissolution rates of irradiated and partly decladded uranium aluminide fuels were determined by single-path flow through tests at 25 °C in J-13 well water and in bicarbonate solutions under oxidising conditions [Wiersma 1998]; similar test were performed with unirradiated uranium-aluminium alloys at 25°C and 90°C. The tests gave dissolution rates of about $0.2 \cdot 10^{-3}$ g U m^{-2} d^{-1} in J-13 well water and 22 to $33 \cdot 10^{-3}$ g U m^{-2} d^{-1} in bicarbonate solutions (20 mM $NaHCO_3$ at pH 8) based on the uranium release from the irradiated fuels (cf. [Gray 1998], [Bechtel 2004]). Dissolution rates in nitric acid (pH 3) were $28 \cdot 10^{-3}$ and $99 \cdot 10^{-3}$ g U m^{-2} d^{-1} for spent UAl_x-Al fuel and an irradiated U-Al-alloy, respectively. Similar tests on unirradiated uranium-aluminium alloys yielded dissolution rates of about $25 \cdot 10^{-3}$ g U m^{-2} d^{-1} at 90 °C in J-13 water. In J-13 water adjusted to pH 11 by NaOH, dissolution rates between $86 \cdot 10^{-3}$ g U m^{-2} d^{-1} and $250 \cdot 10^{-3}$ g U m^{-2} d^{-1} were determined for different U-Al-alloys, clearly emphasising the higher dissolution rates under alkaline conditions (cf. [INEEL 2003]).

Electrochemical corrosion tests on various unirradiated uranium-aluminium alloys revealed a negligible effect of the alloy composition on the corrosion rates [Wiersma 1998], [INEEL 2003]). The increase in temperature from 25 °C to 90 °C was found to have little effect, except for the corrosion rates in nominal J-13 water. The corrosion rates at 90 °C were roughly similar in nominal J-13 water and in J-13 water adjusted to pH 3, but about a factor 10 higher in J-13 water adjusted to pH 11 (cf. Table 5-2). The effect of solution composition was even more pronounced at 25 °C, with a slight increase of the corrosion rates under acidic conditions and an increase in the corrosion rates by a factor of more than 100 compared to J-13 water in the high pH solution.

Table 5-2 Corrosion rates of unirradiated uranium-aluminium alloys in J-13 water and variants thereof determined by electrochemical tests (recalculated after [Wiersma 1998] and [INEEL 2003])

Alloy	Temperature	J-13 - nominal (pH 8.4)	J-13 – low pH (pH 3)	J-13 - high pH (pH 11)
10 UAl	25 °C	25.4 µm a^{-1}	76.2 µm a^{-1}	1422 µm a^{-1}
13.2 UAl	25 °C	15.2 µm a^{-1}	2.5/ 53.3 µm a^{-1}	1524 µm a^{-1}
25 UAl	25 °C	12.7 µm a^{-1}	50.8 µm a^{-1}	1473 µm a^{-1}
10 UAl	90 °C	152.4 µm a^{-1}	57.2 µm a^{-1}	1270 µm a^{-1}
13.2 UAl	90 °C	86.4 µm a^{-1}	94.0 µm a^{-1}	1498 µm a^{-1}
25 UAl	90 °C	152.4 µm a^{-1}	88.9 µm a^{-1}	1270 µm a^{-1}

Moreover, [Kaminski 2002] investigated the corrosion of unirradiated UAl_x fuels by unsaturated intermittent drip tests with a modified J-13 well water at 90 °C for about 6 months under oxidising conditions. The release rates of uranium varied between 0.23 and $2.9 \cdot 10^{-3}$ g m^{-2} d^{-1} at pH 8.4 (average about $1 \cdot 10^{-3}$ g U m^{-2} d^{-1}), depending on the test specimen and test intervals. The release rates were found to be similar in magnitude to the release rates observed in flow-through tests with irradiated UAl_x-fuels [Kaminski 2003] (cf. Table 5-3).

Table 5-3 Uranium release rates from uranium-aluminide fuels under various test conditions using J-13 water relevant to the Yucca Mountain repository (modified after [Kaminski 2003])

Sample	Test	Temperature	Release rate	Source
U-Al-alloy	flow through	25 °C	1.7 … 2.2·10^{-3} g m^{-2} d^{-1}	[Wiersma 1998]
U-Al-alloy	flow through	90 °C	8 … 27·10^{-3} g m^{-2} d^{-1}	[Wiersma 1998]
UAl_x (irradiated)	flow through	25 °C	0.1 … 0.2·10^{-3} g m^{-2} d^{-1}	[Wiersma 1998]
UAl_x (irradiated)	flow through	90 °C	0.3 … 2·10^{-3} g m^{-2} d^{-1}	[Wiersma 1998]
UAl_x	drip	90 °C	0.2 … 2.9·10^{-3} g m^{-2} d^{-1}	[Kaminski 2002]

[Bechtel 2004] reviewed available data and information on the dissolution kinetics of various types of DOE owned spent nuclear fuels to abstract degradation models suitable for use in the Total System Performance Assessment for the license application for the Yucca Mountain repository. The derived best-estimate dissolution model for aluminium-based RRSF was based on the flow through experiments for irradiated UAl_x fuel in J-13 water from [Wiersma 1998], translating into a total matrix dissolution rate of 1.38·10^{-3} g metal m^{-2} d^{-1} at 25 °C and 13.8·10^{-3} g metal m^{-2} d^{-1} at 90 °C. A conservative model was derived from UAl_x dissolution data in $NaHCO_3$-solutions (cf. [Wiersma 1998]), providing a total matrix dissolution rate of 0.16 g metal m^{-2} d^{-1} and 1.6 g metal m^{-2} d^{-1} at 25 °C and 90 °C, respectively [Bechtel 2004]. As an upper limit release model, an instantaneous release of radionuclides upon exposure of the spent fuels to groundwater was assumed. Generally it was reasoned that the oxidation rate of the UAl_x is considered to be controlled by the oxidation of the aluminium metal matrix (cf. [Hilton 2000], [Bechtel 2004]).

The corrosion resistance of UAl_x-Al dispersion fuels has been studied in Germany since the 1990s with respect to the option of direct disposal of RRSF in a deep geological repository in salt formations. Static corrosion experiments performed with irradiated UAl_x-Al fuels from the FRJ-2 reactor in Jülich in $MgCl_2$-rich brines at 90 °C under oxic conditions, partly in presence of metallic waste container materials, revealed that (i) the aluminium cladding has no barrier function in contact with salt brines (ii) with respect to the time scales of long term safety assessments, the RRSF will dissolve immediately in the salt brines, (iii) the corrosion processes are accelerated in the presence of metallic additives, and (iv) radionuclides are mobilised from the RRSF, when the fuel meat becomes accessible to the brine, but parts of the released radionuclide inventory are retained in the secondary phases formed in the corrosion process (cf. [Brodda 1995], [Fachinger 1997], [Fachinger 2000]). In NaCl-rich brines the corrosion and the release of fission products proceeded at a significantly lower rate compared to Mg-rich brines [Fachinger 2000].

[Mazeina 2003a,b] performed static corrosion experiments with unirradiated UAl_x-Al fuel plates from the FRJ-2 reactor and aluminium cladding materials in different media ($MgCl_2$-brine, NaCl-brine and granite water) and partly with iron additives (Fe^0, Fe^{2+}) at 90 °C under anaerobic conditions, to get insight into corrosion mechanisms and to characterise the corrosion products formed. The highest integral corrosion rates were determined in the $MgCl_2$-brine with iron additives (2.6 g m^{-2} d^{-1}), leading to a complete corrosion of the fuel samples within 500 to 600 days [Mazeina 2003a]. The corrosion rates in NaCl-brines and especially in the lowly mineralised granitic water (Grimsel type) were found to be significantly lower (80·10^{-3} g m^{-2} d^{-1} and 2.7·10^{-3} g m^{-2} d^{-1}, respectively). In some cases, the overall corrosion rates of the unirradiated fuel plates exceeded those of aluminium cladding materials under similar conditions [Mazeina 2003b]. Distribution analysis of the corroded material performed at the end of the experiments in $MgCl_2$-brines showed that

more than 90% of the uranium and aluminium released from the corroded fuel elements precipitated in amorphous and crystalline secondary phases [Mazeina 2003a].

Further anaerobic corrosion experiments on unirradiated FRJ-2 fuel plates were performed in $MgCl_2$-brines, clay waters (Mont Terri type) and Äspö-type granitic waters at 90 °C in the presence of Fe^{2+} ions to simulate conditions in a corroding waste container for up to about one year (cf. [Curtius 2005], [Curtius 2006], [Brücher 2007], [Curtius 2010]). The UAl_x-Al fuel plates corroded entirely within this experimental time frame; the total dissolution was complete in $MgCl_2$-brines in about 100 days and required about 370 days in clay and granite waters, respectively. The corrosion rates for the UAl_x-Al fuels calculated by [Curtius 2010] ranged from $2.7 \cdot 10^{-3}$ g m^{-2} d^{-1} in granite and clay waters to $10.8 \cdot 10^{-3}$ g m^{-2} d^{-1} in the $MgCl_2$-rich brine. The inventory of the matrix elements uranium and aluminium determined in solution was less than 5% [Curtius 2010], i.e. the vast majority (> 95%) of these elements were retained in the secondary corrosion products.

Moreover, the corrosion behaviour of irradiated fuel plates from the FRJ-2 reactor were investigated in static corrosion experiments $MgCl_2$-rich brine, granitic waters (Äspö-type) and Mont-Terri type clay waters at 90 °C under anaerobic conditions and in the presence of Fe^{2+} ions for more than three years ([Curtius 2010], [Curtius 2011]). Under these experimental conditions, the fuels corroded completely within 3.5 years, and secondary alteration phases were formed. As expected, the highest corrosion rates for the irradiated UAl_x-Al fuels were observed in the $MgCl_2$-brines ($7.7 \cdot 10^{-3}$ g m^{-2} d^{-1}) whereas the corrosion rates in the granite and clay water were about $1.1 \cdot 10^{-3}$ g m^{-2} d^{-1} ([Curtius 2010], [Curtius 2011]). The secondary phases quantitatively retained the matrix elements uranium and aluminium as well as various radionuclides (e.g. Am, Eu), whereas the inventory of more mobile fission products (e.g. Sr, Cs) was found to be released completely in solution. Table 5-4 summarises the anoxic corrosion rates of UAl_x-Al dispersion fuels obtained in different solutions.

Table 5-4 Comparison of integral corrosion rates of uranium aluminide (UAl_x-Al) dispersion fuels at 90 °C under anoxic conditions determined in static corrosion tests in different test solution

Sample	Solution type	Corrosion rate	Source
UAl_x-Al (unirradiated)	brine ($MgCl_2$)	2.6 g m^{-2} d^{-1}	[Mazeina 2003b]
UAl_x-Al (unirradiated)	brine ($MgCl_2$)	$10.8 \cdot 10^{-3}$ g m^{-2} d^{-1}	[Curtius 2010]
UAl_x-Al (irradiated)	brine ($MgCl_2$)	$7.7 \cdot 10^{-3}$ g m^{-2} d^{-1}	[Curtius 2010]
UAl_x-Al (unirradiated)	brine (NaCl)	$80 \cdot 10^{-3}$ g m^{-2} d^{-1}	[Mazeina 2003b]
UAl_x-Al (unirradiated)	granitic (Grimsel)	$2.7 \cdot 10^{-3}$ g m^{-2} d^{-1}	[Mazeina 2003b]
UAl_x-Al (unirradiated)	granitic (Äspö)	$2.7 \cdot 10^{-3}$ g m^{-2} d^{-1}	[Curtius 2010]
UAl_x-Al (irradiated)	granitic (Äspö)	$1.1 \cdot 10^{-3}$ g m^{-2} d^{-1}	[Curtius 2010]
UAl_x-Al (unirradiated)	clay (Mont Terri)	$2.7 \cdot 10^{-3}$ g m^{-2} d^{-1}	[Curtius 2010]
UAl_x-Al (irradiated)	clay (Mont Terri)	$1.1 \cdot 10^{-3}$ g m^{-2} d^{-1}	[Curtius 2010]

5.2.2. Aqueous corrosion of uranium silicide fuels

Only very few studies are available concerning the corrosion behaviour of uranium silicide fuels in aqueous environments, none of them referring to the dissolution behaviour under highly alkaline or cementitious conditions. [Bourns 1968] and [Feraday 1971] performed corrosion tests on uranium silicide fuels (U_3Si) at elevated temperatures with steam (up to 550 °C) and water (up to 300 °C) within the frame of the development of new fuel types for power reactors. In the frame of criticality assessments for spent nuclear fuel disposal in the Yucca Mountain repository, it was assumed that the fuel matrix of uranium silicide

fuels would corrode at a rate similar to that of metallic aluminium, based on thermodynamic considerations on the stability of U-Al-Si alloys [CRWMS M&O 1998a]. For conditions expected in a failed waste container (pH 9 to 10 due to reaction of J-13 well water with degrading waste forms), a corrosion rate of 0.225 g m^{-2} d^{-1} identical to the corrosion rate for UAl_x-Al-fuels was assumed [CRWMS M&O 1998b] that in consequence would lead to complete corrosion of the aluminium fuel matrix within 10 years [CRWMS M&O 1998a]. Within the parameter selection for the Yucca Mountain viability assessment, it was also assumed that uranium silicide fuel particles would dissolve at about the same rate as the aluminium matrix of the dispersion fuels, which would be at about one tenth of the rate for metallic uranium [Fillmore 1998]. In this respect, [Fillmore 1998] assumed the corrosion behaviour of uranium silicide fuels to be similar to uranium aluminide fuels.

[Wiersma 1998] determined dissolution rates of irradiated and partly decladded U_3Si_2-Al fuels by single-path flow through tests at 25 °C in J-13 well water, sodium bicarbonate solution (20 mM $NaHCO_3$, pH 8), and nitric acid (pH 3) under oxidising conditions. The dissolution rates determined from the uranium release were similar in $NaHCO_3$ and HNO_3 solutions ($36 \cdot 10^{-3}$ g m^{-2} d^{-1}) and distinctively lower in J-13 water ($0.22 \cdot 10^{-3}$ g m^{-2} d^{-1}), with the latter value similar to the rates derived for irradiated uranium aluminide fuels under the same experimental conditions (cf. [Wiersma 1998], [Gray 1998], [INEEL 2003]). Consequently, in the abstraction of waste form degradation models suitable for the performance assessment for the Yucca Mountain repository, the dissolution models derived for uranium aluminide fuels were also applied to describe the corrosion behaviour of other aluminium based fuels like uranium silicide fuels in the repository environment [Bechtel 2004].

Static corrosion experiments with unirradiated U_3Si_2-Al dispersion fuels were performed at the Forschungszentrum Jülich in $MgCl_2$-rich brines, clay pore waters (Mont-Terri-type) and granite water (Äspö-type) at 90 °C under anaerobic conditions in the presence of dissolved Fe^{2+}, to simulate the effects of a corroding waste container (cf. [Curtius 2005], [Curtius 2006], [Brücher 2007], [Curtius 2010]). The corrosion behaviour was found to be similar to uranium aluminide fuels samples under identical conditions, showing complete corrosion of the samples within one year. The highest corrosion rates (determined by the evolution of hydrogen gas) were observed in the $MgCl_2$-brine ($57.4 \cdot 10^{-3}$ g m^{-2} d^{-1}), due to the high chloride concentration and the slightly lower pH [Curtius 2010]. The corrosion rates in clay and granite waters were found to be similar ($23.6 \cdot 10^{-3}$ g m^{-2} d^{-1}) and thus about a factor 2 to 3 lower than in the $MgCl_2$-brine [Curtius 2010]. The inventory of the matrix elements uranium, silicon, and aluminium in solution was found to be less than 5% [Curtius 2010], i.e. more than 95% of these elements were retained in amorphous and crystalline phases formed during the corrosion process.

Similar experiments using irradiated U_3Si_2-Al fuels from the FRG-1 reactor in Geesthacht performed for 3.5 years gave overall corrosion rates of $42.4 \cdot 10^{-3}$ g m^{-2} d^{-1} in $MgCl_2$-rich brines under anoxic conditions at 90 °C (cf. [Brücher 2007], [Curtius 2010], [Curtius 2011]). The corrosion of irradiated fuel samples in synthetic Mont Terri type clay pore water and Äspö type granitic waters progressed with a similar but lower rate of about $7 \cdot 10^{-3}$ g m^{-2} d^{-1} in these experiments [Curtius 2010]. It was generally found that the fuel samples dissolved completely within the experimental time frame of 3.5 years in all test solutions, and the corrosion behaviour of the uranium silicide fuels closely resembled that of irradiated UAl_x-Al fuels. Depending on solution composition, a variety of crystalline and amorphous corrosion products were formed (cf. section 5.2.3) that effectively retained the matrix elements uranium, silicon, and aluminium, as well as many radionuclides (e.g. Am, Pu), whereas the inventories of more mobile radionuclides such as Cs and Sr were completely released into solution (cf. [Curtius 2010], [Curtius 2011], [Curtius 2015]). In Table 5-5 the anoxic corrosion rates of uranium silicide fuels in various test solutions are compiled.

Table 5-5 Comparison of integral corrosion rates of uranium silicide (U_3Si_2-Al) dispersion fuels at 90 °C under anoxic conditions determined in static corrosion tests in different test solution

Sample	Solution type	Corrosion rate	Source
U_3Si_2-Al (unirradiated)	brine ($MgCl_2$)	$57.4 \cdot 10^{-3}$ g m^{-2} d^{-1}	[Curtius 2010]
U_3Si_2-Al (irradiated)	brine ($MgCl_2$)	$42.4 \cdot 10^{-3}$ g m^{-2} d^{-1}	[Curtius 2010]
U_3Si_2-Al (unirradiated)	granitic (Äspö)	$23.6 \cdot 10^{-3}$ g m^{-2} d^{-1}	[Curtius 2010]
U_3Si_2-Al (irradiated)	granitic (Äspö)	$6.9 \cdot 10^{-3}$ g m^{-2} d^{-1}	[Curtius 2010]
U_3Si_2-Al (unirradiated)	clay (Mont Terri)	$23.6 \cdot 10^{-3}$ g m^{-2} d^{-1}	[Curtius 2010]
U_3Si_2-Al (irradiated)	clay (Mont Terri)	$6.9 \cdot 10^{-3}$ g m^{-2} d^{-1}	[Curtius 2010]

5.2.3. Formation of secondary phases

The corrosion of aluminium based fuels leads to the formation of a variety of amorphous and crystalline secondary phases that can effectively retain various radionuclides as well as the released fuel matrix elements (e.g. by sorption, re-precipitation, or structural incorporation into newly formed secondary phases). The amount and nature of the corrosion products depend strongly on the environmental conditions the spent fuels are exposed to (i.e. especially pH and redox conditions and the composition of the aqueous phase) as well as on the nature of the fuel itself (i.e. aluminide or silicide fuel).

In unsaturated intermittent drip tests with J-13 water at 90 °C under oxidizing conditions, [Kaminski 2002] observed the formation of a thin silica-substituted hydrous aluminium oxide gel layer on the surface of unirradiated uranium-aluminide fuels. Moreover, the oxidation of the fuel produced hydrated aluminium and uranyl oxyhydroxide compounds such as dehydrated schoepite ($UO_3 \cdot xH_2O$, $x \cong 0.8$) and bequerelite ($Ca(UO_2)_6O_4(OH)_6 \cdot 8H_2O$). In similar tests, [Kaminski 2005] observed the formation of predominantly silicon-rich colloids (smectite clays) and some aluminium-rich colloids that carried about 99% of the uranium released from the fuel. [Wiersma 1998] observed also the formation of (hydrous) aluminium oxide layers in corrosion test performed on various aluminium based fuels and uranium aluminium alloys under oxidizing conditions. The thickness of the layer depended on solution chemistry, temperature, and flow conditions; the formation of an oxide layer was not detectable in tests performed with high pH J-13 waters at pH 11 [Wiersma 1998].

[Fachinger 2000] and [Brücher 2001] observed the formation of partly gel-like secondary phases in corrosion experiments performed with irradiated UAl_x-Al fuels in salt brines under oxic conditions. In static corrosion tests with unirradiated UAl_x-Al-fuel samples under anoxic conditions at 90 °C in $MgCl_2$-rich brine, Mazeina [2003a] found bischofite ($MgCl_2 \cdot 6H_2O$) and Mg-Al-Cl-hydrotalcite (i.e. a layered double hydroxide, LDH) as crystalline secondary phases after a complete corrosion of the fuel samples, besides an amorphous fraction. The formation of Mg-Al-hydrotalcite (besides an aluminium hydroxide) was also observed in corrosion tests on aluminium cladding materials in $MgCl_2$-brines at elevated temperatures (90 °C) [Mazeina 2003c]. The anoxic corrosion of unirradiated UAl_x-Al-fuels in NaCl-rich brines at 90 °C resulted in the formation of completely amorphous corrosion products [Mazeina 2003b]. Detailed investigations of the secondary phases formed during the anoxic corrosion of (unirradiated) research reactor fuels in $MgCl_2$-rich brine (UAl_x-Al and U_3Si_2-Al) and clay water (UAl_x-Al) were performed using scanning electron microscopy/energy dispersive X-ray spectroscopy and X-ray diffraction, after applying a dedicated separation and enrichment step for the secondary phases (cf. [Curtius 2010], [Klinkenberg 2010], [Klinkenberg 2011], [Neumann 2012] and [Klinkenberg 2014]). The secondary phases identified in these studied are summarised in Table 5-6.

Table 5-6 Secondary phases observed in static anoxic corrosion experiments performed with (unirradiated) UAl_x-Al and U_3Si_2-Al fuels (after [Curtius 2010], [Klinkenberg 2011], [Neumann 2012], [Klinkenberg 2014]) – phases in italics are remains of uncorroded fuels

Phase	Formula	UAl_x-Al	U_3Si_2-Al	UAl_x-Al	U_3Si_2-Al
		$MgCl_2$-brine		Clay water	
UAl_x	UAl_4	+	+	+	-
U_3Si_2	U_3Si_2	-	+	-	+
Mg-LDH	$Mg_6Al_2(OH)_{18}{\cdot}4H_2O$	+	+	-	+
Hibschite	$Ca_3Al_2(SiO_4)_{3-x}(OH)_{4x}$ (x=0.2-1.5)	-	+	-	-
Phillipsite	$(Na,K,Ca)_{1-2}(Si,Al)_8O_{16}{\cdot}6H_2O$	-	+	-	-
Gypsum	$CaSO_4{\cdot}2H_2O$	-	-	+	+
Bassanite	$CaSO_4{\cdot}0.5H_2O$	-	-	+	+
Aluminium	Al	-	-	+	+
Lesukite	$Al_2(OH)_5Cl{\cdot}2H_2O$	+	+	-	-
Bayerite	α-$Al(OH)_3$	+	+	-	-
Gibbsite	γ-$Al(OH)_3$	+	+	-	-
Nordstrandite	$Al(OH)_3$	+	+	-	-
Boehmite	γ-AlO(OH)	-	-	-	+
Iron	Fe	+	+	-	-
Hematite	Fe_2O_3	-	-	+	-
Goethite	α-FeO(OH)	+	+	+	+
Akaganeite	β-FeO(OH)	+	+	-	-
Lepidocrocite	γ-FeO(OH)	+	+	-	-
Lawrencite	$FeCl_2$	+	+	-	-
Fe-LDH	$Fe(OH,Cl)_{2.55}$	+	+	-	-
"clay minerals"	-	-	-	-	+
X-ray amorphous	-	+	+	+	+

The main corrosion products of UAl_x-Al fuels corroded in $MgCl_2$-rich brines were found to be Mg- and Fe-LDH phases and lesukite ($Al_2(OH)_5Cl{\cdot}2H_2O$) with all other crystalline phases present only in traces [Klinkenberg 2014]. Rietveld analyses revealed a high fraction of amorphous phases of approximately 30%, which are expected to include the re-precipitated uranium, which was quantitatively retained in the corrosion products, potentially as $U(OH)_4$ [Klinkenberg 2014]. Similar results with respect to the major corrosion products (LDH and lesukite), the high amount of amorphous phases (about 50 %), and the absence of crystalline uranium phases were obtained in corrosion experiments of U_3Si_2-Al fuels in $MgCl_2$-rich brines ([Neumann 2012], [Klinkenberg 2014]). The corrosion of UAl_x-Al fuel in Mont Terri Water produced a significantly higher amount of amorphous phases (about 80 %) together with some sulphates and iron oxihydroxides [Neumann 2012]. [Klinkenberg 2011] identified boehmite (γ-AlO(OH)) as the main crystalline corrosion product of U_3Si_2-Al fuels in Mont Terri clay waters, besides some Mg-LDH and other accessory phases, with the proportion of Mg-LDH significantly lower compared to corrosion experiments in $MgCl_2$-brines, due to the lower amount of Mg in solution [Klinkenberg 2010]. Approximately 50 % of the solid phase was found to be X-ray amorphous. Similar to the corrosion in brines, in the experiments with clay water, the amorphous phase quantitatively retained the uranium in the system, presumably as amorphous $U(OH)_4$ ([Klinkenberg 2010], [Klinkenberg 2011], [Neumann 2012]).

6. Evaluation

Within a multibarrier concept for the disposal of HLW, the waste form acts as the first barrier against the release of radionuclides from the waste into the repository near-field. In as such, the performance of the waste form under repository conditions is an important issue with respect to the isolation and containment of the radioactive waste and the radionuclides therein from the biosphere. The safety assessment methodology throughout the repository development within OPERA is based on safety functions that are defined as actions or roles that the natural and engineered barriers must perform to prevent the radionuclides present in the disposed wastes posing an unacceptable hazard to humans or the environment (cf. [ONDRAF 2004], [Verhoef 2011a], [Verhoef 2011b]). The five safety functions defined in [Verhoef 2011b] for the OPERA reference concept (incl. inter alia 'physical containment', 'resistance to leaching', and 'transport and retention') were later on replaced by the updated safety functions published in 2009 by ONDRAF/NIRAS [Smith 2009] (cf. [Verhoef 2014a]). The safety functions in [Smith 2009] related to the waste forms and the EBS comprise – with respect to the disposal of HLW – (i) the safety function 'engineered containment (C)', which describes the isolation of the radionuclides from their immediate environment (i.e. the near field water) provided by the supercontainer, and (ii) the safety function 'delay and attenuation of releases (R)'. The latter safety function that is relevant following the engineered containment phase once the physical containment of the supercontainer is impaired and the wastes come into contact with water, includes (i) the 'limitation of contaminant releases from the waste forms (R1)' describing the slow release of radionuclides from the waste, and (ii) the 'retardation and spreading in time of contaminant migration (R3)' related to the radionuclide sorption capacity and the slow diffusive transport in the EBS and the Boom Clay host rock.

The loss of integrity of the engineered containment provided by the supercontainer in the post-closure phase requires a number of subsequent steps and processes, such as

- (fast) resaturation of the repository backfill,
- corrosion/failure of the stainless steel envelope,
- re-saturation of the concrete buffer,
- corrosion/failure of the carbon steel overpack, and finally
- corrosion/failure of the ECN-canister,

before the RRSF in the failed ECN-canisters can come into contact with the near field water at some point in the (far) future. The radionuclides contained in the RRSF can be released, when the fuel meat of the irradiated dispersion fuels becomes accessible to the near field water after failure of the aluminium cladding.

In the following section 6.1 the corrosion rates of and the radionuclide release from RRSF under repository conditions relevant to OPERA are discussed to assess and quantify the safety function R1: 'limitation of contaminant releases from the waste forms' in the context of the envisaged OPERA safety case. Section 6.2 provides an overview on processes that affect the radionuclide migration and may contribute to the retention of the leached radionuclides in the immediate near field (e.g. due to solubility constraints and/or interaction with degradation products from the engineered barrier system) addressing thus the safety function R3: 'retardation and spreading in time of contaminant migration'.

6.1. Radionuclide source term

The performance of a nuclear waste form in the repository environment is dependent on the environmental conditions to which the material will be exposed. Near field factors affecting substantially the radionuclide source term for a waste include the hydrogeological regime and the geochemical conditions (notably pH, redox potential, temperature, gas partial pressures, groundwater/pore water composition), which themselves will evolve over time in the post-closure phase (cf. section 4.2). Due to the uncertainties with respect to the time scales of the engineered containment phase and the degradation stages of the cementitious materials at the time of canister failure, i.e. when the RRSF can come into contact with water, different scenarios with respect to the composition of the near-field water resulting from the interaction of Boom Clay pore water with the cementitious materials are addressed.

As reference scenario, it is assumed here that the conditions in the supercontainer pore water at the time of canister failure are representative for the stage II of concrete degradation (i.e. portlandite stage), based on the expected lifetime of the overpack and the long duration of stage II of up to several 100,000 years (cf. [Lemmens 2012], [Kursten 2015]). Due to the relatively low heat output of the heat-generating wastes in the OPERA concept and the rather insignificant temperature excursion in the HLW section during the first decades (cf. [Kursten 2015]), ambient conditions (i.e. about 25 °C in 500 m depth in the Netherlands) are assumed at the time of canister failure. Moreover, the oxygen available at the time of repository closure will have been consumed, for example due to corrosion of metals during the degradation of EBS, leading to anoxic or reducing conditions at that time. The relevant environmental conditions for this scenario can thus be described by an anoxic/reducing near field water at pH 12.5 controlled by portlandite dissolution (i.e. the near field water can be described as a saturated $Ca(OH)_2$ solution) at ambient temperature. Potential deleterious effects of the co-disposal of HLW and LILW in the OPERA disposal concept (e.g. ingress of oxidising species or complexing organic ligands released from the LILW) are disregarded at that point by assuming an appropriate design and layout of the disposal facility (e.g. by placing low permeability seals and plugs between the different repository sections).

The durability (corrosion resistance) of aluminium in alkaline solutions and cementitious environments has been studied and discussed extensively in the past (e.g. [Straumanis 1949a,b], [Takatani 1982], [Takatani 1983], [Zhang 2009], [Hoch 2010]), although only few data on corrosion rates determined under anoxic or reducing conditions are available (e.g. [Fujisawa 1997]). Taking into account the high (initial) corrosion rates observed in $Ca(OH)_2$ solutions (cf. [Takatani 1982], [Takatani 1983]) or in mortar equilibrated water at pH 12.2 [Fujisawa 1997] and the thickness of the cladding layer (i.e. typically 0.38 mm), it can be concluded that under highly-alkaline near field conditions, the aluminium cladding does not function as a durable barrier in the longer-term. The observed initial corrosion rates of aluminium in alkaline $Ca(OH)_2$-solutions (or in cementitious materials) are very large (i.e. over 1 mm a^{-1}). This means for the reference scenario that after the near-field water comes into contact with the RRSF, a typical 0.38 mm cladding will fail rather fast. In this context it has to be noted that the typically observed decrease in aluminium corrosion rates after the initial period of rapid corrosion is thought to be dependent on preserving the (unstable) corrosion product layer (i.e. complex Al-Ca-compounds) adhering to the surface, e.g. by embedding the aluminium in a solid or pulverised mortar (e.g. [Hoch 2010]). This decrease in corrosion rates was not observed in corrosion experiments in mortar equilibrated water under anoxic conditions, i.e. in a situation comparable to the RRSF in a failed canister, where no stable corrosion product layer could form on the aluminium surface [Fujisawa 1997].

Information on the corrosion behaviour of the uranium aluminides and/or uranium silicides present in the fuel meats of RRSF under conditions relevant to deep geological disposal are generally sparse. Some corrosion studies on RRSF were performed under atmospheric conditions with respect to conditions expected in the Yucca Mountain repository (cf. [Wiersma 1998], [Kaminiski 2003]), whereas researchers in Germany investigated the corrosion behaviour of UAl_x-Al and U_3Si_2-Al fuels in salt brines, clay and granite waters under anoxic conditions (e.g. [Curtius 2015]). However, investigations on the corrosion behaviour of RRSF under conditions representative for an anoxic cementitious near field are lacking to date.

Corrosion experiments performed with unirradiated and irradiated research reactor fuel plates under anoxic conditions in salt brines, clay waters and granite waters revealed complete dissolution of these fuel types within a time frame of a few years, indicating a very low corrosion resistance under anoxic repository conditions after the fuel comes in contact with water (i.e. after failure of the waste canister due to corrosion). The highest corrosion rates were observed in $MgCl_2$-rich brines and lower rates (about a factor 3) in clay and granite waters [Curtius 2015]. With respect to an assessment of the behaviour of RRSF in a cementitious environment relevant to the OPERA safety case, the following experimental observations are important and have been included in the subsequent considerations:

- the corrosion behaviour of uranium silicide fuels appears to be similar to that of uranium aluminide fuels, both fuel types exhibiting a rather low corrosion resistance (e.g. [Fillmore 1998], [INEEL 2003], [Curtius 2012]);
- the corrosion rates of uranium aluminides and uranium silicides in the fuel meats are thought to be similar to metallic aluminium (e.g. [Dodd 2000]);
- corrosion experiments at pH 11 in modified J-13 water emphasise the higher dissolution rates of uranium aluminides under alkaline conditions (cf. [INEEL 2003]).

Taking also into account that (i) the metallic aluminium in the fuel meat will have a similar corrosion behaviour as the aluminium cladding of the fuel, (ii) the particle size of the uranium aluminides and uranium silicides dispersed in the fuel meat is rather small (40 to 150 µm), and (iii) the corrosion rates of metallic uranium under anoxic and highly alkaline conditions are also high (e.g. [Hoch 2010]), it can be expected that the corrosion behaviour of the fuel meat is comparable to the corrosion behaviour of aluminium and consequently the life time of the fuel meat under highly alkaline conditions is relatively short. Generally, it can be concluded that for the reference conditions addressed here (pH 12.5, anoxic/reducing) both the cladding and fuel meat will dissolve completely within a very short period (i.e. probably several years). Thus cladding and fuel meat do not form a long-term barrier with respect to radionuclide retention. With respect to the time scales relevant for geological disposal, RRSF will corrode instantaneously after coming into contact with the near field water. Thus from a safety assessment perspective after failure of the waste canisters, the radionuclide inventory will be instantaneously released from the RRSF.

Alternatively to the reference scenario, in case of an early canister failure scenario, it might be assumed that the conditions in the near field are representative for concrete during degradation stage I, depending at the time of the loss of physical containment of the waste. In this scenario, the pH in the near field water would be higher compared to the reference scenario (up to pH ~13.5, cf. section 4.2) and the pore water composition dominated by KOH and NaOH. In this case, an even faster corrosion of the cladding and the fuel meat can be assumed, due to the increased solubility and corrosion rates of aluminium under more alkaline conditions, the lack of potential secondary phases that could passivate the aluminium, and the assumed further increase in uranium aluminide/silicide dissolution rates with increasing pH (similar to metallic aluminium and uranium).

In the longer term, i.e. after concrete degradation stage II, a decrease in the pore water pH buffered by CSH with decreasing Ca/Si ratios is to be expected (as well as changes in the physical properties of the concrete), with the pore water composition finally approaching the composition of the groundwater in the surrounding Boom Clay. Although the corrosion rates of the aluminium cladding and the fuel meat are expected to be lower than in the other scenarios due to the decrease in pH, experimental evidence exists that, in the presence of ferrous ions from the corrosion of waste canisters or overpacks, RRSF exhibits a rather low corrosion resistance also in pore waters representative for clay environments (cf. [Curtius 2006], [Klinkenberg 2011], [Curtius 2015]).

Thus it can be generally concluded that − for all scenarios considered here − the life time of the RRSF is rather short after coming into contact with the near field water, and it is sensible to assume an instantaneous corrosion of and radionuclide release from the waste form RRSF within OPERA.

However, the fast disintegration and corrosion of the fuel matrix does not necessarily imply that all the radionuclides become available as dissolved species that can migrate into the repository near and far field. There is evidence that under anoxic conditions some radionuclides (e.g. uranium and plutonium isotopes) are practically completely retained in the secondary products formed during the corrosion of RRSF due to solubility limitations or by sorption/uptake (cf. [Curtius 2006], [Klinkenberg 2011], [Curtius 2012], [Curtius 2015]). Although no experimental evidence on the amount and nature of the corrosion products of RRSF formed under cementitious conditions exists so far, it might be assumed that the uranium is quantitatively retained in the corrosion products as amorphous $U(OH)_4$ (or UO_2xH_2O), similarly as observed in clay, granite, or salt systems, due to the low solubility of uranium under these conditions (cf. section 6.2.1) and the expected low water exchange rates in a failed waste canister. The potential retention of safety relevant long-lived fission and activation products (e.g. selenium-79, iodine-129, or carbon-14), which have been observed to be retained e.g. by sorption to or uptake by Mg-LDH formed during RRSF corrosion in brines or clay waters (cf. [Curtius 2015]) is a rather open issue, since no experimental results on the nature of crystalline or amorphous secondary phases formed during corrosion of RRSF in a cementitious near field (e.g. maybe Ca-aluminates, cf. section 5.1) and their potential for radionuclide retention are available to date.

Regarding a potential quantitative retention of uranium (and perhaps also a retention of plutonium-IV under reducing conditions) in the amorphous fraction of the RRSF corrosion products inside a failed waste canister, the potential risk of the occurrence of critical configurations (e.g. due to accumulation of fissile material at the bottom/wall of the waste canister) and the effects of a potential criticality excursion in the OPERA disposal facility should be assessed in detail in the future, since, according to [Verhoef 2016], the amount of fissile material in an ECN-canister loaded with either HEU or LEU RRSF exceeds the critical mass (cf. section 3.3).

6.2.Radionuclide migration in the near-field

The radionuclides released due to dissolution or leaching of a waste form, i.e. in this case the fast corrosion of RRSF, are not necessarily in a mobile form that can readily migrate in the EBS or the repository host rock. The released radionuclides may precipitate in a less soluble secondary phase or may be incorporated in or sorbed by crystalline or amorphous phases formed during the degradation of the waste form, depending on the chemical environment and the secondary phases present. Moreover, the (degrading) near field materials may provide sinks for various radionuclides, for example due to sorption onto container corrosion products such as magnetite, including also reduction of radionuclides in higher valence states to less soluble forms in lower valence states and their precipitation. In the expected highly alkaline cementitious near field within the

supercontainer buffer, the various cement phases may limit the radionuclide mobility due to sorption (e.g. on CSH-phases) or structural uptake (e.g. in AF_m-phases); moreover the concentrations of certain radionuclides may be limited by the low solubility of their hydroxides under high pH conditions.

In general, it can be expected that the highest radionuclide concentrations will occur in the repository near-field and will decrease along the migration path to the far-field, due to further retardation processes, such as sorption on materials present in the engineered or natural barriers (i.e. in this case the Boom Clay), or due to dilution. In section 6.2.1 approaches to the evaluation of maximum radionuclide concentration in the repository near field are discussed, section 6.2.2 provides some information on the sorption of radionuclides in a cementitious near field.

6.2.1. Solubility limitation in a cementitious near-field

The dissolved concentrations of radionuclides in the cementitious near field are determined by a variety of processes such as the release rates from the degrading waste forms, the potential formation of secondary solid phases when exceeding a solubility limit, and/or the sorption onto or uptake by solid repository materials (e.g. also by solid solution formation). Due to the complex interactions of the various processes and the large number of parameters that may affect the radionuclide behaviour (e.g. pH, Eh, solution composition and presence of complexing ligands, nature and availability of solid phases and their surfaces/interfaces), it is difficult to accurately determine the maximum radionuclide concentrations in the repository near field. One possible approach to the determination of maximum concentrations of radionuclides in a geological repository is the calculation of the solubility of radionuclides by using chemical thermodynamic data and assuming potential solubility limiting phases (cf. [Wanner 2007]). According to [Wang 2013a], it is justified within the radioactive waste community that the solubility determined by equilibrium calculations represents the maximum released radionuclide concentration.

[Wang 2013a] evaluated the solubility of various radionuclides in the pore water of the concrete buffer of a supercontainer used for the disposal of HLW in in Boom Clay in Belgium. The solubility limits were mainly derived using a thermodynamic approach by calculation of the equilibrium with a solubility controlling solid phase, and are partly based on the review of experimental data in the literature for cementitious conditions. In a first step, [Wang 2013a] modelled the interaction of the cement buffer with Boom Clay pore water, using the reference Boom Clay pore water from the Mol site [de Craen 2004], to derive the pore water composition in the concrete buffer for the different cement degradation stages (cf. section 4.2.1). The pore water compositions simulated by this approach for the various stages of cement degradation (i.e. Stage I: NaOH and KOH pore water; stage II: portlandite stage, stage III: buffering by CSH-phases) are provided in Table 6-1. According to [Wang 2013a], the estimation of the redox potential within the supercontainer buffer is difficult due to uncertainties regarding the redox controlling mechanisms and the thermodynamic data. In general, it is expected that the conditions in the repository near field in the HLW repository in Boom Clay are reducing [Wang 2013a]. The radionuclide solubilities evaluated by [Wang 2013a] for the supercontainer near field are summarised in Table 6-2. According to [Wang 2013a] the most influential chemical parameter on the solubility was the pH. With respect to the maximum solubility of uranium provided by [Wang 2013a] it should be noted that these concentrations were derived for U^{VI}, assuming that the repository conditions might be to oxidising for uranium to prevail as U^{IV}. In the case that the redox potential would be negative enough to favour U^{IV} in solution (i.e. less than ~670 mV in stage I and less than about ~550 mV in stage II), significantly lower uranium solubilities (10^{-8} to 10^{-9} mol L^{-1}) might occur (cf. [Berner 2003]).

Table 6-1 Simulated pore water composition in the near field concrete at 25 °C [Wang 2013a] – concentrations in mmol L^{-1}

Parameter	Stage I	Stage II	Stage III
pH	13.5 … 12.5	12.5	12.5 … 10.5
Na	141 … 15	15	15
K	370 … 0.2	0.2	0.2
Ca	0.7 … 15.4	15.4	15.4 … 1.4
Mg	10^{-7} … 10^{-6}	10^{-6}	10^{-6} … 10^{-4}
Al	0.08 … 0.008	0.008	0.008 … 0.5
Si	0.01 … 0.002	0.002	0.002 … 5
CO_3	0.4 … 7 10^{-3}	7 10^{-3}	7 10^{-3} … 0.02
SO_4	8 … 0.04	0.04	0.04 … 5.7

With respect to the proposed Swiss cementitious repository for ILW in the Opalinus Clay, [Berner 2003] carried out solubility calculations for various radionuclides in the cementitious stage II pore water (cf. Table A-3), which are provided in Table A-6 for comparison. More recently, [Berner 2014] re-evaluated the solubility limits for safety relevant elements in the pore water of a concrete system for use in the provisional safety analysis for deep geological repository for long-lived ILW (cf. Table A-7). The solubility calculations were performed for the degradation stage characterised by portlandite saturation (Stage II, cf. Table A-4 for the pore water composition) using the updated NAGRA/PSI Chemical Thermodynamic Database 12/07 [Thoenen 2014], whereas the evaluations in [Berner 2003] were based on the NAGRA/PSI Chemical Thermodynamic Database 01/01 [Hummel 2002].

6.2.2. Sorption of radionuclides in a cementitious near field

The mobility of radionuclides in cementitious materials depends on the chemical behaviour of the particular element in high pH systems as well as on the chemical, physical and mineralogical properties of the solid material (e.g. pore water pH, degradation state, amount and nature of cement minerals, aggregates and accessory phases, specific surface areas, interface properties, etc.) and the presence of complexing ligands and competing ions. The retardation of radionuclides by sorption onto cementitious materials can encompass processes like ion exchange (e.g. radium and/or strontium uptake by CSH, e.g. [Tits 2006]), surface complexation (e.g. caesium sorption by CSH, e.g. [Heath 2000], [Iwaida 2002]) or structural uptake and solid solution formation (e.g. uptake of selenium or iodine by AF_m phases, e.g. [Baur 2003], [Aimoz 2012]) or combinations thereof.

The sorption of radionuclides to cementitious materials and radionuclide retardation under cementitious near-field conditions has been intensively discussed within the context of nuclear waste disposal and is still in the focus of international research activities, for example in the EC-Horizon 2020 research project CEBAMA (www.cebama.eu). Various case specific sorption databases for radionuclide-cement interactions have been developed in the past decades (e.g. [Wieland 2002], [Wang 2009b], [Suyama 2012], [Wang 2013b], [Wieland 2014]), which can provide an overview on the radionuclide retardation expected in various cementitious systems under different environmental conditions. However, at present no directly applicable data sets are at hand to describe the sorption of radionuclides in a cementitious repository in Boom Clay in the Netherlands.

Table 6-2 Solubilities of selected elements in a cementitious supercontainer near field [Wang 2013a] – concentrations in mol kg^{-1} (VL: very low, NL: not limited)

Element	Stage	Upper bound	95% confidence limit for upper bound	Lower bound	95% confidence limit for lower bound
	I	6E-5		VL	
Ag	II	6E-6		VL	
	III	6E-6		VL	
Am	I – III	3E-9	3E-10 … 3E-8	3E-9	3E-10 … 3E-8
	I	1E-4		<1E-4	
Be	II	<1E-4		<1E-4	
	III	<1E-4		<1E-4	
	I	3E-4		8E-6	
C	II	8E-6		8E-6	
	III	1E-5		8E-6	
	I	1.5E-2		7E-4	
Ca	II	1.5E-2		1.5E-2	
	III	1.5E-2		1.4E-3	
Cl	I - III	NL		NL	
Cm	I - III	3E-9	3E-10 … 3E-8	3E-9	3E-10 … 3E-8
Cs	I - III	NL		NL	
I	I - III	NL		NL	
	I	9E-4		5E-6	
Mo	II	5E-6		5E-6	
	III	4E-5		5E-6	
	I	1.1E-5	2E-6 … 2E-5	7E-9	4E-9 … 8E-9
Nb	II	7E-9	4E-9 … 8E-9	7E-9	4E-9 … 8E-9
	III	8E-7	1.8E-7 … 4.2E-7	7E-9	4E-9 … 8E-9
Ni	I - III	2.9E-7	2.4E-7 … 3.4E-7	2.9E-7	2.4E-7 … 3.4E-7
Np (IV)	I - III	1E-8		1E-9	
Pa	I - III	1E-8		1E-8	
	I	NL		NL	
Pb	II	NL		5E-2	
	III	NL		1E-4	
	I	1E-4		1E-5	
Pd	II	1E-5		1E-5	
	III	1E-5		4E-6	
Pu (IV)	I – III	1E-8		1E-11	
	I	1E-6		7E-9	
Ra	II	1E-6		1E-6	
	III	1E-6		1E-8	
	I	NL		5E-4	
Se	II	NL		2E-5	
	III	NL		1E-11	
	I	2E-6		1E-8	
Sn	II	1E-8		1E-8	
	III	1E-7		1E-8	
	I	2.5E-3		1E-4	
Sr	II	2.5E-3		2.5E-3	
	III	2.5E-3		3.4E-4	
	I	NL		1E-6 Tc^{IV}	
Tc	II	NL		1E-7 Tc^{IV}	
	III	NL		NL	
Th	I – III	1E-8	1E-9 … 1E-7	1E-8	1E-9 … 1E-7
	I	3E-6	2.6E-7 … 7E-6	2E-6	1E-6 … 6E-6
U(VI)	II	2E-6	1E-6 … 6E-6	2E-6	1E-6 … 6E-6
	III	3E-5		2E-6	1E-6 … 6E-6
Zr	I	3E-8	5E-9 … 1E-7	2E-8	3.6E-10 … 1E-6
	II - III	2E-8	3.6E-10 … 1E-6	2E-8	3.6E-10 … 1E-6

7. Conclusions

The RRSF from test and research reactors in the Netherlands to be disposed of in a deep geological repository comprise UAl_x-Al and U_3Si_2-Al dispersion fuels with aluminium cladding, containing HEU (up to 93 wt.% ^{235}U) and LEU (up to 20 wt.% ^{235}U), respectively. The generic disposal concept for HLW such as RRSF in Boom Clay pursued in the context of OPERA is based on the Belgian supercontainer concept. In this concept, the EBS makes extensive use of cementitious materials as buffer within the supercontainer, as backfilling grout, and in the construction material for the disposal gallery linings. Thus the near-field chemistry will be governed by the degradation of cementitious materials in the long-term and an anoxic and highly alkaline repository near field will prevail probably for some hundreds of thousands of years post closure.

Experimental investigations on the corrosion behaviour and performance of RRSF in the repository environment are rather limited, and studies regarding the behaviour of RRSF under cementitious near field conditions are lacking to date. The durability of the aluminium cladding under highly alkaline conditions is low, thus after the near-field water comes into contact with the RRSF, a typical 0.38 mm aluminium cladding will fail rather fast. Thus the aluminium cladding does not function as a durable barrier in the longer-term, and radionuclides can be leached from the fuel meat after coming into contact with the near field water rather soon after canister failure. Based on experimental evidence regarding the low durability of RRSF under anoxic repository conditions in salt, clay and granite environments, and the assumed analogous low corrosion resistance of the fuel meat compared to the aluminium matrix and cladding in cementitious conditions, the life time of the fuel meat corroding in a highly alkaline environment is expected to be relatively short (i.e. few years). With respect to the time scales relevant for the safety assessment of a geological repository it can generally be concluded that RRSF will corrode instantaneously after coming into contact with the cementitious near field water. Thus it is sensible to assume an instantaneous corrosion of and radionuclide release from the waste form RRSF after failure of the canisters within the OPERA safety case.

However, the fast dissolution process does not necessarily imply that all radionuclides released from the fuel matrix will be mobile and can migrate into the repository near and far field, since the radionuclides can be retained by amorphous and/or crystalline corrosion products formed during the degradation of the RRSF. For example, it has been observed in corrosion experiments under anoxic conditions addressing RRSF disposal in salt, clay, or granitic systems that the uranium released during the corrosion process is practically quantitatively retained in amorphous corrosion products, presumably as amorphous UOH_4 (or alternatively $UO_2(am)\cdot xH_2O$). Moreover, the migration of radionuclides released from the corroding RRSF may further be delayed by sorption to other near field materials such as corrosion products from the metallic waste canisters/overpacks or retention/uptake in the cementitious materials present in the supercontainer buffer or the repository backfill.

In the case that the fissile uranium (and perhaps also fissile plutonium) is more or less completely retained in the corrosion products, a critical configuration inside the corroding waste canister cannot be excluded since the amount of fissile material in an ECN-canister loaded with either HEU or LEU RRSF that might accumulate on the canister bottom exceeds the critical mass. Moreover, within the OPERA disposal concept, two ECN-canisters overpacked in one supercontainer.

In order to increase the mechanistic understanding of the behaviour of RRSF under OPERA disposal conditions, to build further confidence in the OPERA safety case, and evaluate safety margins with respect to the geological disposal of RRSF, in our opinion the following issues should be addressed in more detail in future research activities:

- Near field conditions at the time of canister failure: The geochemical conditions the wastes are exposed to after canister failure should be further constrained, for example, by coupled reactive transport simulations of the interaction of typical Boom Clay groundwaters expected in various regions of the Netherlands with the cementitious EBS materials. In this context it is suggested to look in more detail on the effect of the stainless steel envelope on the timescales of the resaturation of the supercontainer buffer and the lifetime of the overpack/waste canister.
- Corrosion rates of RRSF in alkaline conditions: The corrosion rates of RRSF in solutions representative for different concrete degradation states and the radionuclide release behaviour should be determined experimentally under anoxic conditions to support the assumptions for the OPERA safety case.
- Corrosion products/secondary phases: Corrosion experiments with (unirradiated) fuel plates should be performed to determine the nature and amounts of secondary phases formed during the corrosion of RRSF and evaluate their thermodynamic stability and their radionuclide retention potential.
- Criticality: The potential of the occurrence of critical configurations due to accumulation of fissile material (e.g. amorphous uranium phases) inside the corroding waste canister should be evaluated and, if necessary, the effects of a potential criticality excursion in the OPERA disposal facility should be assessed.
- Pre-disposal conditioning: Depending on the outcome of the aforementioned evaluations, it might be worthwhile to consider further pre disposal treatment measures for the RRSF stored at COVRA, such as repacking, encapsulation, or conditioning (e.g. melt-dilute process), to reduce, for example, criticality risks, or enhance the life time of the RRSF under repository conditions.

8. References

[Ahlf 1993] Ahlf J, Zurita A (eds.) *High Flux Reactor (HFR) Petten - Characteristics of the installation and the irradiation facilities*, Nuclear Science and Technology, Commission of the European Communities – Joint Research Centre, EUR 15151 EN (1993) 1-196.

[Aimoz 2012] Aimoz L, Wieland E, Taviot-Gueho C, Dähn R, Vepa M, Churakov SV, *Structural insight into iodide uptake by AFm phases*, Environ Sci Technol 46 (2012) 3874-3881.

[Armstrong 1996] Armstrong RD, Braham VJ, *The mechanism of aluminum corrosion in alkaline solutions*, Corros Sci 38 (1996) 1463-1471.

[Atkins 1992] Aktins M, Glasser F, *Application of Portland cement-based materials to radioactive waste immobilization*, Waste Manage 12 (1992) 105-131.

[Baur 2003] Baur I, Johnson CA, *The solubility of selenate-AF$_t$ ($3CaO{\cdot}Al_2O_3{\cdot}3CaSeO_4{\cdot}37.5H_2O$) and selenate-AF$_m$ ($3CaO{\cdot}Al_2O_3{\cdot}CaSeO_4{\cdot}xH_2O$)*, Cem Concr Res 33 (2003) 1741-1748.

[Beattie 2012] Beattie TM, Williams SJ, *An overview of near-field evolution research in support of the UK geological disposal programme*, Min Mag 76 (2012) 2995–3001.

[Bechtel 2004] Bechtel SAIC, *DSNF and other waste form degradation abstraction,* Bechtel SAIC Company ANL-WIS-MD-000004 REV 04 (2004) 1-57.

[Bel 2006] Bel JJP, Wickham SM, Gens RMF, *Development of the supercontainer design for deep geological disposal of high-level heat emitting radioactive waste in Belgium*, Mat Res Soc Symp Proc 932 (2006) 1-10.

[Berner 1988] Berner UR, *Modelling the incongruent dissolution of hydrated cement minerals,* Radiochim Acta 44/55 (1988) 387-393.

[Berner 1992] Berner UR, *Evolution of pore water chemistry during degradation of cement in a radioactive waste repository environment*, Waste Manage 12 (1992) 201-219.

[Berner 2003] Berner U, *Radionuclide concentration limits in the cementitious near-field of an ILW repository*, NAGRA Technical Report NTB 02-22 (2003) 1-48.

[Berner 2014] Berner U, *Solubility of radionuclides in a concrete environment for provisional safety analyses for SGT-E2*, NAGRA Technical Report NTB 14-07 (2014) 1-81.

[Binger 1957] Binger WW, Marstiller CB, *Aluminum alloys for handling high-purity water*, Corrosion 13 (1957) 59-64.

[Bourns 1968] Bourns WT, *Corrosion testing of uranium silicide fuel specimens*, Atomic Energy of Canada Ltd, AECL-2718 (1968) 1-43.

[Braak 1987] Braak JR, *De lage flux reactor te Petten*, ECN report ECN-87-172 (1987) 1-102.

[Brodda 1995] Brodda BG, Fachinger J, *Corrosion behavior of spent MTR fuel elements in a drowned salt mine repository*, Mat Res Soc Symp Proc 353 (1995) 593-600.

[Brücher 2001] Brücher H, Curtius H, Fachinger J, *R&D for back-end options for irradiated research reactor fuel in Germany*, Transactions 5th Topical Meeting on Research Reactor Fuel Management, April 1 to 3, 2001, Aachen, Germany (2001) 99-103.

[Brücher 2007] Brücher H, Curtius H, *Investigations into the behaviour of research reactor fuel elements in repository relevant aquatic phases*. Transactions 11th International Topical Meeting Research Reactor Fuel Management (RRFM) and Meeting of the International Group on Reactor Research (IGORR), Lyon, France, 11– 15 March 2007 (2007) 1-5.

[Cachoir 2015] Cachoir C, Mennecart T, *Spent fuel dissolution in supercontainer conditions - Reporting period 2009-2012*, External Report SCK•CEN ER-231 (2015) 1-140.

[Carlsson 2014] Carlsson T, Kotiluoto P, Vilkamo O, Kekki T, Auterinen I, Rasilainen K, *Chemical aspects on the final disposal of irradiated graphite and aluminium*, VTT Technology Report 156 (2014) 1-57.

[Chandra 1990] Chandra N, Dhar S, Saxena BK, *Corrosion of aluminium in aqueous solutions of different pH*, J Electrochem Soc India 39 (1990) 160-164.

[Chatalov 1952] Chatalov AY, *Effet du pH sur le comportement électrochimique des méteaux et leur résistance à la corrosion*, Dokl Akad Nauk SSSR 86 (1952) 775-777.

[Curtius 2005] Curtius H, Brücher H, *R&D for the final disposal of irradiated research reactor fuel elements*, 9th International Topical Meeting on Research Reactor Fuel Management, 10-13 April 2005, Budapest, Hungary (2005) 164-168.

[Curtius 2006] Curtius H, Kaiser G, Paparigas Z, Ufer K, Müller E, Enge R, Brücher H, Untersuchungen zum Verhalten von Forschungsreaktor-Brennelementen (FR-BE) in den Wirtsgesteinsformationswässern möglicher Endläger, Berichte des Forschungszentrums Jülich 4237 (2006) 1-120.

[Curtius 2010] Curtius H, Kaiser G, Paparigas Z, Hansen B, Neumann A, Klinkenberg M, Müller E, Brücher H, Bosbach D, *Wechselwirkung mobilisierter Radionuklide mit sekundären Phasen in endlagerrelevanten Formationswässern*, Berichte des Forschungszentrums Jülich 4333 (2010) 1-170.

[Curtius 2011] Curtius H, Kaiser G, Müller E, Bosbach D, *Radionuclide release from research reactor spent fuel*, J Nucl Mater 416 (2011) 211-215.

[Curtius 2015] Curtius H, Bosbach D, Deissmann G, *Corrosion of spent fuel from research and prototype reactors under conditions relevant to geological disposal*, Key Topics in Deep Geological Disposal: Conference Report, KIT Scientific Reports 7696 (2015) 176-180.

[CRWMS M&O 1998a] Civilian Radioactive Waste Management System Management & Operating Contractor, *Evaluation of codisposal viability for aluminum-clad DOE-owned spent fuel: Phase II Degraded codisposal waste package internal criticality*, Dl#: BBA000000-01717-5705-00017 REV 01 (1998) 1-75.

[CRWMS M&O 1998b] Civilian Radioactive Waste Management System Management & Operating Contractor, *Geochemical and physical analysis of degradation modes of HEU in a codisposal waste package with HLW canisters*, Dl#: BBA000000-01717-0200-00059 REV 01 (1998) 1-114.

[de Craen 2004] de Craen M, Wang L, van Geet M, Moors H, *Geochemistry of Boom Clay pore water at the Mol site*, Scientific Report SCK•CEN-BLG-990 (2004) 1-179.

[de Vries 1997] de Vries JW, Gibcus HPM, de Leege PFA, *The HOR core conversion program development and licensing experiences*, 20. International meeting on Reduced Enrichment for Research and Test Reactors (RERTR), Jackson Hole, WY United States, 5-10 October 1997 (1997) 1-8.

[de Vries 2006] de Vries JW, de Leege PFA, Gibcus HPM, *HOR HEU/LEU core conversion: 8 years experience*, Transactions 10th International Topical Meeting on Research Reactor Fuel Management, 30. April-3. May 2006, Sofia, Bulgaria (2006) 255-259.

[Diomidis 2014] Diomidis N, *Scientific basis for the production of gas due to corrosion in a deep geological repository*, NAGRA Arbeitsbericht NAB 14-21 (2014) 1-64.

[Dodd 2000] Dodd DH, Grupa JB, Houkema M, de Haas JBM, Van der Kaa T, Veltkamp AC, *Direct disposal of spent fuel from test and research reactors in the Netherlands - A preliminary investigation*, NRG 21406/00.30934/P (2000) 1-90.

[Drace 2013] Drace Z, Ojovan MI, *A summary of IAEA coordinated research project on cementitious materials for radioactive waste management*, in: Bart F, Cau-dit-Coumes C, Frizon F, Lorente S (eds) Cement-based materials for nuclear waste storage, Springer (2013) 3-11.

[Fachinger 1997] Fachinger J, Brücher H, Rainer H, *Behavior of spent aluminum cladded metallic uranium fuel in concentrated salt brines*, 1st International Topical Meeting on Research Reactor Fuel Management, February 5 to 7, 1997, Bruges, Belgium (1997) 127-130.

[Fachinger 2000] Fachinger J, Curtius H, *Long term behavior of direct disposed MTR fuel elements in saline brines*, in: Rammlmaier D, Mederer J, Oberthür T, Heimann RB, Pentinghaus H (eds): Applied Mineralogy in Research, Economy, Technology, Ecology and Culture, Balkema, Rotterdam (2000) 531-534.

[Feraday 1971] Feraday MA, *The oxidation, hydriding and aqueous corrosion of U_3Si alloys*, Atomic Energy of Canada Ltd, AECL-3862 (1971) 1-43.

[Fillmore 1998] Fillmore DL, *Parameter selection for Department of Energy spent nuclear fuel to be used in the Yucca Mountain viability assessment*, Idaho National Engineering Laboratory, INEEL/EXT-98-00666 (1998) 1-27.

[Ferrand 2013] Ferrand K, *Topical report on tests on vitrified (V)HLW waste in Supercontainer disposal conditions (status 2011)*, External Report SCK•CEN ER-195 (2013) 1-464.

[Fujisawa 1997] Fujisawa R, Cho T, Sugahara K, Takizawa Y, Horikawa Y, Shiomi T, Hironaga M, *The corrosion behaviour of iron and aluminum under waste disposal conditions*, Mat Res Soc Symp Proc 465 (1997) 675-682.

[Giffaut 2014] Giffaut E, Grivé M, Blanc P, Vieillard P, Colàs E, Gailhanou H, Gaboreau S, Marty N, Madé B, Duro L, *Andra thermodynamic database for performance assessment: ThermoChimie*, Appl Geochem 49 (2014) 225–236.

[Gimenez 1981] Gimenez P, Rameau JJ, Reboul MC, *Experimental pH potential diagram of aluminum for sea water*, Corrosion 37 (1981) 673–682.

[Glasser 2011] Glasser FP, *Application of inorganic cements to the conditioning and immobilisation of radioactive wastes*, in: Ojovan MI (ed) Handbook of advanced radioactive waste conditioning technologies, Woodhead (2011) 67–135.

[Gray 1998] Gray WJ, *Corrosion of aluminum-based spent fuel under geological disposal conditions*, Proceedings Third topical meeting on DOE Spent Nuclear Fuel and Fissile Materials Management, September 8-11, 1998, Charleston, SC, USA (1998) 697-698.

[Grogan 1992] Grogan HA, Worgan KJ, Smith GM, Hodkinson DP, *Post-disposal implications of gas generated from a repository for low and intermediate level wastes*. NAGRA Technical Report NTB 92-07 (1992) 1-58.

[Harris 2002] Harris AW, Manning MC, Tearle WM, Tweed CJ, *Testing of models of the dissolution of cements - leaching of synthetic C-S-H gels*. Cem Concr Res 32 (2002) 731-746.

[Hart 2014] Hart J, *Determination of the inventory Part A: Radionuclides*, OPERA report OPERA-PU-NRG1112A (2014) 1-47.

[Heath 2000] Heath TG, Illet DJ, Tweed CJ, *Development of a near-field sorption model for a cementitious repository*, UK Nirex report AEAT/R/ENV/0229 (2000) 1-41.

[Hilton 2000] Hilton BA, *Review of oxidation rates of DOE spent nuclear fuel: Part 1: Metallic fuel*, Argonne National Laboratory ANL-00/24 (2000) 1-85.

[Hoch 2010] Hoch AR, Smart NR, Wilson JD, Reddy, B, *A survey of reactive metal corrosion data for use in the SMOGG Gas generation model*, Report Serco SA/ENV-0895 Issue 2 (2010) 1-197.

[Hoch 2012] Hoch AR, Baston GMN, Glasser FP, Hunter FMI, Smith V, *Modelling evolution in the near field of a cementitious repository*, Min Mag 76 (2012) 3055–3069.

[Höglund 1991] Höglund LO, Bengtsson A, *Some chemical and physical processes related to the long-term performance of the SFR repository*, SKB SFR 01-06 (1991).

[Hofman 2015] Hofman GL, Kim YS, *Dispersion fuels*, Materials Science and Technology (2015) 1-94.

[Howe 1956] Howe JP, *The metallurgy of reactor fuels*, in: Finniston HM, Howe JP (eds) Progress in Nuclear Energy, McGraw Hill (1956) 481–510.

[Hummel 2002] Hummel W, Berner U, Curti E, Pearson FJ, Thoenen T, *Nagra/PSI Chemical Thermodynamic Data Base 01/01*, NAGRA Technical Report NTB 02-16 (2002) 1-565.

[IAEA 2009] International Atomic Energy Agency, *Corrosion of research reactor aluminium clad spent fuel in water*, Technical Reports Series TRS 418 (2009) 1-209.

[INEEL 2003] Idaho National Engineering and Environmental Laboratory, *Review of DOE spent nuclear fuel release rate test results*, Report DOE/SNF/REP-073 (2003) 1-199.

[Iwaida 2002] Iwaida T, Nagasaki S, Tanaka S, Yaita T, Tachimori S, *Structure alteration of C-S-H (calcium silicate hydrated phases) caused by sorption of cesium*, Radiochim Acta 90 (2002) 677-681.

[Jobe 1997] Jobe DL, Lemire RJ, Taylor P, *Iron oxide redox chemistry and nuclear fuel disposal*, AECL-11667, COG-96-487-1 (1997) 1-48.

[Kaminski 2001] Kaminski MD, Goldberg MM, C*orrosion of breached aluminide fuel under potential repository conditions*, International High Level Radioactive Waste Management Conference, April 29 - May 3, 2001, Las Vegas, NV (2001) 1-6.

[Kaminski 2002] Kaminski MD, Goldberg MM, *Aqueous corrosion of aluminium-based nuclear fuel*, J Nucl Mater 347 (2002) 77-87.

[Kaminski 2003] Kaminski MD, *Aqueous corrosion of aluminum-based nuclear fuel*, Argonne National Laboratory ANL-CMT-03/1 (2003) 1-133.

[Kim 2012] Kim YS, *Uranium intermetallic fuels (U-Al, U-Si, U-Mo)* Chapter 3.14 in: Comprehensive Nuclear Materials Volume 3: Advanced Fuels/Fuel Cladding/Nuclear Fuel Performance Modeling and Simulation (2012) 391–422.

[King 2000] King F, Stroes-Gascoyne S, *An assessment of the long-term corrosion behavior of C-steel and the impact on the redox conditions inside a nuclear fuel waste disposal container*, Ontario Power Generation Report No 06819-REP-01200-10028-R00 (2000).

[Kinoshita 2013] Kinoshita H, Swift P, Utton C, Carro-Mateo B, Marchand G, Collier N, Milestone N, *Corrosion of aluminium metal in OPC- and CAC-based cement matrices*, Cem Concr Res 50 (2013) 11–18.

[Klinkenberg 2010] Klinkenberg M, Curtius H, Neumann A, Bosbach D, *Corrosion of research reactor fuel elements in Mont Terri clay pore water - treatment, preparation and identification of secondary phases*, Clays in natural & engineered barriers for radioactive waste confinement, 4th International Meeting, March 2010, Nantes, France (2010) 1-2.

[Klinkenberg 2011] Klinkenberg M, Curtius H, Neumann A, Bosbach D, *Corrosion of research reactor fuel elements in Mont Terri clay pore water*, Euroclay 2011, 26 June 2011 to 01 July 2011, Antalya, Turkey (2011) 1.

[Klinkenberg 2014] Klinkenberg M, Neumann A, Curtius H, Kaiser G, Bosbach D, *Research reactor fuel element corrosion under repository relevant conditions: separation, identification, and quantification of secondary alteration phases of UAl_x-Al in $MgCl_2$-rich brine,* Radiochim Acta 102 (2014) 311–324.

[Kosakowski 2013] Kosakowski G, Berner U, *The evolution of clay rock/cement interfaces in a cementitious repository for low- and intermediate level radioactive waste*, Phys Chem Earth 64 (2013) 65–86.

[Krupka 1998] Krupka KM, Serne RJ, *Effects on radionuclide concentrations by cement/ground-water interactions in support of performance assessment of low-level radioactive waste facilities*, Pacific Northwest National Laboratory PNNL-11408 (1998) 1-142.

[Kursten 2004] Kursten B, Smailos E, Azkarate I, Werme L, Smart NR, Santarini G, *State-of the-art document on the COrrosion BEhaviour of COntainer MAterials (COBECOMA)*, European Commission, Contract No FIKW-CT-20014-20138, Final Report (2004) 1-299.

[Kursten 2015] Kursten B, Druyts F, *Assessment of the uniform corrosion behaviour of carbon steel radioactive waste packages with respect to the disposal concept in the geological Dutch Boom Clay formation*, OPERA-PU-SCK513 (2015) 1-107.

[Kursten 2016] Kursten B, *pers comm* (2016)

[Lam 1997] Lam PS, Sindelar RL, Peacock jr. HB, Vapour corrosion of aluminium cladding alloys and aluminium-uranium fuel materials in storage environments, Westinghouse Savannah River Company WSRC-TR-97-0120 (1997) 1-45.

[Lam 1999] Lam PS, Sindelar RL, Barrett KY, *Corrosion of aluminum-uranium alloys in water vapor at 200 °C*, Mat Res Soc Symp Proc 327 (1999) 121–129.

[Lemmens 2012] Lemmens K, Mennecart T, Cachoir C, *Spent fuel dissolution in Belgian supercontainer conditions: source term and compatibility*, Mat Res Soc Symp Proc 1475 (2012) 131-136.

[Lillard 2005] Lillard JA, Hanrahan RA, Corrosion of uranium and uranium alloys, in: Cramer SD, Covino jr BS, (eds) ASM Handbook, Volume 13B: Corrosion: Materials (2005) 370-384.

[Lindgren 1994] Lindgren M, Pers K, *Radionuclide release from the near-field of SFL 3-5, A preliminary study*, SKB Arbetsrapport AR 94-54 (1994).

[Mazeina 2003a] Mazeina L, Curtius H, Fachinger J, Odoj R, *Characterisation of secondary products of uranium-aluminium material test reactor fuel element corrosion in repository-relevant brine*. J Nucl Mater 323 (2003) 1-7.

[Mazeina 2003b] Mazeina L, *Investigation of the corrosion behaviour of U-Al material test reactor fuel elements in repository-relevant solutions and characterisation of the secondary phases formed*, Berichte des Forschungszentrums Jülich 4063 (2003) 1-116.

[Mazeina 2003c] Mazeina L, Curtius H, Fachinger J, *Formation of hydrotalcite-like compounds during corrosion experiments on MTR-FE-Al cladding*, Clay Miner 38 (2003) 35-40.

[McKee 1948] McKee AB, Brown RH, *Resistance of aluminum to corrosion in solutions containing various anions and cations*, Corrosion 3 (1948) 595-612.

[McWhirter 1952] McWhirter JW, Draley JE, *Aqueous corrosion of uranium and alloys: Survey of project literature*, Argonne National Laboratory ANL-4862 (1952) 1-49.

[MEAAI, 2014] Ministry of Economic Affairs, Agriculture and Innovation & Ministry of Foreign Affairs, *National report of the Kingdom of the Netherlands for the fifth review conference on the Joint Convention of the safety of spent fuel management and on the safety of radioactive waste management* (2014) 1-112.

[Meeussen 2014] Meeussen JCL, Rosca-Bocancea E, *Determination of the inventory Part B: Matrix composition*, OPERA report OPERA-IR-NRG1112B (2014) 1-23.

[Moreno 2001] Moreno L, Skagius K, Södergren S, Wiborgh M, *PROJECT SAFE Gas related processes in SFR*, SKB Report R-01-11 (2001) 1-130.

[NAGRA 2002] NAGRA, *Project Opalinus Clay Safety Report. Demonstration of disposal feasibility for spent fuel, vitrified high-level waste and long-lived intermediate-level waste (Entsorgungsnachweis)*, NAGRA Technical Report NTB 02-05 (2002) 1-360.

[NAGRA 2004] NAGRA, *Effects of post-disposal gas generation in a repository for spent fuel, high-level waste and long-lived intermediate level waste sited in Opalinus Clay*, NAGRA Technical Report NTB 04-06 (2004) 1-151.

[NAGRA 2008] NAGRA, *Effects of post-disposal gas generation in a repository for low- and intermediate-level waste sited in the Opalinus Clay of Northern Switzerland*, NAGRA Technical Report NTB 08-07 (2008) 1-138.

[Narayan 1988] Narayan R, Sheriff KP, *Electrochemical behaviour of aluminium in NaCl-anodic polarisation in alkaline solutions*, Key Eng Mater 20-28 (1988) 295-303.

[Neall 1994] Neall F, *Modelling of the near-field chemistry of the SMA repository at the Wellenberg site: Application of the extended cement degradation model*, NAGRA Technical Report NTB 94-03 (1994) 1-45.

[NRG 2012] Nuclear Research & Consultancy Group (NRG), *Information package HFR LEU fuel elements and control rods*, NRG-25138.116255 rev B (2012) 1-20 (Confidential document not published openly).

[Neumann 2012] Neumann A, *Bildung von sekundären Phasen bei tiefengeologischer Endlagerung von Forschungsreaktor-Brennelementen − Struktur- und Phasenanalyse*. Schriften des Forschungszentrums Jülich, Reihe Energie & Umwelt 153 (2012) 1-229.

[Openshaw 1964] Openshaw PR, Shreir LL, *Oxidation of uranium-aluminium intermetallic compounds II. Nature and surface topography of oxide films*, Corros Sci 4 (1964) 335-344.

[ONDRAF 2004] ONDRAF/NIRAS, *Multi-criteria analysis on the selection of a reference EBS design for vitrified high level waste*, NIROND 2004-03 (2004) 1-120.

[ONDRAF 2013] ONDRAF/NIRAS, *ONDRAF/NIRAS Research, Development and Demonstration (RD&D) Plan for the geological disposal of high-level and/or long-lived radioactive waste including irradiated fuel if considered as waste*, NIROND-TR 2013-12 E (2013) 1-411.

[Paramasivam 2001] Paramasivam M, Iyer SV, *Influence of alloying additives on corrosion and hydrogen permeation through commercial aluminium in alkaline solution*, J Appl Electrochem 31 (2001) 115-119.

[Pourbaix 1974] Pourbaix M, *Atlas of electrochemical equilibria in aqueous solutions*. National Association of Corrosion Engineers, Houston, TX, USA (1974) 1-644.

[Prítrský 2006] Prítrský J, Matejovič I, Ondra F, Nečas V, *Assessment of gas producing radioactive waste disposal*, J Electr Eng 57 (2006) 235-237.

[Rodwell 1999] Rodwell WR, Harris AW, Horseman ST, Lalieux P, Müller W, Ortiz Amaya L, Preuss K, *Gas migration and two-phase flow through engineered and geological barriers for a deep repository for radioactive waste. A joint EC/NEA status report*, EUR 19122 EN (1999) 1-429.

[Savage 2002] Savage D, Stenhouse M, *SFR 1 vault database*, SKI Report 02:53 (2002) 1-39.

[Seetharam 2015] Seetharam S, Jacques D, *Potential degradation processes of the cementitious EBS components, their potential implications on safety functions and conceptual models for quantitative assessment*, OPERA-PU-SCK514 (2015) 1-90.

[Setiadi 2006] Setiadi A, Milestone NB, Hill J, Hayes M, *Corrosion of aluminium and magnesium in BFS composite cements*, Adv Appl Ceram 105 (2006) 191-196.

[Sindelar 1996] Sindelar RL, Peacock jr. HB, Lam PS, Iyer NC, Louthan jr. MR, *Acceptance criteria for interim dry storage of aluminium-alloy clad spent nuclear fuels*, Westinghouse Savannah River Company WSRC-TR-95-0347 (1996) 1-34.

[Skagius 1999] Skagius K, Lindgren M, Pers K, *Gas generation in SFL 3-5 and effects on radionuclide release*, SKB Report R-99-16 (1999) 1-63.

[Smart 1998] Smart NR, Blackwood DJ, *An investigation of the effects of galvanic coupling on the corrosion of container and waste metals in cementitious environments*, AEA Technology Report AEAT-0251 Issue C (1998).

[Smart 2004] Smart NR, Blackwood DJ, Marsh GP, Naish CC, O'Brien TM, Rance AP, Thomas MI, *The anaerobic corrosion of carbon and stainless steels in simulated cementitious repository environments: A summary review of Nirex research*, AEA Technology Report AEAT/ERRA-0313 (2004) 1-87.

[Smith 2009] Smith P, Cornélis B, Capoeut M, Van Geet M, *The long-term safety strategy for the geological disposal of radioactive waste*, NIROND-TR-2009-12E (2009) 1-52.

[Stecher-Rasmussen 1996] Stecher-Rasmussen F, Vroegindeweij C, Freudenreich WE, de Haas JBM, Verbakel WFAR, *Development of the ECN Argonaut reactor for BNCT studies*, In: Mishima Y (ed) Cancer Neutron Capture Therapy, Plenum Press (1996) 319-325.

[Straumanis 1949a] Straumanis ME, Brakšs N, *The rate of solution of highest purity aluminum in sodium hydroxide solutions*, J Electrochem Soc 95 (1949) 98-106.

[Straumanis 1949b] Straumanis ME, Brakšs N, *The rate of solution of high purity aluminum in various bases*, J Electrochem Soc 96 (1949) 21-26.

[Sukiman 2013] Sukiman NL, Zhou X, Birbilis N, Hughes AE, Mol JMC, Garcia SJ, Zhou X, Thompson GE, *Durability and corrosion of aluminium and its alloys: Overview, property space, techniques and developments*, In: Ahmad Z (ed) Aluminium alloys - New trends in fabrication and applications, InTech (2013) 49-97.

[Suyama 2012] Suyama T, Tachi Y, *Development of sorption database (JAEA-SDB): Update of sorption data including soil and cement systems*, JAEA-Data/Code 2011-022 (2012) 1-35.

[Tabrizi 1991] Tabrizi MR, Lyon SB, Thompson GE, Ferguson JM, *The long term corrosion of aluminium in alkaline media*, Corros Sci 32 (1991) 733-742.

[Takatani 1982] Takatani Y, Yamakawa K, Yoshizawa S, *Corrosion behaviour of aluminium in alkaline solution*, J Soc Mater Sci Jpn 31 (1982) 1024-1030.

[Takatani 1983] Takatani Y, Yamakawa K, Yoshizawa S, *Corrosion behaviour of aluminum alloys in saturated calcium hydroxide solution*, J Soc Mater Sci Jpn 32 (1983) 1218-1222.

[Thijssen 2006] Thijssen PJM, *HEU/LEU Conversion of the Petten HFR*, Transactions 10th International Topical Meeting on Research Reactor Fuel Management, 30 April - 3 May 2006, Sofia, Bulgaria (2006) 250-254.

[Thoenen 2014] Thoenen T, Hummel W, Berner U, Curti E, *The PSI/Nagra Chemical Thermodynamic Database 12/07*, NAGRA Working Report NAB 14-49 (2014) 1-372.

[Tits 2006] Tits J, Iijima K, Wieland E, Kamei G, *The uptake of radium by calcium silicate hydrates and hardened cement paste*, Radiochim Acta 94 (2006) 637-643.

[van den Berghe 2010] van den Berghe S, Leenaers A, Koonen E, Sannen L, *From high to low enriched uranium fuel in research reactors*, Adv Sci Tec 73 (2010) 78-90.

[van Humbeeck 2007] van Humbeeck H, de Bock C, Bastiaens W, *Demonstrating the construction and backfilling feasibility of the supercontainer design for HLW*, Proceedings RepoSafe, International Conference on Radioactive Waste Disposal in Geological Formations, Braunschweig, November 6 – 9 2007 (2007) 336-345.

[Verhoef 2011a] Verhoef E, Neeft E, Grupa J, Poley A, *Outline of a disposal concept in clay,* OPERA-PG-COV008 (2011) 1-17.

[Verhoef 2011b] Verhoef EV, Schröder T, *Research plan*, OPERA-PG-COV004 (2011) 1-24.

[Verhoef 2014a] Verhoef EV, Neeft EAC, Grupa JB, Poley AD, *Outline of a disposal concept in clay*, OPERA-PG-COV008_rev1 (2014) 1-18.

[Verhoef 2014b] Verhoef EV, de Bruin AMG, Wiegers RB, Deissmann G, *Cementitious materials in OPERA disposal concept in Boom Clay*, OPERA-PG-COV020 (2014) 1-17.

[Verhoef 2016] Verhoef EV, Neeft EAC, Deissmann G, Filby A, Wiegers RB, Kers DA, *Waste families in OPERA*, OPERA-PG-COV023 (2016) 1-39.

[Vujičić 1985] Vujičić V, Lovreček B, *A study of the influence of pH on the corrosion rate of aluminium*, Surf Technol 25 (1985) 49-57.

[Waber 1952] Waber JT, *A review of the corrosion of uranium and its alloys*, Los Alamos Scientific Laboratory, LA-1524 (1952) 1-47.

[Wang 2009a] Wang L, *Near-field chemistry of a HLW/SF repository in Boom Clay - scoping calculations relevant to the supercontainer design*, External Report SCK•CEN ER-17 (2009) 1-53.

[Wang 2009b] Wang L, Martens E, Jacques D, de Cannière P, Berry J, Mallants D, *Review of sorption values for the cementitious near field of a near surface radioactive waste disposal facility*, NIROND-TR 2008-23 E (2009) 1-419.

[Wang 2013a] Wang L, *Solubility of radionuclides in Supercontainer concrete*, External Report SCK•CEN ER-239 (2013) 1-43.

[Wang 2013b] Wang L, Ochs M, Mallants D, Vielle-Petit L, Martens E, Jacques D, de Cannière P, Berry JA, Leterme B, *A new radionuclide sorption data base for benchmark cement accounting for geochemical evolution of cement*, in: Bart F, Cau-dit-Coumes C, Frizon F, Lorente S (eds) Cement-based materials for nuclear waste storage, Springer (2013) 103-112.

[Wersin 2003] Wersin P, Johnson LH, Schwyn B, Berner U, Curti E, *Redox conditions in the near field of a repository for SF/HLW and ILW in Opalinus Clay*, NAGRA Technical Report NTB 02-13 (2003) 1-38.

[Wersin 2004] Wersin P, Schwyn B, *Project Opalinus Clay: Integrated Approach for the development of geochemical databases used for safety assessment*, NAGRA Technical Report NTB 03-06 (2004) 1-71.

[Wiborgh 1986] Wiborgh M, Höglund LO, Pers K, *Gas formation in a L/ILW repository and gas transport in the host rock*, NAGRA Technical Report NTB 85-17 (1986) 1-132.

[Wickham 2008] Wickham S, *Evolution of the near-field of the ONDRAF/NIRAS repository concept for category B and C wastes*, NIROND TR-2007-07 E (2008) 1-140.

[Wieland 2001] Wieland E, *Experimental studies on the inventory of cement-derived colloids in the pore water of a cementitious backfill material*, NAGRA Technical Report NTB 01-02 (2001) 1-104.

[Wieland 2002] Wieland E, Van Loon LR, *Cementitious near-field sorption data base for performance assessment of an ILW repository in Opalinus Clay*, NAGRA Technical Report NTB 02-20 (2002) 1-87.

[Wieland 2014] Wieland E, *Sorption data base for the cementitious near field of L/ILW and ILW repositories for provisional safety analyses for SGT-E2*, NAGRA Technical Report NTB 14-08 (2014) 1-104.

[Wiersma 1998] Wiersma BJ, Mickalonis JI, *Preliminary report on the dissolution rate and degradation of aluminum spent nuclear fuels in repository environments*, Westinghouse Savannah River Company WSRC-TR-98-00290 (1998) 1-29.

[Wintergerst 2009] Wintergerst M, Dacheux N, Datcharry F, Herms E, Kapusta B, *Corrosion of the AlFeNi alloy used for the fuel cladding in the Jules Horowitz research reactor*, J Nucl Mater 48 (2009) 113-119.

[WNN 2013a] http://www.world-nuclear-news.org/NN-State_aid_for_Pallas_reactor_cleared-1807135.html 18.07.2013, accessed on 01.03.2016.

[WNN 2013b] http://www.world-nuclear-news.org/WR-LFR-fuel-removed-from-Petten-0612134.html, 06.12.2013, accessed on 01.03.2016.

[Zhang 2009] Zhang J, Klasky M, Letellier BC, *The aluminum chemistry and corrosion in alkaline solutions*, J Nucl Mater 384 (2009) 175–189.

Appendix 1

Table A-1 Activity per ECN canister filled with 33 spent research fuel elements after 130 years decay time [Verhoef 2016]

Radionuclide	Spent HEU-fuel Activity [Bq]	Spent LEU Fuel Activity [Bq]	Radionuclide	Spent HEU-fuel Activity [Bq]	Spent LEU Fuel Activity [Bq]
Ac-226			Np-237	2.76E+09	4.24E+09
Ac-227			Pa-231	1.41E+06	1.41E+06
Ag-108m			Pa-233		
Am-241	1.03E+12	1.38E+13	Pa-234		
Am-242m			Pb-202		
Am-243	2.18E+09	3.54E+10	Pb-210		
Ba-133			Pb-214		
Be-10			Pd-107	1.04E+08	1.36E+08
Bi-207			Pm-145		
Bi-214			Po-209		
C-14	6.57E+07	6.57E+07	Pu-238	4.95E+12	8.25E+12
Ca-41			Pu-239	9.11E+10	1.56E+12
Cd-113m			Pu-240	6.83E+10	1.47E+12
Cf-249			Pu-241	7.00E+10	9.44E+11
Cf-251			Pu-242	3.37E+08	5.29E+09
Cf-252			Pu-244	4.91E+05	4.91E+06
Cl-36	0.00E+00		Ra-226	8.78E+05	8.78E+05
Cm-241			Re-186		
Cm-243	1.27E+11	1.27E+12	Sb-125		
Cm-244	1.94E+09	1.94E+10	Se-79	2.97E+09	9.46E+08
Cm-245	1.48E+07	1.48E+08	Si-32		
Cm-246	1.85E+06	1.85E+07	Sm-146		
Cm-247	2.63E+05	2.63E+06	Sm-151	6.73E+11	1.09E+13
Cm-248	1.62E+06	1.62E+07	Sn-121m		
Co-60			Sn-126	2.57E+09	1.90E+11
Cs-135	1.35E+09	2.10E+10	Sr-90	3.80E+13	5.31E+13
Cs-137	4.39E+13	6.53E+13	Tc-99	1.11E+11	1.11E+11
Eu-152			Tc-99m		
Eu-152m			Th-229	1.31E+04	1.31E+04
H-3			Th-230	3.22E+07	3.22E+07
Ho-166m			Th-231		
I-129	2.04E+08	2.78E+08	Th-234		
K-40			Ti-44		
Kr-81			U-232	2.95E+09	2.95E+10
Kr-85	1.19E+11	3.63E+10	U-233	1.83E+06	1.83E+06
Mo-93			U-234	2.81E+10	4.29E+10
Mo-99			U-235	4.72E+08	5.32E+08
Nb-93m			U-236	3.80E+09	6.79E+09
Nb-94	1.34E+06	1.34E+06	U-238	1.01E+07	9.39E+08
Ni-59			U-239		
Ni-63	7.06E+03	7.06E+03	Zr-93	1.67E+10	1.67E+10

Table A-2 Inventory of radionuclides relevant for the long-term safety originating from spent research reactor fuels, control assemblies, and uranium filters in the year 2130 [Hart 2014]

Radionuclide	Half-Life [years]	Activity [Bq]
Ni-63	1.006E+02	4.20E+07
Se-79	3.770E+05	1.45E+09
Kr-85	1.075E+01	1.34E+14
Sr-90	2.879E+01	1.45E+16
Zr-93	1.530E+06	6.09E+10
Tc-99	2.140E+05	4.61E+11
Pd-107	6.500E+06	9.68E+08
Sn-126	1.000E+05	9.45E+09
Cs-137	3.004E+01	1.67E+16
Sm-147	1.060E+11	1.34E+05
Sm-151	9.000E+01	2.90E+13
U-232	6.880E+01	1.40E+06
U-233	1.592E+05	2.05E+08
U-234	2.457E+05	4.16E+12
U-235	7.038E+08	9.32E+10
U-236	2.370E+07	6.60E+11
U-238	4.468E+09	9.91E+10
Np-237	2.140E+06	4.29E+11
Pu-238	8.770E+01	1.00E+15
Pu-239	2.411E+04	1.45E+14
Pu-240	6.563E+03	1.19E+14
Pu-241	1.433E+01	4.19E+14
Pu-242	3.735E+05	4.24E+11
Am-241	4.328E+02	1.16E+15
Am-243	7.365E+03	2.79E+12
Cm-244	1.800E+01	5.58E+12
Th-230	7.540E+04	3.78E+09
Pa-231	3.276E+04	2.53E+08
Th-232	1.405E+10	3.60E+03

Appendix 2

Table A-3 **Predicted composition of cementitious pore waters in a repository in Opalinus Clay and reference Opalinus Clay pore water ([Berner 2003], [Wersin 2004]) - concentrations in mmol L^{-1}**

	Initial stage water (Stage 1)	Reference water (Stage 2)	Opalinus Clay porewater
pH	13.44	12.55	7.24
E_H	-430 mV	-750 … -230 mV	-167 mV
Na	101	169	169
K	303	5.7	5.65
Ca	0.84	20.1	0.0105
Mg	$<10^{-4}$	10^{-4}	7.48
Al	0.01	0.005	<0.001
Si	0.05	0.016	0.178
CO_3	0.204	0.01	2.7
SO_4	0.75	0.10	24
Cl	-	160	160

Table A-4 **Predicted composition of cementitious pore waters in an ILW repository in Opalinus Clay (after 10,000 years exchange with Opalinus Clay) [Berner 2014] and reference Opalinus Clay pore water used in the modelling study [Kosakowski 2013] - concentrations in mol kg^{-1}**

	Concrete pore water (Stage 2)	Opalinus Clay pore water
pH	12.54	7.26
E_H	-498 mV	-168.5 mV
Na	$4.228 \cdot 10^{-2}$	$1.646 \cdot 10^{-1}$
K	$3.310 \cdot 10^{-3}$	$2.594 \cdot 10^{-3}$
Ca	$1.806 \cdot 10^{-2}$	$1.247 \cdot 10^{-2}$
Mg	$1.107 \cdot 10^{-8}$	$9.591 \cdot 10^{-3}$
Al	$6.912 \cdot 10^{-6}$	$1.750 \cdot 10^{-8}$
Si	$3.432 \cdot 10^{-5}$	$1.802 \cdot 10^{-4}$
CO_3	$8.064 \cdot 10^{-6}$	$2.172 \cdot 10^{-3}$
SO_4	$4.711 \cdot 10^{-5}$	$2.479 \cdot 10^{-2}$
Cl	$3.752 \cdot 10^{-2}$	$1.602 \cdot 10^{-1}$

Appendix 3

Table A-5 Corrosion rates of aluminium under alkaline conditions

Material	Conditions	Method	Test duration	Corrosion rate [µm a^{-1}]	Source
Al	pH 10, 25 °C		7 d	20	McKee 1948
Al	pH 8, 25 °C		st	0.9	Chatalov 1952
Al	pH 10.2, 25 °C		st	102	Chatalov 1952
Al	pH 12, 25 °C		st	3,244	Chatalov 1952
Al-alloy	pH 10, 60 °C		7 d	248	Binger 1957
Al	pH 9.4, 25 °C	ML	1 h	113	Vujicic 1985
Al	pH 10, 25 °C	ML	1 h	634	Vujicic 1985
Al	pH 11, 25 °C	ML	1 h	7,082	Vujicic 1985
Al (98.5%)	pH 10, NaOH/NaCl	EM		870	Narayan 1988
Al (98.5%)	pH 12, NaOH/NaCl	EM		8,700	Narayan 1988
Al (99.999%)	pH 10, NaOH, 0.1 M NaCl	EM		210	Chandra 1990
Al (>99.5%)	pH 10, NaOH, 30 °C	ML	20 d	52	Tabrizi 1991
Al (>99.5%)	pH 10, NaOH, 30 °C	ML	40 d	41	Tabrizi 1991
Al (>99.5%)	pH 10, NaOH, 30 °C	ML	80 d	19	Tabrizi 1991
Al (>99.5%)	pH 11, NaOH, 30 °C	ML	20 d	108	Tabrizi 1991
Al (>99.5%)	pH 11, NaOH, 30 °C	ML	40 d	100	Tabrizi 1991
Al (>99.5%)	pH 11, NaOH, 30 °C	ML	80 d	33	Tabrizi 1991
Al (>99.5%)	pH 12, NaOH, 30 °C	ML	20 d	520	Tabrizi 1991
Al (>99.5%)	pH 11, NaOH, 30 °C	ML	40 d	106	Tabrizi 1991
Al (>99.5%)	pH 10, NaOH, 30 °C, 1000 ppm Cl^-	ML	40 d	48	Tabrizi 1991
Al (>99.5%)	pH 10, NaOH, 60 °C	ML	40 d	61	Tabrizi 1991
Al (>99.5%)	pH 11, NaOH, 60 °C	ML	40 d	219	Tabrizi 1991
Al (>99.5%)	pH 11, NaOH, 60 °C	ML	40 d	63	Tabrizi 1991
Al (>99.5%)	pH 10, NaOH, 60 °C, 1000 ppm Cl^-	ML	40 d	24	Tabrizi 1991
Al (2S)	0.01 M NaOH (pH ▫12)	ML	30 m	244,000	Paramasivam 2001
Al (3S)	0.01 M NaOH (pH ▫12)	ML	30 m	365,000	Paramasivam 2001
Al (26S)	0.01 M NaOH (pH ▫12)	ML	30 m	103,000	Paramasivam 2001
Al (57S)	0.01 M NaOH (pH ▫12)	ML	30 m	97,000	Paramasivam 2001
Al 5025	$Ca(OH)_2$ (pH ~12.5), 30 °C	ML	1 d	12,647	Takatani 1982
Al 5025	$Ca(OH)_2$ (pH ~12.5), 30 °C	ML	10 d	1,521	Takatani 1982
Al 5025	$Ca(OH)_2$ (pH ~12.5), 30 °C	ML	30 d	538	Takatani 1982
Al 1050	$Ca(OH)_2$ (pH ~12.5), 30 °C	ML	1 d	17,733	Takatani 1982
Al 1050	$Ca(OH)_2$ (pH ~12.5), 30 °C	ML	10 d	1,816	Takatani 1982
Al 1050	$Ca(OH)_2$ (pH ~12.5), 30 °C	ML	30 d	599	Takatani 1982
Al 2017	$Ca(OH)_2$ (pH ~12.5), 30 °C	ML	1 d	3,664	Takatani 1983
Al 2017	$Ca(OH)_2$ (pH ~12.5), 30 °C	ML	10 d	612	Takatani 1983
Al 2017	$Ca(OH)_2$ (pH ~12.5), 30 °C	ML	30 d	275	Takatani 1983

methods: ML: mass loss, EM: electrochemical methods, H2: H_2-gas evolution
duration: d: days, h: hours, m: minutes, st: short term

Table A-5 Corrosion rates of aluminium under alkaline conditions (*continued*)

Material	Conditions	Method	Test duration	Corrosion rate [µm a^{-1}]	Source
Al 3003	$Ca(OH)_2$ (pH ~12.5), 30 °C	ML	1 d	7,731	Takatani 1983
Al 3003	$Ca(OH)_2$ (pH ~12.5), 30 °C	ML	10 d	975	Takatani 1983
Al 3003	$Ca(OH)_2$ (pH ~12.5), 30 °C	ML	30 d	384	Takatani 1983
Al 7072	$Ca(OH)_2$ (pH ~12.5), 30 °C	ML	1 d	5,545	Takatani 1983
Al 7072	$Ca(OH)_2$ (pH ~12.5), 30 °C	ML	10 d	2,096	Takatani 1983
Al 7072	$Ca(OH)_2$ (pH ~12.5), 30 °C	ML	30 d	894	Takatani 1983
Al 1050	$Ca(OH)_2$ (pH ~12.5), 30 °C	ML	1 d	10,974	Takatani 1983
Al 1050	$Ca(OH)_2$ (pH ~12.5), 30 °C	ML	10 d	1,382	Takatani 1983
Al 1050	$Ca(OH)_2$ (pH ~12.5), 30 °C	ML	30 d	482	Takatani 1983
Al 5052	$Ca(OH)_2$ (pH ~12.5), 30 °C	ML	1 d	13,968	Takatani 1983
Al 5052	$Ca(OH)_2$ (pH ~12.5), 30 °C	ML	10 d	1,625	Takatani 1983
Al 5052	$Ca(OH)_2$ (pH ~12.5), 30 °C	ML	30 d	583	Takatani 1983
Al 6063	$Ca(OH)_2$ (pH ~12.5), 30 °C	ML	1 d	13,910	Takatani 1983
Al 6063	$Ca(OH)_2$ (pH ~12.5), 30 °C	ML	10 d	6,047	Takatani 1983
Al 6063	$Ca(OH)_2$ (pH ~12.5), 30 °C	ML	30 d	3,154	Takatani 1983
Al (JIS A 1070)	mortar equil. water, pH 12.2, 15 °C	H2	1 d	10,200	Fujisawa 1997
Al (JIS A 1070)	mortar equil. water, pH 12.2, 15 °C	H2	4 d	7,400	Fujisawa 1997
Al (JIS A 1070)	mortar equil. water, pH 12.2, 15 °C	H2	40 d	6,700	Fujisawa 1997
Al (JIS A 1070)	embedded in mortar grains, 15 °C	H2	initial	20,000	Fujisawa 1997
Al (JIS A 1070)	embedded in mortar grains, 15 °C	H2	> 1000 h	1 ... 10	Fujisawa 1997
Al (JIS A 1070)	embedded in mortar	H2	initial	500	Fujisawa 1997
Al (JIS A 1070)	embedded in mortar	H2	> 1000 h	1 ... 10	Fujisawa 1997
Al	embedded in BFA-OPC-mortar, RT?	H2	0 ... 7 d	2,250	Kinoshita 2013
Al	embedded in BFA-OPC-mortar, RT?	H2	7 ... 28 d	22	Kinoshita 2013
Al	embedded in PFA-CAC-mortar, RT?	H2	0 ... 7 d	152	Kinoshita 2013
Al	embedded in PFA-CAC-mortar, RT?	H2	7 ... 28 d	217	Kinoshita 2013

methods: ML: mass loss, EM: electrochemical methods, H2: H_2-gas evolution
duration: d: days, h: hours, m: minutes, st: short term

The experimental data on the aluminium dissolution rates, which are often reported in units of mass release per surface area and time (e.g. g m^{-2} d^{-1}), as normalised release rates (g m^{-2}), or specific hydrogen evolution rates (e.g. ml H_2 cm^{-2} d^{-1}), depending on the type of experiment, were recalculated to corrosion rates in units of µm a^{-1}. For the conversion a density of 2700 kg m^{-3} and a molar mass of 26.98 g mol^{-1} for aluminium were used throughout this review. In many cases the rate data were not explicitly given in the references but had to be taken from digitized graphs/figures and are thus associated with some uncertainty.

Appendix 4

Table A-6 **Calculated and recommended radionuclide solubility limits in the cementitious near field (pH 12.55, E_H -230 mV, 25 °C) of an ILW repository [Berner 2003] - concentrations in mol L^{-1} (NL: not limited)**

Element	Calculated			Recommended		
	Lower limit	Maximum solubility	Upper limit	Lower limit	Maximum solubility	Upper limit
Cm	-	-	-	3E-10	2E-9	1E-8
Am	3E-10	2E-9	1E-8	-	-	-
Pu	1E-11	4E-11	2E-10	-	-	-
Np	3E-9	5E-9	1E-8	-	-	-
U	-	NL	-	-	1E-8	5E-7
Pa	-	-	-	-	~1E-8	-
Th	8E-10	3E-9	1E-8	-	-	-
Ra	-	1E-5	-	1E-6	-	2E-2
Cs	-	NL	-	-	-	-
I	-	NL	-	-	-	-
Tc	-	NL	-	-	-	-
Nb	-	NL	-	-	-	-
Se	-	NL (~0.1)	-	7E-6	1E-5	2E-5
Cl	-	NL	-	-	-	-
C_{inorg}	-	-	-	-	9.7E-6	2E-4
Ac	-	-	-	4E-9	2E-6	2E-5
Sn	1E-8	1E-7	2E-7	-	-	-
Pd	-	insignificantly low	-	8E-8	8E-7	8E-6
Zr	-	6E-6	-	6E-7	-	6E-5
Sr	-	3E-3	-	1E-3	-	6E-3
Ni	1E-8	3E-7	8E-6	-	-	-
Po	-	-	-	-	-	-
Pb	-	-	-	-	3E-3	2E-2
Hf	-	-	-	6E-7	6E-6	6E-5
Ho	-	-	-	4E-9	2E-6	2E-5
Eu	-	2E-6	2E-5	4E-9	-	-
Pm	-	-	-	4E-9	2E-6	2E-5
Sb	-	NL	-	-	-	-
Cd	-	-	-	-	4E-6	3E-5
Ag	-	-	-	-	insignificantly low	3E-6
Ru	-	-	-	-	-	high
Mo	-	-	-	-	3E-5	2E-3
Co	-	-	-	-	7E-7	8E-6

Table A-7: Calculated radionuclide solubilities in cementitious environments (recommended values, lower and upper guideline values) [Berner 2014] compared to earlier evaluations ([NAGRA 2002], [Berner 2003])

Concrete pore water, portlandite stage, pH 12.54				[NAGRA 2002], [Berner 2003]		
Element	Recommended value	Lower guideline value	Upper guideline value	Reference case	Lower limit	Upper limit
	[mol kg^{-1} H_2O]	[mol kg^{-1} H_2O]	[mol kg^{-1} H_2O]	[mol L^{-1}]	[mol L^{-1}]	[mol L^{-1}]
Be	2.3×10^{-4}	9.3×10^{-5}	4.6×10^{-4}	--	--	high
C_{inorg}	8.1×10^{-6}			2×10^{-4}	1×10^{-4}	4×10^{-4}
Cl	3.8×10^{-2}			high	high	high
K	3.3×10^{-3}			5.7×10^{-3}	-	-
Ca	1.8×10^{-2}			1.8×10^{-3}	-	-
ISA a)	2.0×10^{-2}					
ISA b)			2.9×10^{-2}			
Co	5.4×10^{-7}	3.8×10^{-11}	1.7×10^{-5}	7×10^{-7}	7×10^{-7}	7×10^{-6}
Ni	3.0×10^{-6}	1.0×10^{-7}	2.3×10^{-4}	3×10^{-7}	1×10^{-8}	8×10^{-6}
ISA a)	3.5×10^{-6}					
ISA b)			4.7×10^{-6}			
Se(-II)	2.1×10^{-6}	7.2×10^{-11}	high	1×10^{-5}	7×10^{-6}	7×10^{-4}
Sr	2.4×10^{-3}	--	--	3×10^{-3}	2×10^{-3}	6×10^{-3}
Zr	4.5×10^{-9}	6.8×10^{-11}	1.3×10^{-4}	6×10^{-6}	6×10^{-7}	6×10^{-5}
ISA a)	4.9×10^{-7})					
Nb(V)	high	high	high	high	high	high
Mo(VI)	7.2×10^{-6}	3.6×10^{-6}	2.0×10^{-5}	3×10^{-5}	3×10^{-6}	2×10^{-3}
Tc(IV)	1.8×10^{-6}	2.9×10^{-8}	1.8×10^{-6}	high	3×10^{-7}	high
Pd	8.5×10^{-7}	insignificant	2.5×10^{-5}	8×10^{-7}	--	--
Ag	1.8×10^{-6}	2.9×10^{-14}	1.7×10^{-4}	insignificant	--	--
Sn(IV)	1.0×10^{-7}	5.0×10^{-8}	2.0×10^{-7}	1×10^{-7}	1×10^{-7}	8×10^{-6}
I	1.8×10^{-7}	1.8×10^{-8}	1.8×10^{-7}	high	high	high
Cs	high	high	high	high	high	high
Sm	4.6×10^{-7}	8.9×10^{-11}	4.6×10^{-7}	2×10^{-6}	2×10^{-7}	2×10^{-5}
ISA a)	2.9×10^{-4}					
Eu	1.9×10^{-6}	3.8×10^{-9}	2.7×10^{-5}	2×10^{-6}	4×10^{-9}	2×10^{-5}
ISA a)	5.0×10^{-4}	1.1×10^{-6}				
ISA b)			2.2×10^{-3}			
Ho	1.9×10^{-7}	1.8×10^{-11}	1.9×10^{-7}	2×10^{-6}	4×10^{-9}	2×10^{-5}
ISA a)	1.2×10^{-4}					
Pb	4.6×10^{-3}	1.7×10^{-3}	4.6×10^{-3}	3×10^{-3}	--	2×10^{-2}
Po(IV)	6.4×10^{-8}	1.6×10^{-10}	6.4×10^{-8}	high	high	high
Ra	9.7×10^{-7}	2.1×10^{-7}	1.7×10^{-5}	1×10^{-5}	1×10^{-6}	2×10^{-5}
Ac	(1.9×10^{-6})	(3.8×10^{-9})	(2.7×10^{-5})	2×10^{-6}	4×10^{-9}	2×10^{-5}
ISA a)	5.0×10^{-4})					
Th	1.3×10^{-9}	1.6×10^{-10}	6.4×10^{-8}	3×10^{-9}	8×10^{-10}	1×10^{-8}
ISA a)	9.5×10^{-7}		6.0×10^{-6}			
ISA b)			3.0×10^{-5}			

ISA a): calculations including 5×10^{-3} [mol kg^{-1} H_2O] of $(K^+)ISA^-$
ISA b): calculations with solid $Ca(ISA)_2(cr)$ present.

Table A-7: Calculated radionuclide solubilities in cementitious environments (recommended values, lower and upper guideline values) [Berner 2014] compared to earlier evaluations ([NAGRA 2002], [Berner 2003]) *(continued)*

Concrete pore water, portlandite stage, pH 12.54				[NAGRA 2002], [Berner 2003]		
Element	Recommended value	Lower guideline value	Upper guideline value	Reference case	Lower limit	Upper limit
	[mol kg^{-1} H_2O]	[mol kg^{-1} H_2O]	[mol kg^{-1} H_2O]	[mol L^{-1}]	[mol L^{-1}]	[mol L^{-1}]
Pa(V)	1.8×10^{-6}	1.8×10^{-7}	1.8×10^{-5}	1×10^{-8}	1×10^{-8}	High
ISA a)	(2.3×10^{-6})					
U(VI)	7.0×10^{-7}	1.7×10^{-8}	1.4×10^{-4}	1×10^{-8}	1×10^{-8}	5×10^{-7}
ISA a)	8.4×10^{-7}					
ISA b)			1.1×10^{-6}			
Np(IV)	1.0×10^{-9}	2.5×10^{-11}	4.0×10^{-8}	5×10^{-9}	3×10^{-9}	1×10^{-8}
ISA a)	3.5×10^{-9}					
ISA b)			1.9×10^{-8}			
Pu(IV)	2.3×10^{-12}	2.3×10^{-13}	8.2×10^{-8}	4×10^{-11}	1×10^{-11}	1×10^{-10}
ISA a)	(8.1×10^{-12})					
ISA b)			(4.4×10^{-11})			
Am	5.4×10^{-10}	2.2×10^{-12}	1.1×10^{-8}	2×10^{-9}	3×10^{-10}	1×10^{-8}
ISA a)	8.9×10^{-8}	4.4×10^{-9}				
ISA b)			3.5×10^{-7}			
Cm	1.1×10^{-9}	1.5×10^{-10}	8.6×10^{-9}	2×10^{-9}	3×10^{-10}	1×10^{-8}
(ISA a)	(1.8×10^{-7})					
(ISA b)			(7.1×10^{-7})			

ISA a): calculations including 5×10^{-3} [mol kg^{-1} H_2O] of $(K^+)ISA^-$
ISA b): calculations with solid $Ca(ISA)_2$(cr) present.

OPERA
Meer informatie:

Postadres
Postbus 202
4380 AE Vlissingen

T 0113-616 666
F 0113-616 650
E info@covra.nl

www.covra.nl